

University of Windsor

Scholarship at UWindor

Electronic Theses and Dissertations

Theses, Dissertations, and Major Papers

1-1-1972

Cylindrical shells made of corrugated sheets.

M. N. El-Atrouzy
University of Windsor

Follow this and additional works at: <https://scholar.uwindsor.ca/etd>

Recommended Citation

El-Atrouzy, M. N., "Cylindrical shells made of corrugated sheets." (1972). *Electronic Theses and Dissertations*. 6110.

<https://scholar.uwindsor.ca/etd/6110>

This online database contains the full-text of PhD dissertations and Masters' theses of University of Windsor students from 1954 forward. These documents are made available for personal study and research purposes only, in accordance with the Canadian Copyright Act and the Creative Commons license—CC BY-NC-ND (Attribution, Non-Commercial, No Derivative Works). Under this license, works must always be attributed to the copyright holder (original author), cannot be used for any commercial purposes, and may not be altered. Any other use would require the permission of the copyright holder. Students may inquire about withdrawing their dissertation and/or thesis from this database. For additional inquiries, please contact the repository administrator via email (scholarship@uwindsor.ca) or by telephone at 519-253-3000ext. 3208.

INFORMATION TO USERS

This manuscript has been reproduced from the microfilm master. UMI films the text directly from the original or copy submitted. Thus, some thesis and dissertation copies are in typewriter face, while others may be from any type of computer printer.

The quality of this reproduction is dependent upon the quality of the copy submitted. Broken or indistinct print, colored or poor quality illustrations and photographs, print bleedthrough, substandard margins, and improper alignment can adversely affect reproduction.

In the unlikely event that the author did not send UMI a complete manuscript and there are missing pages, these will be noted. Also, if unauthorized copyright material had to be removed, a note will indicate the deletion.

Oversize materials (e.g., maps, drawings, charts) are reproduced by sectioning the original, beginning at the upper left-hand corner and continuing from left to right in equal sections with small overlaps.

ProQuest Information and Learning
300 North Zeeb Road, Ann Arbor, MI 48106-1346 USA
800-521-0600

UMI[®]

CYLINDRICAL SHELLS MADE OF CORRUGATED SHEETS

*A Dissertation
Submitted to the Faculty of Graduate Studies
through the Department of Civil Engineering
in Partial Fulfillment of the Requirements
for the Degree of Doctor of Philosophy
at The University of Windsor.*

By

M. N. El-Atrouzy

Windsor, Ontario, Canada:

1972

UMI Number: DC52690

INFORMATION TO USERS

The quality of this reproduction is dependent upon the quality of the copy submitted. Broken or indistinct print, colored or poor quality illustrations and photographs, print bleed-through, substandard margins, and improper alignment can adversely affect reproduction.

In the unlikely event that the author did not send a complete manuscript and there are missing pages, these will be noted. Also, if unauthorized copyright material had to be removed, a note will indicate the deletion.

UMI[®]

UMI Microform DC52690
Copyright 2008 by ProQuest LLC
All rights reserved. This microform edition is protected against
unauthorized copying under Title 17, United States Code.

ProQuest LLC
789 East Eisenhower Parkway
P.O. Box 1346
Ann Arbor, MI 48106-1346

AAW2182

© M. N. El-Atrouzy 1972

412165

APPROVED BY:

A. L. Smith

G. Abdul-Samed

Shorston

J. B. Kennedy

Paul Fazio

ACKNOWLEDGEMENTS

First of all, the author wishes to thank the Almighty God for His constant guidance and blessings.

The author then wishes to thank his advisor, Dr. G. Abdel-Sayed, for his assistance, counsel, and encouragement.

Thanks are also due to the laboratory technicians of the Department of Civil Engineering for their assistance in the experimental work and to the staff of the Computer Centre for providing the many hours of computer time required for the theoretical analyses.

The material for experimental work, provided free of charge, from WESTEEL ROSCO LTD. is greatly appreciated.

This research study was made possible through a financial assistance from the N.R.C. of Canada.

Finally, the author is deeply indebted to his parents for their concern and moral support.

ABSTRACT

This study is presented to establish methods of analysis and practical applications of cylindrical shells, made of corrugated sheets.

The present approach is based on treating the corrugated sheets as orthotropic shells, and deals with their applications in shell roofs and grain bins.

The differential equations, governing the behaviour of orthotropic shells, are established in an exact as well as simplified form.

The cases of practical shells, which are solved here, include single and group of shells with longitudinal stiffeners in valleys only, and with longitudinal stiffeners in valleys and crown, as well as half barrels supported along their four edges. Simplified design formulae and tables are prepared for use in practice.

An experimental program was undertaken with full scale shell roofs. The experimental results showed good agreement with those obtained theoretically.

Simplified differential equations, governing the behaviour of bins made of corrugated sheets, are derived. Particular and homogeneous solutions are superimposed to satisfy the governing equations as well as the boundary conditions.

A study on the effect of geometry of corrugation configuration on the load capacity of the shell is also made.

CONTENTS

	Page
ACKNOWLEDGEMENTS	i
ABSTRACT	ii
LIST OF FIGURES	v
LIST OF TABLES	vii
NOMENCLATURE	viii
CHAPTERS	
I. INTRODUCTION	1
II. MATHEMATICAL FORMULATIONS	5
III. APPLICATIONS OF CYLINDRICAL SHELLS MADE OF CORRUGATED SHEETS IN ROOFING	14
IV. EXPERIMENTAL VERIFICATION	41
V. APPLICATIONS OF CYLINDRICAL SHELLS MADE OF CORRUGATED SHEETS IN GRAIN BINS	50
VI. EFFECT OF GEOMETRY OF CORRUGATION ON THE LOAD CAPACITY OF THE SHELL	62
VII. OBSERVATIONS AND CONCLUSIONS	67
APPENDICES	
APPENDIX (I): DERIVATION OF EXACT CHARACTERISTIC EQUATION OF ORTHOTROPIC SHELLS	101
APPENDIX (II): STRESS-RESULTANTS AND DISPLACE- MENTS DUE TO BENDING	107
APPENDIX (III): SIMPLIFIED FORMULAE AND DESIGN TABLES FOR SHELL ROOFS MADE OF CORRUGATED SHEETS	122
APPENDIX (IV): FLOW CHARTS	132
REFERENCES	135
VITA AUCTORIS	137

LIST OF FIGURES

Figure		Page
1	Arc-and-tangent type of corrugation.	70
2	Infinitesimal element of shell surface with the applied internal stress-resultants.	70
3	Coordinate system for roofs.	71
4	Types of Boundary Conditions of shell roofs.	72
5	Effect of " ρ " on shell roofs for different values of (L/R) .	73
6	Relation between percentage of error in the roots of the simplified characteristic equation vs. the ratio (L/R) .	74
7	Comparison between the present solution and the beam-method.	75
8	Comparison between Case (I) and Case (IV) of boundary conditions.	76
9-a	A picture showing the shell model tested.	77
9-b	A picture showing the loading system used.	77
9-c	General arrangements of the shell roof tested in the lab.	78
10,11	Comparison between theoretical and experimental results of first experiment.	79
12..19	Comparison between theoretical and experimental results of second experiment.	81
20,21	Comparison between theoretical and experimental results of third experiment.	89
22	Coordinate-system for grain bins.	91
23	Boundary conditions for grain bins.	91
24	Circular bin under frictional forces stiffened by longitudinal ribs.	92

Figure		Page
25	Relation between (h/b_a) and (λ_e/b_a) for the determination of the effective width of corrugated sheets.	93
26	Relation between (h/b_a) and (λ_e/h) for the determination of the effective width of corrugated sheets.	94
27	Comparison between the values of u-displacement when using the standard and <u>1st</u> alternative shapes of corrugation.	95
28	A picture showing the shape of dimpled corrugated sheet.	96
29-a	Stress-strain curves for dimpled corrugated sheets.	97
29-b		98
30	Relation between maximum percentage of error in the roots of the simplified characteristic equation for different values of (D_x/D_ϕ) vs. the ratio (L/R) .	99
31	Comparison between the present solution and the beam-method for third alternative.	100

LIST OF TABLES

Table		Page
(III.1)	Values of roots of characteristic equations (23 & 25) for different ratios of (L/R).	32
(1,2,3)	Results and analysis of first experiment.	44
(4...7)	Results and analysis of second experiment.	46
(I)	Design tables for shell roofs stiffened at valleys only.	124
(II)	Design tables for shell roofs stiffened at valleys and crown.	125
(III)	Design tables for half barrels supported on four edges on earth.	126
(IV)	Design tables for an inner shell of a multiple group of shells stiffened at valleys only.	127
(V)	Design tables for an inner shell of a multiple group of shells stiffened at valleys and crown.	128
(A,B,C)	Maximum intensity of snow load for different cases of boundary conditions.	129

NOMENCLATURE

$A, B, C,$ $D, E, F,$ $G, H, A^*,$ $B^*, C^*,$ E^*, F^*	- Integration constants.
B_x	- Bending rigidity in the x-direction.
B_ϕ	- Bending rigidity in the ϕ -direction.
$B_{x\phi}$	- Torsional rigidity.
b_a	- Spacing of vertical stiffeners in grain bins.
c	- Corrugation pitch.
D_x	- Axial rigidity in the x-direction.
D_ϕ	- Axial rigidity in the ϕ -direction.
$D_{x\phi}$	- Shear rigidity in the x- ϕ plane.
E	- Modulus of elasticity of steel.
E_x	- Apparent strain rigidity in the x-direction.
f	- Half depth of corrugation.
h	- Height of grain bin.
k	- A parameter equals π/L .
l	- Developed length of corrugation.
L	- Span of shell.
m	- The 8-roots of the characteristic equation.
P_x	- Component of external load in the x-direction.
P_ϕ	- Component of external load in the ϕ -direction.
P_z	- Component of external load in the z-direction.
M_x	- Longitudinal bending moments.
M_ϕ	- Transversal bending moments.

NOMENCLATURE con't

- $M_{x\phi}$ - Torsional moments.
- N_x - Direct longitudinal stress-resultant.
- N_ϕ - Direct transversal stress-resultant.
- $N_{x\phi}$ - Membrane shearing forces.
- Q_x - Longitudinal shearing forces.
- Q_ϕ - Transversal shearing forces.
- R - Radius of curvature of the shell.
- t - Average thickness of the sheet.
- u - Displacement component in the x -direction.
- v - Displacement component in the ϕ -direction.
- w - Radial displacement normal to the shell surface.
- x, ϕ, z - Coordinates.
- α - Real part in the roots of the characteristic equation.
- β - Imaginary part in roots of the characteristic equation.
- λ - A parameter equals $(\pi R/L)$.
- λ_e - Effective width of corrugated sheets.
- μ - Poisson's ratio.
- ϕ_e - Half the central angle.
- ρ - A reduction factor to account for the effect of slip at sheet-to-sheet and sheet-to-frame connections.
- ϵ_x - Axial strain in the x -direction.
- ϵ_ϕ - Strain in the tangential direction.

NOMENCLATURE con't

- $\gamma_{x\phi}$ - Shear strain in the $x-\phi$ plane.
 θ - Rotation of the tangent of shell surface.

CHAPTER (I)
INTRODUCTION

The use of light gauge corrugated sheets goes back to the beginning of this century. For a long time, corrugated sheets were being used as coverings, without any attention being paid to their structural capability. The main reason for not considering them as structural materials, was the lack of a sound basis for connecting these sheets together, to form a continuous medium. Nilson⁽¹⁸⁾ was the first to study the behaviour of these sheets when assembled. His study laid the foundation for the use of corrugated sheets, as shear diaphragms, to replace shear bracings. Furthermore, his investigation postulated the possibility of using these sheets in folded plate roofs⁽¹⁹⁾, in which they carry mainly the shear forces, (the tension and compression are being carried by longitudinal stiffeners).

Parallel to these studies of practical applications, extensive study of the mechanical properties of such assembly was carried out by Luttrell⁽¹⁷⁾, Bryan⁽²⁰⁾, EL-Dakhkhini⁽²⁰⁾ and the author⁽⁸⁾.

In Canada and the U.S.A., corrugated sheets are produced with cylindrical curvature. Up to the present time, they are being used in grain bins and farm buildings without

a reliable method of design. Therefore, it is the author's conviction that a precise method of analysis for cylindrical shells made of corrugated sheets would open the way for another economical practical use of such materials.

Furthermore, shells have better load-carrying characteristics than folded plates, (under a uniformly distributed load), since they translate the applied loads into mainly membrane forces. Moreover, shells offer an efficient use of thin steel sheets in longspan structures, as the corrugations minimize the problems of local and overall buckling.

Corrugated sheets, with cylindrical curvature, are usually produced, using the arc-and-tangent type of corrugations. The present thesis examines shells made of this type of corrugation and suggests alternatives for better performance.

In this study, the corrugated sheets are treated as orthotropic materials. In Chapter (II), the mathematical formulations of the theoretical model are dealt with. Exact and simplified governing differential equations are derived from these formulations.

In Chapter (III), the applications in roofing are presented. The practical cases of boundary conditions are discussed and the method of solution is given. The general differential equation of the 8th order in the radial displacement, w , governing the behaviour of orthotropic shells is established. The membrane analysis of the shell, under different cases of loading, is also given in this

chapter. In this membrane solution, the boundary conditions are not satisfied. Subsequently, a bending solution of the governing differential equation, with no surface loading, is superimposed in order to satisfy the boundary conditions. The practical cases of boundary conditions, which are solved here, include single shells and groups of shells with longitudinal stiffeners in valleys only, and with longitudinal stiffeners in valleys and crown, as well as half barrels supported along their four edges. Simplified design formulae and tables were prepared for use in practice.

Also undertaken in the course of the present study, was an experimental program planned to test shells having different cases of boundary conditions. These experimental investigations, together with a comparison of the theoretical and experimental results, are given in Chapter (IV).

The differential equations, governing the behaviour of grain bins, made of corrugated sheets, are obtained in Chapter (V). Particular and homogeneous solutions are superimposed to satisfy the governing equations, as well as the boundary conditions. Curves were prepared for the determination of the effective width of corrugated sheets, stiffened by vertical ribs, under frictional forces. The study of the effect of the slip at sheet-to-sheet and sheet-to-frame connections is made for both shell roofs and grain bins.

Chapter (VI) deals with the effect of geometry of corrugation on the load capacity of the shell. Other

corrugation configurations are suggested for better performance of the shell.

The observations and conclusions of the present study are given in Chapter (VII).

CHAPTER (II)
MATHEMATICAL FORMULATIONS

In this analysis, the theoretical model represents a shell, made of an elastic orthotropic material in which the mechanical properties are equal to the average properties of the corrugated sheets.

II.1 Mechanical Properties:

For the arc-and-tangent type of corrugation, figure (1), the mechanical properties are^(1,8):

$$D_{\phi} = \left(\frac{\ell}{c}\right) \cdot t \cdot E \quad (1-a)$$

$$D_x = \frac{E \cdot t}{6(1-\mu^2)} \left(\frac{t}{f}\right)^2 \quad (1-b)$$

$$D_{x\phi} = \rho \frac{E \cdot t}{2(1+\mu)} \left(\frac{c}{\ell}\right) \quad (1-c)$$

$$B_{\phi} = 0.522 E \cdot t \cdot f^2 \quad (1-d)$$

$$B_x = \frac{E \cdot t^3}{12(1-\mu^2)} \left(\frac{c}{\ell}\right) \quad (1-e)$$

$$B_{x\phi} = \frac{E \cdot t^3}{12(1+\mu)} \left(\frac{\ell}{c}\right) \quad (1-f)$$

in which: D_x and D_{ϕ} are the axial rigidity in the x- and ϕ -directions respectively; $D_{x\phi}$ = shear rigidity in the x- ϕ

plane; B_x and B_ϕ = bending rigidity in the xz - and ϕz -plane respectively; $B_{x\phi}$ = torsional rigidity; t = average thickness of the sheet; c = corrugation pitch; ℓ = developed length of corrugation per pitch; f = half depth of corrugation; E = modulus of elasticity of steel; μ = Poisson's ratio; and ρ = a reduction factor to account for the effect of slip at sheet-to-sheet and sheet-to-frame connections ⁽¹⁾. These properties were verified experimentally in Reference (8).

II.2. Governing Differential Equations:

The differential equations governing the behaviour of the shell are obtained by using the previously mentioned properties, Equations (1-a, b...f), together with the equilibrium conditions and geometric relationships of an infinitesimal element, $dx \cdot R \cdot d\phi$.

II.2.(a). Conditions of Equilibrium:

Referring to figure (2), the conditions of equilibrium are:

$$\frac{\partial N_x}{\partial x} + \frac{1}{R} \left(\frac{\partial N_{\phi x}}{\partial \phi} \right) + p_x = 0 \quad (2-a)$$

$$\frac{\partial N_\phi}{\partial \phi} + R \left(\frac{\partial N_{x\phi}}{\partial x} \right) - Q_\phi + R p_\phi = 0 \quad (2-b)$$

$$\frac{\partial Q_\phi}{\partial \phi} + R \left(\frac{\partial Q_x}{\partial x} \right) + N_\phi + R p_z = 0 \quad (2-c)$$

$$\frac{\partial M_{\phi}}{\partial \phi} + R \left(\frac{\partial M_{x\phi}}{\partial x} \right) - RQ_{\phi} = 0 \quad (2-d)$$

$$R \left(\frac{\partial M_x}{\partial x} \right) + \frac{\partial M_{\phi x}}{\partial \phi} - RQ_x = 0 \quad (2-e)$$

$$R(N_{x\phi} - N_{\phi x}) + M_{\phi x} = 0 \quad (2-f)$$

where: p_x , p_{ϕ} and p_z are the components of external loading in the x , ϕ and z -directions respectively, R is the radius of curvature.

Eliminating the transverse shears, Q_x and Q_{ϕ} , from equations (2-a,...f), by making use of equations (2-d,e), this system of equilibrium equations can be reduced to the following:

$$N'_x + \frac{N^{\circ}_{\phi x}}{R} + p_x = 0 \quad (3-a)$$

$$RN^{\circ}_{\phi} + R^2 N'^2_{x\phi} - M^{\circ}_{\phi} - RM^{\circ}_{x\phi} + R^2 p_{\phi} = 0 \quad (3-b)$$

$$M^{\circ\circ}_{\phi} + RM^{\circ}_{x\phi} + RM^{\circ}_{\phi x} + R^2 M''^2_x + RN_{\phi} + R^2 p_z = 0 \quad (3-c)$$

$$R(N_{x\phi} - N_{\phi x}) + M_{\phi x} = 0 \quad (3-d)$$

where: $()' = \frac{\partial ()}{\partial x}$; $()^{\circ} = \frac{\partial ()}{\partial \phi}$.

II.2.(b). Geometric Relationships:

The geometric relationships of cylindrical shells are (10):

$$\epsilon_x = \frac{\partial u}{\partial x} + z \frac{\partial^2 w}{\partial x^2} \quad (4-a)$$

$$\epsilon_\phi = \frac{1}{R} \frac{\partial v}{\partial \phi} - \left(\frac{1}{R+z} \right) w + \frac{z}{R} \left(\frac{1}{R+z} \right) \frac{\partial^2 w}{\partial \phi^2} \quad (4-b)$$

$$\gamma_{x\phi} = \left(\frac{R+z}{R} \right) \frac{\partial v}{\partial x} + \left(\frac{1}{R+z} \right) \frac{\partial u}{\partial \phi} + \left(\frac{z}{R} + \frac{z}{R+z} \right) \frac{\partial^2 w}{\partial x \partial \phi} \quad (4-c)$$

II.2.(c) Elastic Relationships:

Making use of the elastic law, together with the previous geometric relationships, Equation (4), the following expressions can be obtained for the stress-resultants of orthotropic shells (10):

$$N_\phi = - \frac{D}{R} \phi (\dot{w} - \dot{v}) - \frac{B}{R^3} \phi (w + \ddot{w}) \quad (5-a)$$

$$N_x = D_x \dot{u} + \frac{B_x}{R} \ddot{w} \quad (5-b)$$

$$N_{\phi x} = \frac{D_{x\phi}}{R} (\dot{u} + R\dot{v}) + \frac{B_{x\phi}}{2R^3} (\dot{u} - R\dot{w}) \quad (5-c)$$

$$N_{x\phi} = \frac{D_{x\phi}}{R} (\dot{u} + R\dot{v}) + \frac{B_{x\phi}}{2R^2} (\dot{v} + \dot{w}) \quad (5-d)$$

$$M_{\phi} = - \frac{B}{R^2} (\dot{w} + \ddot{w}) \quad (5-e)$$

$$M_{x\phi} = - \frac{B_x}{R} (R\dot{w} + \dot{u}) \quad (5-f)$$

$$M_{\phi x} = - \frac{B_{x\phi}}{2R^2} (2R\dot{w} - \dot{u} + R\dot{v}) \quad (5-g)$$

$$M_{x\phi} = - \frac{B_{x\phi}}{2R^2} (2R\dot{w} + 2R\dot{v}) \quad (5-h)$$

Substituting for the stress-resultants from Equation (5) into the equilibrium equations, Equations (3a-c), the following three governing differential equations in u , v and w , are obtained:

$$D_x \ddot{u} + \frac{B_x}{R} \dddot{w} + D_{x\phi} \left(\frac{\ddot{u}}{R^2} + \frac{\dot{v}}{R} \right) + \frac{B_{x\phi}}{2R^3} \left(\frac{\ddot{u}}{R} - \dot{w} \right) + p_x = 0 \quad (6-a)$$

$$D_{\phi} (\dot{v} - \dot{w}) + D_{x\phi} (R\dot{u} + R^2\dot{v}) + \frac{3B_{x\phi}}{2} (\ddot{v} + \ddot{w}) + R^2 p_{\phi} = 0 \quad (6-b)$$

$$D_{\phi} (\dot{v} - \dot{w}) - \frac{B_{\phi}}{R^2} (\dot{w} + 2\ddot{w} + \dot{w}) - (R^2 B_x \ddot{w} + R B_x \dddot{u}) - (2 B_{x\phi} \ddot{w} + \frac{3B_{x\phi}}{2} \dot{v} - \frac{B_{x\phi}}{2R} \dot{u}) + R^2 p_z = 0 \quad (6-c)$$

The fourth condition of equilibrium, Equation (3-d), is self-satisfied.

II.3. Simplifications:

The system of equations, Equations (6-a,b,c), is derived with minor approximations, (lateral strain and non-linear terms of the strain expressions are neglected). It encounters a number of terms which have insignificant effects on the results of the corrugated sheet shells. These terms may be neglected, and this system of equations can be simplified if the following assumptions are made in the derivation:

The structural action of a cylindrical shell can be approximated by combining the structural actions of a flat membrane corresponding to the developed shell loaded in its own plane; of a plate, formed by the developed shell loaded at right angles to its plane; and of the shell regarded as a flexible membrane.

Thus, Equations (2), (4) and (5), can be reduced to a simpler form, based on the following arguments which were first proposed by Donnell⁽⁶⁾ for isotropic shells. Firstly, in connection with the equations of equilibrium, it can be argued that the transverse shearing force, Q_ϕ , appearing in equation (2-b), (which represents the condition $\Sigma \phi = 0$), may be dropped, as it does not occur in the corresponding equations of equilibrium of the flat membrane or the membrane shell. Therefore, the equilibrium equations, Equations (3-a, b, c), reduce to:

$$N_x' + \frac{N_{\phi x}}{R} + p_x = 0 \quad (7-a)$$

$$N_{\phi}' + RN_{x\phi}' + Rp_{\phi} = 0 \quad (7-b)$$

$$M_{\phi}'' + RM_{x\phi}'' + RM_{\phi x}'' + R^2 M_x'' + RN_{\phi}' + R^2 p_z = 0 \quad (7-c)$$

Secondly, in connection with the strain expressions, the effect of changes of curvature on the strains is assumed to be negligible, therefore, Equations (4-a,b,c) are simplified to:

$$\epsilon_x = \frac{\partial u}{\partial x} \quad (8-a)$$

$$\epsilon_{\phi} = \frac{1}{R} \left(\frac{\partial v}{\partial \phi} - w \right) \quad (8-b)$$

$$\gamma_{x\phi} = \frac{\partial v}{\partial x} + \frac{1}{R} \left(\frac{\partial u}{\partial \phi} \right) \quad (8-c)$$

Thirdly, the changes of curvature and twist, are considered to be insignificantly affected by the "stretching" displacements, u and v . Thus, these expressions are reduced to:

$$\chi_x = - \frac{\partial^2 w}{\partial x^2}$$

$$\chi_{\phi} = - \frac{\partial^2 w}{R^2 \partial \phi^2}$$

$$\chi_{x\phi} = - \frac{\partial^2 w}{R \partial x \partial \phi}$$

Utilizing Equations (8-a,b,c) together with the elastic law, the stress-resultants N_x , N_ϕ , $N_{x\phi}$ and $N_{\phi x}$ are reduced to:

$$N_x = D_x u \quad (9-a)$$

$$N_\phi = -\frac{D_\phi}{R} (w - \dot{v}) \quad (9-b)$$

$$N_{x\phi} = N_{\phi x} = \frac{D_{x\phi}}{R} (\dot{u} + R\dot{v}) \quad (9-c)$$

and the moments are:

$$M_x = -B_x \frac{\partial^2 w}{\partial x^2} \quad (9-d)$$

$$M_\phi = -\frac{B_\phi}{R^2} \frac{\partial^2 w}{\partial \phi^2} \quad (9-e)$$

$$M_{x\phi} = M_{\phi x} = -\frac{B_{x\phi}}{R} \frac{\partial^2 w}{\partial x \partial \phi} \quad (9-f)$$

Substituting Equations (9-a,...f) into Equations (7-a,b,c), the following simplified system of governing differential equations, is obtained:

$$D_x \ddot{u} + D_{x\phi} \left(\frac{\ddot{u}}{R^2} + \frac{\dot{v}}{R} \right) + p_x = 0 \quad (10-a)$$

$$D_\phi (\ddot{v} - \dot{w}) + D_{x\phi} (R\dot{u} + R^2\ddot{v}) + R^2 p_\phi = 0 \quad (10-b)$$

$$D_\phi (\dot{v} - w) - (R^2 B_x \overset{''''}{w} + 2B_{x\phi} \overset{''''}{w} + \frac{B_\phi}{R^2} \overset{''''}{w}) + R^2 p_z = 0 \quad (10-c)$$

The solution presented in the following chapters are based on the simplified system of equations, Equations (10-a,b,c). The validity of this system of equations and the degree of accuracy obtained from them are discussed in Chapter (III).

CHAPTER (III)
 APPLICATIONS OF CYLINDRICAL SHELLS
 MADE OF CORRUGATED SHEETS IN ROOFING

III.1. Introduction:

This chapter suggests some economical applications of the cylindrical corrugated sheets used in shell roofs. The practical cases of boundary conditions are discussed and the solutions are given.

Referring to Figure (3), the chosen coordinate system is shown. The origin, 0, is designated at the mid-span of the left edge of the shell. The span of the shell is "L" and half the central angle is " ϕ_e ".

III.2. Boundary Conditions:

The shell roof is supported by two end trusses as shown in Figure (4). Thus, at these ends, the shell undergoes no deflection and is considered to be free from moments. The following boundary conditions are to be satisfied at $x = \pm \frac{L}{2}$.

$$w = 0 \quad \text{(I-a)}$$

$$M_x = 0 \quad \text{(I-b)}$$

$$N_x = 0 \quad \text{(I-c)}$$

$$N_\phi = 0 \quad \text{(I-d)}$$

The boundary conditions along the straight edges differ according to the type of shell as shown in Figures (4-a,c...e). Their boundary conditions are as follows:

CASE (I): Single shell with longitudinal stiffeners in valleys only.

Referring to Figure (4-a), the boundary conditions are as follows:

At $\phi = 0$; and $\phi = 2\phi_e$:

$$M_\phi = 0 \quad (\text{I-i})$$

$$Q_\phi = 0 \quad (\text{I-ii})$$

$$N_\phi = 0 \quad (\text{I-iii})$$

$$u_{\text{shell}} = u_{\text{stiffener}} \quad (\text{I-iv})$$

The first condition means that the torsional resistance of the edge stiffener is neglected. The second and third mean that the bending rigidity of the edge stiffener is also neglected. The fourth condition indicates that the longitudinal displacement, u , at the edge of the shell equals the longitudinal displacement of the edge stiffener.

CASE (II): Single shell with longitudinal stiffeners in valleys and crown.

In this case, Figure (4-b), the following boundary conditions are to be satisfied:

At $\phi = 0$;

$$M_\phi = 0 \quad (\text{II-i})$$

$$Q_\phi = 0 \quad (\text{II-ii})$$

$$N_\phi = 0 \quad (\text{II-iii})$$

$$u_{\text{shell}} = u_{\text{stiffener}} \quad (\text{II-iv})$$

At $\phi = \phi_e$ (i.e. along the crown);

$$Q_\phi = 0 \quad (\text{II-v})$$

$$\theta = 0 \quad (\text{II-vi})$$

$$v = 0 \quad (\text{II-vii})$$

$$u_{\text{shell}} = u_{\text{stiffener}} \quad (\text{II-viii})$$

Equations (II-v,vi,vii) are clear from symmetry.

The 8th equation, Equation (II-viii), is as explained before.

For an antisymmetrical loading, the boundary conditions at $\phi = \phi_e$ becomes:

$$M_\phi = 0 \quad (\text{II-}\bar{\text{v}})$$

$$w = 0 \quad (\text{II-}\bar{\text{vi}})$$

$$N_\phi = 0 \quad (\text{II-}\bar{\text{vii}})$$

$$u_{\text{shell}} = u_{\text{stiffener}} \quad (\text{II-}\bar{\text{viii}})$$

CASE (III): Half barrel supported along the four edges.

In this case, Figure (4-c), the following boundary conditions are to be satisfied:

At $\phi = 0$ and $\phi = 2\phi_e$;

$$w = 0 \quad (\text{III-i})$$

$$M_\phi = 0 \quad (\text{III-ii})$$

$$v = 0 \quad (\text{III-iii})$$

$$u_{\text{shell}} = u_{\text{stiffener}} \quad (\text{III-iv})$$

which means that there is a hinge-like support along the straight edges of the shell.

CASE (IV): Inner shell of a multiple group of shells with longitudinal stiffeners in valleys only.

A design approximation is usually made in the treatment of an interior shell of a multiple group by treating it as a symmetrical problem.

Referring to Figure (4-d), the boundary conditions to be satisfied in this case are:

At $\phi = 0; \phi = 2\phi_e$:

$$w \sin\phi_e + v \cos\phi_e = 0 \quad (\text{IV-i})$$

$$\theta = 0 \quad (\text{IV-ii})$$

$$N_\phi \sin\phi_e - Q_\phi \cos\phi_e = 0 \quad (\text{IV-iii})$$

$$u_{\text{shell}} = u_{\text{stiffener}} \quad (\text{IV-iv})$$

Equation (IV-i) indicates that the horizontal components of the displacements, w and v , are zero. This can easily be seen from symmetry. Equations (IV-ii) states that the rotation of the tangent should be zero, due to symmetry. The physical meaning of Equation (IV-iii) is that the vertical components of the internal forces N_ϕ and Q_ϕ , at the edge of the shell, are set equal to zero. This means that the bending rigidity of the edge stiffener is neglected. Equation (IV-iv) is identical with the corresponding formula of CASE (I).

CASE (V): Inner shell of a multiple group of shells with longitudinal stiffeners in valleys and crown.

Referring to Figure (4-e), the eight boundary conditions to be fulfilled here are as follows:

At $\phi = 0;$

$$w \sin\phi_e + v \cos\phi_e = 0 \quad (\text{V-i})$$

$$\theta = 0 \quad (V-ii)$$

$$N_{\phi} \sin \phi_e - Q_{\phi} \cos \phi_e = 0 \quad (V-iii)$$

$$u_{\text{shell}} = u_{\text{stiffener}} \quad (V-iv)$$

These equations are similar to those given in CASE (IV).

$$\text{At } \phi = \phi_e;$$

$$Q_{\phi} = 0 \quad (V-v)$$

$$\theta = 0 \quad (V-vi)$$

$$v = 0 \quad (V-vii)$$

$$u_{\text{shell}} = u_{\text{stiffener}} \quad (V-viii)$$

These equations are the same as those discussed in the second case of boundary conditions.

III.3. Method of Solution

The solution is carried out in three steps:

- (a) A membrane solution with the surface loads acting on the shell.
- (b) A bending solution of the unloaded shell.
- (c) Superposition of the results of (a) and (b) to satisfy the boundary conditions that exist along the straight edges of the shell.

III.3. (a) Membrane Solution:

In the membrane solution, the shell is idealized as a membrane incapable of resisting bending stresses. This membrane solution is valid for all types of shells. Thus, omitting the terms due to bending in the Equilibrium Equations (3-a,b,c), the following system of equations is

obtained:

$$N'_x + \frac{N_{x\phi}}{R} + p_x = 0 \quad (11-a)$$

$$RN'_\phi + R^2 N'_{x\phi} + R^2 p_\phi = 0 \quad (11-b)$$

$$RN_\phi + R^2 p_z = 0 \quad (11-c)$$

(i) Membrane Solution Under Own Weight:

The own weight, g , can be expressed in a Fourier series as follows:

$$g = \frac{4g}{\pi} \left\{ \cos \frac{\pi x}{L} - \frac{1}{3} \cos \frac{3\pi x}{L} + \frac{1}{5} \cos \frac{5\pi x}{L} \dots \right\}$$

Whenever the load is uniform in the x -direction, it is usually adequate to consider the first term of this series. The components of the own weight in the x - ϕ and z -directions can be written as follows:

$$g_x = 0 \quad (12-a)$$

$$g_\phi = -\frac{4g}{\pi} \sin(\phi_e - \phi) \cos \frac{\pi x}{L} \quad (12-b)$$

$$g_z = \frac{4g}{\pi} \cos(\phi_e - \phi) \cos \frac{\pi x}{L} \quad (12-c)$$

Using the equilibrium equations (11-a,b,c), and substituting for the loading (Equations 12-a,b,c), the membrane solution for the stress-resultants N_x , N_ϕ and $N_{x\phi}$ are obtained.

$$N_{\phi} = -\frac{4gR}{\pi} \cos(\phi_e - \phi) \cos kx \quad (13-a)$$

$$N_x = -\frac{8gL^2}{R\pi^3} \cos(\phi_e - \phi) \cos kx \quad (13-b)$$

$$N_{x\phi} = \frac{8gL}{\pi^2} \sin(\phi_e - \phi) \sin kx \quad (13-c)$$

The three displacement components are obtained from equations (9-a,b,c) as follows:

$$u = \frac{-8g}{Rk^3 \pi D_x} \cos(\phi_e - \phi) \sin kx \quad (13-d)$$

$$v = -\frac{8g}{\pi} \left[\frac{1}{k^3 D_{x\phi}} + \frac{1}{R^2 k^4 D_x} \right] \sin(\phi_e - \phi) \cos kx \quad (13-e)$$

$$w = \frac{8g}{\pi} \left[\frac{1}{k^3 D_{x\phi}} + \frac{1}{R^2 k^4 D_x} \right] \cos(\phi_e - \phi) \cos kx \quad (13-f)$$

in which $k = \frac{\pi}{L}$.

(ii) Membrane Solution Under Snow Load "p".

The snow load can be expressed in a Fourier series as follows:

$$p = \frac{4p \cos(\phi_e - \phi)}{\pi} \left\{ \cos \frac{\pi x}{L} - \frac{1}{3} \cos \frac{3\pi x}{L} + \frac{1}{5} \cos \frac{5\pi x}{L} \dots \right\}$$

As in the case of the own weight, g , the load is uniform in the x -direction and the first term in the series is

usually sufficient. Then the three load components are:

$$p_x = 0 \quad (14-a)$$

$$p_\phi = -\frac{4p}{\pi} \cos(\phi_e - \phi) \sin(\phi_e - \phi) \cos \frac{\pi x}{L} \quad (14-b)$$

$$p_z = \frac{4p}{\pi} \cos^2(\phi_e - \phi) \cos \frac{\pi x}{L} \quad (14-c)$$

Substituting equations (14-a,b,c) into the equilibrium equations (11-a,b,c), the membrane solution for the stress-resultants are obtained. Utilizing Equations (9-a,b,c), the three displacement components are also obtained as follows:

$$N_\phi = -\frac{4pL}{\pi} \cos^2(\phi_e - \phi) \cos kx \quad (15-a)$$

$$N_x = -\frac{12p}{R\pi k^2} \cos 2(\phi_e - \phi) \cos kx \quad (15-b)$$

$$N_{x\phi} = \frac{6pL}{\pi^2} \sin 2(\phi_e - \phi) \sin kx \quad (15-c)$$

$$u = \frac{-12p}{Rk^3 \pi D_x} \cos 2(\phi_e - \phi) \sin kx \quad (15-d)$$

$$v = \frac{-6p}{\pi} \left[\frac{1}{k^2 D_{x\phi}} + \frac{4}{R^2 k^4 D_x} \right] \sin 2(\phi_e - \phi) \cos kx \quad (15-e)$$

$$w = \frac{12p}{\pi} \left[\frac{1}{D_{x\phi} k^2} + \frac{4}{R^2 k^4 D_x} \right] \cos 2(\phi_e - \phi) \cos kx \quad (15-f)$$

(iii) Membrane Solution Under Wind Loading:

Many factors affect wind load on shell roofs. The load may take any non-symmetrical shape, depending upon the geometrical dimensions of the shell, and the direction of the wind. The effects of non-symmetrical loading may be divided into two cases; (1) symmetrical and, (2) antisymmetrical. It is possible to obtain the solution under any case of loading, using the principle of superposition. The following two cases can be used for the determination of the membrane solution under wind loading:

(iii)-a. Symmetrical Case of Wind Suction:

The load is expressed in a Fourier series as previously stated and the three components p_x^* , p_ϕ^* and p_z^* are given by:

$$p_x^* = 0 \quad (16-a)$$

$$p_\phi^* = 0 \quad (16-b)$$

$$p_z^* = \frac{-4p^*}{\pi} \cos(\phi_e - \phi) \cos kx \quad (16-c)$$

The following membrane solutions for the stress-resultants are obtained using the equilibrium equations (11-a,b,c).

$$N_{\phi} = \frac{4p^* R}{\pi} \cos (\phi_e - \phi) \cos kx \quad (17-a)$$

$$N_x = \frac{4p^*}{\pi k^2 R} \cos (\phi_e - \phi) \cos kx \quad (17-b)$$

$$N_{x\phi} = \frac{-4p^*}{\pi k} \sin (\phi_e - \phi) \sin kx \quad (17-c)$$

The three displacement components are obtained from Equations (9-a,b,c).

$$u = \frac{4p^*}{\pi D_x k^3 R} \cos (\phi_e - \phi) \sin kx \quad (17-d)$$

$$v = \frac{4p^*}{\pi} \left[\frac{1}{D_{x\phi} k^2} + \frac{1}{D_x k^4 R^2} \right] \sin (\phi_e - \phi) \cos kx \quad (17-e)$$

$$w = \frac{-4p^*}{\pi} \left[\frac{1}{D_{x\phi} k^2} + \frac{1}{D_x k^4 R^2} \right] \cos (\phi_e - \phi) \cos kx \quad (17-f)$$

(iii)-b. Antisymmetrical Case of Loading:

The three load components are:

$$p_x^* = 0 \quad (16-d)$$

$$p_{\phi}^* = 0 \quad (16-e)$$

$$p_z^* = \frac{4p^*}{\pi} \sin \frac{\pi\phi}{\phi_e} \cos kx \quad (16-f)$$

The membrane solution is obtained by substituting Equations (16-d,e,f) into the equilibrium Equations (11-a,b,c) as follows:

$$N_{\phi} = \frac{-4p^*R}{\pi} \sin \frac{\pi\phi}{\phi_e} \cos kx \quad (17-g)$$

$$N_x = \frac{-4p^*L^2}{R\pi\phi_e^2} \sin \frac{\pi\phi}{\phi_e} \cos kx \quad (17-h)$$

$$N_{x\phi} = \frac{4p^*L}{\pi\phi_e} \cos \frac{\pi\phi}{\phi_e} \sin kx \quad (17-i)$$

The three displacement components are obtained using equations (9-a,b,c) as follows:

$$u = \frac{-4p^*L^3}{\pi^2\phi_e^2RD_x} \sin \frac{\pi\phi}{\phi_e} \sin kx \quad (17-j)$$

$$v = \frac{-4p^*L^2}{\pi^2\phi_e} \left[\frac{1}{D_{x\phi}} + \frac{L^2}{\phi_e^2R^2D_x} \right] \cos \frac{\pi\phi}{\phi_e} \cos kx \quad (17-k)$$

$$w = \frac{4p^*L^2}{\pi\phi_e^2} \left[\frac{1}{D_{x\phi}} + \frac{L^2}{\phi_e^2R^2D_x} \right] \sin \frac{\pi\phi}{\phi_e} \cos kx \quad (17-l)$$

If isotropic properties are considered, these equations yield the well known membrane solution for isotropic shells.

III.3.(b) Bending Solution:

Since the load is considered in the membrane solution, then p_x , p_{ϕ} and p_z are replaced by zero in Equations (10-a,b,c). The bending solution is governed by the following system of homogeneous differential equations:

$$D_x \ddot{u} + D_{x\phi} \left(\frac{\ddot{u}}{R^2} + \frac{\ddot{v}}{R} \right) = 0 \quad (18-a)$$

$$D_\phi (\ddot{v} - \dot{w}) + D_{x\phi} (R\ddot{u} + R^2\ddot{v}) = 0 \quad (18-b)$$

$$D_\phi (\dot{v} - w) - (R^2 B_x \ddot{w} + 2B_{x\phi} \ddot{w} + \frac{B_\phi}{R^2} \ddot{w}) = 0 \quad (18-c)$$

Eliminating u and v from Equations (18-a,b,c), it is possible to obtain one governing differential equation in the radial displacement, w , as follows:

Differentiating Equation (18-b) twice with respect to x :

$$D_\phi (\ddot{v} - \dot{w}) + D_{x\phi} (R\ddot{u} + R^2\ddot{v}) = 0 \quad (19-a)$$

Applying the operator $R \left(\frac{\partial^2}{\partial x \partial \phi} \right)$ to Equation (18-a):

$$R D_x \ddot{u} + D_{x\phi} \left(\frac{1}{R} \ddot{u} + \ddot{v} \right) = 0 \quad (19-b)$$

Differentiating Equation (18-b) twice with respect to ϕ :

$$D_\phi (\ddot{v} - \dot{w}) + D_{x\phi} (R\ddot{u} + R^2\ddot{v}) = 0 \quad (19-c)$$

From Equations (19-b) and (19-c), it can be shown that:

$$R^3 D_x \ddot{u} = D_\phi (\ddot{v} - \dot{w})$$

$$\text{or } R \ddot{u} = \frac{D_\phi}{R^2 D_x} (\ddot{v} - \dot{w}) \quad (20-a)$$

Substituting Equation (20-a) into Equation (19-a):

$$D_{\phi} (\overset{\dots}{v} - \overset{\dots}{w}) + D_{x\phi} \left(\frac{D_{\phi}}{D_x R^2} (\overset{\dots}{v} - \overset{\dots}{w}) + R^2 \overset{\dots}{v} \right) = 0 \quad (20-b)$$

Differentiating Equation (18-c) twice with respect to x and once with respect to ϕ :

$$D_{\phi} (\overset{\dots}{v} - \overset{\dots}{w}) = (R^2 B_x \overset{\dots}{w} + 2B_{x\phi} \overset{\dots}{w} + \frac{B_{\phi}}{R^2} \overset{\dots}{w}) \quad (20-c)$$

Substituting Equation (20-c) into Equation (20-b)

then:

$$R^2 B_x \overset{\dots}{w} + 2B_{x\phi} \overset{\dots}{w} + \frac{B_{\phi}}{R^2} \overset{\dots}{w} + D_{x\phi} \left[\frac{D_{\phi}}{D_x R^2} (\overset{\dots}{v} - \overset{\dots}{w}) + R^2 \overset{\dots}{v} \right] = 0 \quad (20-d)$$

Applying the operation $\frac{1}{D_x R^2} \left(\frac{\partial^3}{\partial \phi^3} \right)$ to Equation (18-c) yields:

$$\frac{D_{\phi}}{D_x R^2} (\overset{\dots}{v} - \overset{\dots}{w}) = \frac{B_x}{D_x} \overset{\dots}{w} + \frac{2B_{x\phi}}{D_x R^2} \overset{\dots}{w} + \frac{B_{\phi}}{D_x R^4} \overset{\dots}{w} \quad (20-e)$$

Substituting Equation (20-e) into Equation (20-d):

$$R^2 B_x \overset{\dots}{w} + 2B_{x\phi} \overset{\dots}{w} + \frac{B_{\phi}}{R^2} \overset{\dots}{w} + D_{x\phi} \left[\frac{B_x}{D_x} \overset{\dots}{w} + \frac{2B_{x\phi}}{D_x R^2} \overset{\dots}{w} + \frac{B_{\phi}}{D_x R^4} \overset{\dots}{w} + R^2 \overset{\dots}{v} \right] = 0 \quad (20-f)$$

Differentiating Equation (20-f) with respect to ϕ gives:

$$\begin{aligned}
 \overset{\dots}{V} = & - \left[\frac{B_x \overset{\dots}{\dots}}{D_{x\phi}} w + \frac{2B_{x\phi} \overset{\dots}{\dots}}{R^2 D_{x\phi}} w + \frac{B_\phi \overset{\dots}{\dots}}{R^4 D_{x\phi}} w + \frac{B_x \overset{\dots}{\dots}}{R^2 D_x} w \right. \\
 & \left. + \frac{2B_{x\phi} \overset{\dots}{\dots}}{R^4 D_x} w + \frac{B_\phi \overset{\dots}{\dots}}{R^6 D_x} w \right] \quad (20-g)
 \end{aligned}$$

Differentiating Equation (18-c) four times with respect to x , then:

$$\overset{\dots}{V} = \overset{\dots}{W} + \frac{R^2 B_x \overset{\dots}{\dots}}{D_\phi} w + \frac{2B_{x\phi} \overset{\dots}{\dots}}{D_\phi} w + \frac{B_\phi \overset{\dots}{\dots}}{R^2 D_\phi} w \quad (20-h)$$

Equating Equations (20-g) and (20-h):

$$\begin{aligned}
 & \frac{R^2 B_x \overset{\dots}{\dots}}{D_\phi} w + \frac{2B_{x\phi} \overset{\dots}{\dots}}{D_\phi} w + \frac{B_\phi \overset{\dots}{\dots}}{R^2 D_\phi} w + w + \frac{B_x \overset{\dots}{\dots}}{D_{x\phi}} w \\
 & + \frac{2B_{x\phi} \overset{\dots}{\dots}}{R^2 D_{x\phi}} w + \frac{B_\phi \overset{\dots}{\dots}}{R^4 D_{x\phi}} w + \frac{B_x \overset{\dots}{\dots}}{R^2 D_x} w + \frac{2B_{x\phi} \overset{\dots}{\dots}}{R^4 D_x} w \\
 & + \frac{B_\phi \overset{\dots}{\dots}}{R^6 D_x} w = 0 \quad (20-i)
 \end{aligned}$$

Multiplying both sides of Equation (20-i) by $R^6 \begin{bmatrix} D_x \\ B_\phi \end{bmatrix}$, then:

$$\begin{aligned}
& \overset{\dots}{w} + \left[\frac{D_x}{D_{x\phi}} + \frac{2B_{x\phi}}{B_\phi} \right] R^2 \overset{\dots}{w} + \left[\frac{D_x}{D_\phi} + \frac{2B_{x\phi} D_x}{B_\phi D_{x\phi}} + \frac{B_x}{B_\phi} \right] R^4 \overset{\dots}{w} \\
& + \left[\frac{2B_{x\phi} D_x}{B_\phi D_\phi} + \frac{B_x D_x}{B_\phi D_{x\phi}} \right] R^6 \overset{\dots}{w} + \left[\frac{D_x B_x}{D_\phi B_\phi} \right] R^8 \overset{\dots}{w} \\
& + \left[\frac{D_x R^6}{B_\phi} \right] \overset{\dots}{w} = 0 \tag{21}
\end{aligned}$$

Equation (21) is the eight-order partial differential equation governing the bending behaviour of cylindrical orthotropic shells. If isotropic properties are considered for the shell, Equation (21) yields the well known Donnell's equation.

Taking into account the chosen coordinate system, the bending solution can be assumed as follows:

$$w = H e^{m\phi} \cos \frac{\lambda x}{R}, \quad \lambda = \frac{\pi R}{L} \tag{22}$$

With this Levy-type solution, the boundary conditions (I-a,b,c,d), are automatically satisfied since the resulting bending solution for w , N_x , M_x and N_ϕ , given in Appendix (II), are equal to zero when $x = \pm \frac{L}{2}$.

Substituting Equation (22) into Equation (21), the following characteristic equation is obtained:

$$\begin{aligned}
& m^8 + m^6 \left\{ -\lambda^2 \left[\frac{D_x}{D_{x\phi}} + \frac{2B_{x\phi}}{B_\phi} \right] \right\} + m^4 \left\{ \lambda^4 \left[\frac{D_x}{D_\phi} \right. \right. \\
& \left. \left. + \frac{2B_{x\phi} D_x}{B_\phi D_{x\phi}} + \frac{B_x}{B_\phi} \right] \right\} + m^2 \left\{ -\lambda^6 \left[\frac{2B_{x\phi} D_x}{B_\phi D_\phi} \right. \right. \\
& \left. \left. + \frac{B_x D_x}{B_\phi D_{x\phi}} \right] \right\} + \left\{ \lambda^8 \left[\frac{D_x B_x}{D_\phi B_\phi} \right] + \lambda^4 \left[\frac{D_x R^2}{B_\phi} \right] \right\} = 0
\end{aligned}
\tag{23}$$

This characteristic equation is approximate because it is obtained from the simplified governing differential Equation (21).

To discuss the accuracy of Equation (23), a comparison is made between its roots and those of the exact characteristic equation. This exact characteristic equation is obtained by using the exact governing differential Equations (6-a,b,c), together with the following assumed displacement components

$$w = A^* e^{m\phi} \cos \frac{\lambda x}{R} \tag{24-a}$$

$$u = B^* e^{m\phi} \sin \frac{\lambda x}{R} \tag{24-b}$$

$$v = C^* e^{m\phi} \cos \frac{\lambda x}{R} \tag{24-c}$$

Equations (24-a,b,c) are substituted in the governing differential Equations (6-a,b,c) after replacing

p_x , p_ϕ and p_z by zero. The resulting homogeneous system of equations can be written in a matrix form as follows:

$$\begin{bmatrix} (-D_x \lambda^2 + D_{x\phi} m^2 + K_{x\phi} m^2) & (-D_{x\phi} m \lambda) & (-K_x \lambda^3 - K_{x\phi} m^2) \\ (D_{x\phi} m \lambda) & (D_\phi m^2 - D_{x\phi} \lambda^2 - 3K_{x\phi} \lambda^2) & (D_\phi m + 3K_{x\phi} m \lambda^2) \\ (K_x \lambda^3 + K_{x\phi} m^2 \lambda) & (D_\phi m + 2K_{x\phi} m \lambda^2 + K_{x\phi} m \lambda^2) & (D_\phi + K_\phi m^4 + 2K_\phi m^2 \\ & & + K_\phi + K_x \lambda^4 \\ & & - 4K_{x\phi} m^2 \lambda^2) \end{bmatrix} \times \begin{bmatrix} A^* \\ B^* \\ C^* \end{bmatrix} = 0$$

where: $K_x = \frac{B_x}{R^2}$, $K_\phi = \frac{B_\phi}{R^2}$ and $K_{x\phi} = \frac{B_{x\phi}}{2R^2}$.

A non-trivial solution of this system of equations can be obtained only if the determinant of the left hand side matrix is equal to zero. This condition leads to the exact characteristic equation. The derivation of this equation is given in Appendix (I); its final form is as follows:

$$\begin{aligned} & m^8 + m^6 \left[2 - \lambda^2 \left(\frac{D_x}{D_{x\phi}} + \frac{2B_{x\phi}}{B_\phi} \right) + \frac{B_x}{B_\phi} \right] + m^4 \left[\lambda^4 \left(\frac{D_x}{D_\phi} + \frac{2D_x B_{x\phi}}{D_{x\phi} B_\phi} \right) \right. \\ & \left. - \lambda^2 \left(\frac{2D_x}{D_{x\phi}} + \frac{4B_{x\phi}}{B_\phi} \right) + 1 \right] + m^2 \left[-\lambda^6 \left(\frac{D_x B_x}{D_{x\phi} B_\phi} \right) \right. \\ & \left. + \frac{2D_x B_{x\phi}}{D_\phi B_\phi} + \lambda^4 \left(\frac{2D_x}{D_\phi} - \frac{2B_x}{B_\phi} + \frac{3D_x B_{x\phi}}{D_{x\phi} B_\phi} \right) - \lambda^2 \left(\frac{2B_{x\phi}}{B_\phi} + \frac{D_x}{D_{x\phi}} \right) \right] \\ & \left. + \left[\lambda^8 \left(\frac{D_x B_x}{D_\phi B_\phi} \right) + \lambda^4 \left(\frac{D_x R^2}{B_\phi} + \frac{3D_x B_{x\phi}}{2D_{x\phi} B_\phi} + \frac{D_x}{D_\phi} \right) \right] = 0 \quad (25) \end{aligned}$$

If isotropic properties are considered for the shell, Equation (25) yields the well known Flugge (Dischinger) characteristic equation, which is used as a yardstick for the comparison of theories of isotropic shells⁽¹³⁾.

The roots of either Equation (23) or Equation (25) can be written as follows:

$$m = \pm \alpha_1 \pm i\beta_1, \quad m = \pm \alpha_2 \pm i\beta_2 \quad (26)$$

and the displacement "w" as:

$$w = \left\{ e^{\alpha_1 \phi} (A \cos \beta_1 \phi + B \sin \beta_1 \phi) + e^{-\alpha_1 \phi} (C \cos \beta_1 \phi + D \sin \beta_1 \phi) + e^{\alpha_2 \phi} (E \cos \beta_2 \phi + F \sin \beta_2 \phi) + e^{-\alpha_2 \phi} (G \cos \beta_2 \phi + H \sin \beta_2 \phi) \right\} \cos \frac{\lambda x}{R} \quad (27)$$

where: (A,B,...H) are arbitrary real constants to be calculated by satisfying the boundary conditions.

The values of the set of roots of Equation (26) are considered to be exact, when calculated from Equation (25), and approximate when calculated from the simplified Equation (23). The deviation between these sets of roots increases with the increase of the ratio $\frac{L}{R}$. This can be seen from Table (III.1), which shows the values of the roots for different ratios $\frac{L}{R}$, using the two characteristic Equations (23) and (25).

TABLE (III.1):

Values of Roots of Characteristic Equations (23 & 25)
for Different Ratios of (L/R).

L/R	Characteristic Equation No.	α_1	β_1	α_2	β_2
1.5	25	3.164364	1.363599	1.310111	3.293497
	23	3.230135	1.336994	1.338256	3.227086
2.0	25	2.721240	1.188397	1.125996	2.871890
	23	2.797089	1.157908	1.158728	2.795109
2.5	25	2.416942	1.069511	0.9994159	2.586171
	23	2.501633	1.035696	1.036284	2.500215
3.0	25	2.190921	0.9822185	0.9052359	2.376776
	23	2.283567	0.9454834	0.9459297	2.282490
3.5	25	2.014175	0.9147102	0.8314314	2.215229
	23	2.114107	0.8753661	0.8757205	2.113251
4.0	25	1.870837	0.8605449	0.7714272	2.085988
	23	1.977519	0.8188437	0.8191339	1.976819
4.5	25	1.751393	0.815705	0.7212826	1.979750
	23	1.864387	0.7720242	0.7722672	1.863801
5.0	25	1.649747	0.7782271	0.6784737	1.890576
	23	1.768686	0.7324146	0.7326222	1.768184
5.5	25	1.561788	0.7459581	0.6412982	1.814461
	23	1.686355	0.6983370	0.6985170	1.685921
6.0	25	1.484623	0.7179042	0.6085605	1.748604
	23	1.614545	0.6686123	0.6687703	1.614164

Figure (5) shows the maximum percentage of error versus (L/R) . It also shows a corresponding curve for the simplified equation of concrete shells (Donnell's equation). The simplified Donnell's equation is generally accepted for concrete shells when $L/R \leq 1.6$ ⁽²¹⁾. Figure (5) shows that it is permissible to use Equation (23) in corrugated sheet shells for higher ratio of (L/R) provided that the same degree of approximation is not exceeded.

Stress-resultants and Displacement Components
due to Bending:

For the longitudinal, transversal and torsional moments, the following relations apply (equations 9 - d, e, f):

$$M_x = -B_x w'' \quad (28-a)$$

$$M_\phi = -\frac{B_\phi}{R^2} w'' \quad (28-b)$$

$$M_{x\phi} = -\frac{B_{x\phi}}{R} w'' \quad (28-c)$$

Using Equations (27) and (28-a,b,c), the explicit expressions for the bending moments are obtained in terms of the 8-unknown constants A,B,...H. Utilizing the equilibrium Equations (7-a,b,c), (after replacing p_x , p_ϕ and p_z by zero), with Equation (27), the explicit expressions for the stress-resultants are obtained.

The displacements, u and v , are determined by using Equation (27) together with Equation (29):

$$u = \frac{N_x}{D_x} \quad , \quad v = \frac{N_{x\phi}}{D_x} - \frac{\dot{u}}{R} \quad (29-a,b)$$

Also the rotation of the tangent, θ , is obtained from the following equation (10):

$$\theta = \frac{1}{R} (v + \dot{w}) \quad (30)$$

All of these displacements and stress-resultants are expressed in terms of the unknown constants A, B,...H. These equations are given in Appendix (II) because they are too lengthy to present here.

III.4. Theoretical Results:

The membrane and bending solution are superimposed and the integration constants A, B,...H, are calculated for each type of shell satisfying the boundary conditions discussed earlier in this chapter. A computer program for all of the theoretical work has been developed for every case of boundary conditions for the IBM system 360/50 at the University of Windsor. This program is prepared for the computer library* and can be used to solve orthotropic shell roofs, stiffened at the valleys only, as well as shells stiffened at the valleys and crown.

A sample of simplified design tables and formulae are given in Appendix (III) for practical use for various types of shell roofs with arc-and-tangent type of corrugations. A snow load was selected in the preparation of these tables.

*Civil Engineering Program Library
Department of Civil Engineering, McMaster University,
Hamilton, Ontario.

The analysis of a simply supported cylindrical shell by the use of tables is illustrated in an example at the end of Appendix (III).

Tables (A,B & C), are prepared to give the maximum intensity of snow load for each type of shells, provided that the maximum displacement "w" does not exceed 1/100 of the span.

Figures (8-a,b) show the comparison between single shell and inner symmetrical shell of a multiple group. From these curves it can be observed that any inner shell will have values of stress-resultants in between the two solved cases. It also justifies the assumption previously stated for case (IV) of boundary condition.

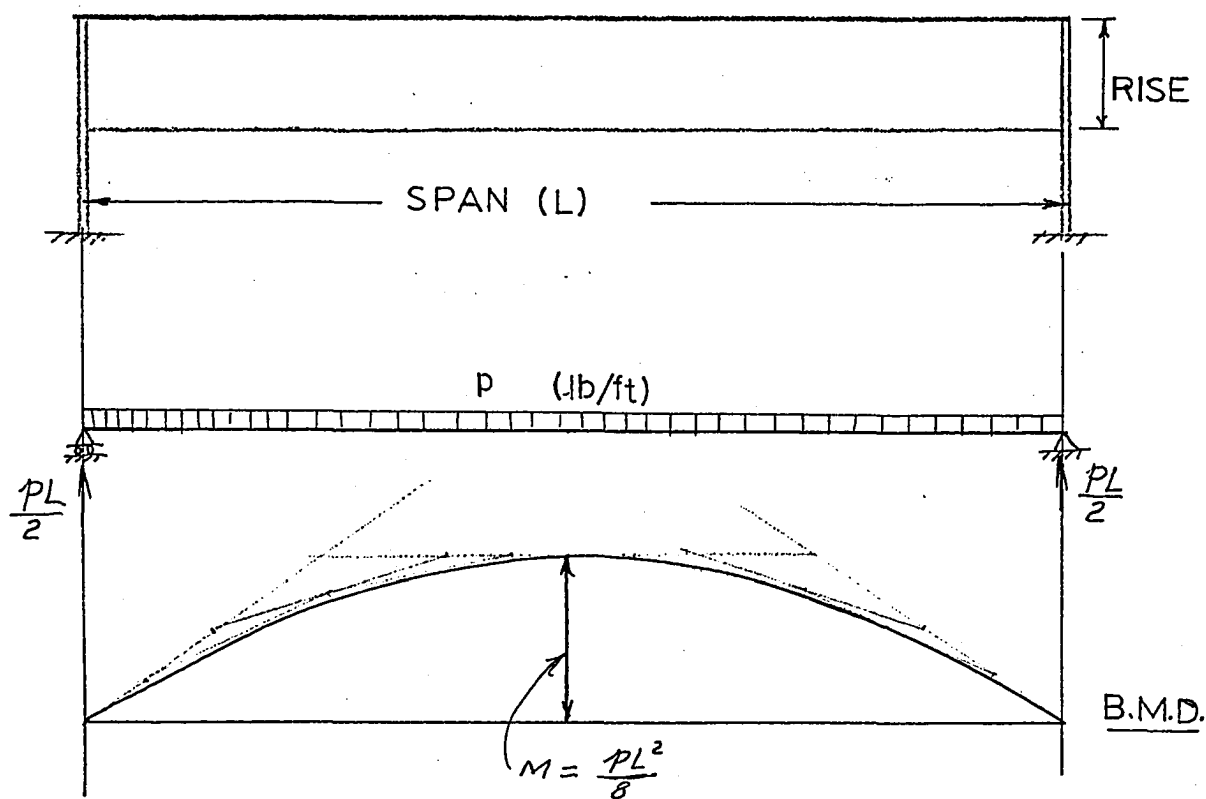
III.5. Effect of Slip at Sheet-to-sheet and Sheet-to-frame Connections:

The shear rigidity, D_x , given earlier by Equation (1-c) in Chapter (II) incorporates a reduction factor, ρ , to account for the effect of slip at sheet-to-sheet and sheet-to-frame connections. This shear slip was studied previously by the author and it was found that the values of " ρ " varied from 0.0 to 1.0⁽⁸⁾.

Figure (6) shows the effect of " ρ " on the values of the displacement "w" for different ratios of (L/R). From this figure, it is clear that the value of " ρ " has insignificant effect on the shell roofs. Also, the effect of " ρ " on the calculated stresses is even less than its effect on "w". Therefore, the number of connectors between the sheets can be reduced to the minimum required to carry the loading without being concerned about the rigidity.

III.6. Application of the Approximate Beam-Method:

The solution presented using the differential equations is valid for short shells. It also encounters considerable calculations and a lengthy program. Therefore, it is interesting to examine the application of the beam-method of analysis which is approximate, and easy to apply.



Moreover, the beam-method is known to lead to good results in the case of long shells where the presented solution fails.

The shell is treated here as a beam in the longitudinal direction and as an arch in the lateral direction. Accompanied by the usual assumptions of the theory of elasticity, the following three assumptions are to be added as a basis for the beam-method in shells:

- (1) The deformation of the cross-section in its plane are neglected.
- (2) The shear deformation caused by $N_{x\phi}$ and $N_{\phi x}$ is neglected (Navier Hypothesis).
- (3) The longitudinal moment, M_x , and the torsional moment $M_{x\phi}$ are neglected.

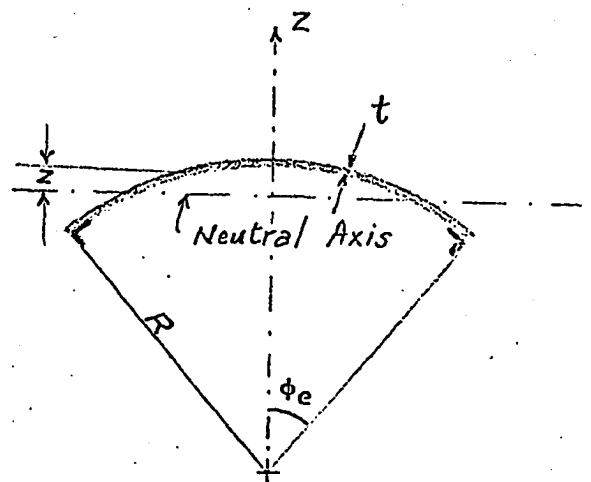
The beam calculations are made in the usual manner as follows:

A. Beam Analysis:

The values of N_x can be calculated by using the formula:

$$N_x = \frac{M \cdot z \cdot t}{I_{N.A.}} \quad (31-a)$$

Where: "M" is the bending moment at any cross-section



calculated in the same procedure as for the simply supported beam and " $I_{N.A.}$ " is the moment of inertia about the Neutral Axis. $N_{x\phi}$ is calculated using the well-known formula:

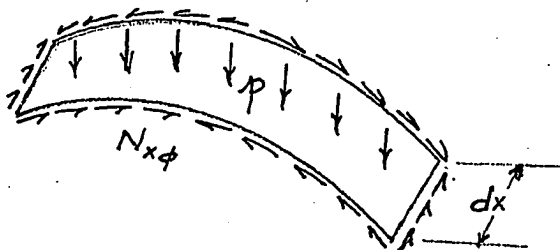
$$N_{x\phi} = \frac{VQ}{2I_{N.A.}} \quad (31-b)$$

Where: "V" is the vertical shearing force at the cross-section, computed in the same manner as a simple beam; and "Q" is the first moment of area up to the point under consideration about the Neutral Axis, found from the expression:

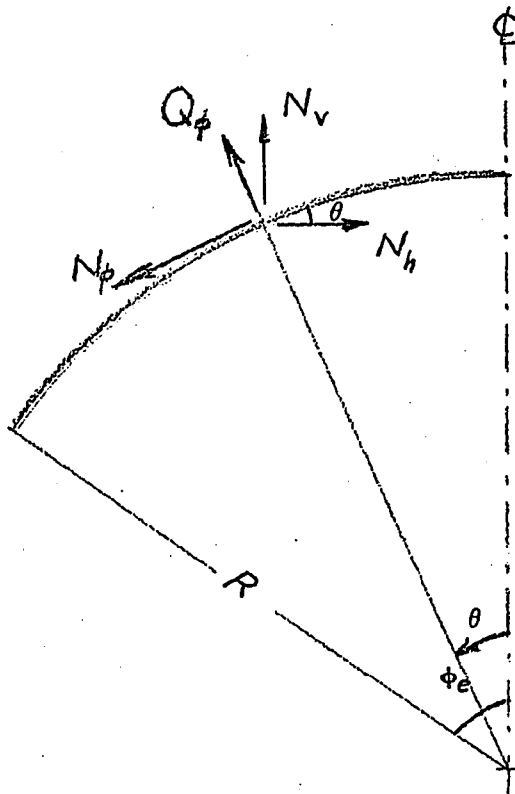
$$Q = 2tR^2 \left(\sin\phi - \frac{\phi}{\phi_e} \sin\phi_e \right) \quad (31-c)$$

B. Arch Analysis:

The second step in the beam-method may be described as the arch analysis. The object of this step is to compute " M_ϕ ", " Q_ϕ " and " N_ϕ ". Referring to the above strip, dx (cut from the shell), the equilibrium of the arch is maintained



by two sets of forces - the load acting on the strip and the specific shear $\frac{\partial N}{\partial x} x\phi$. The specific shear at any point, acting tangentially on the shell arch, can be resolved into horizontal and vertical components. It is evident that the sum of the vertical components of the specific shear balances the load on the shell arch, and the horizontal components of the specific shear which are symmetrically disposed about the crown balance themselves. The transversal bending moment, M_ϕ , at any point in the arch may be calculated as the algebraic sum of the moments caused by the loading and the horizontal and vertical components of the specific shears.



$$N_h = \int \frac{\partial N_{x\phi}}{\partial x} \cos\theta \, ds, \quad ds = R d\phi \quad (31-d)$$

$$N_v = \int \left[\frac{\partial N_{x\phi}}{\partial x} \sin\theta + p \right] ds \quad (31-e)$$

$$Q_\phi = N_v \cos\theta + N_h \sin\theta \quad (31-f)$$

$$M_\phi = \int Q_\phi \, ds \quad (31-g)$$

$$N_\phi = \int \frac{\partial N_{x\phi}}{\partial x} \cdot R \cdot d\phi \quad (31-h)$$

This beam-method is used to compare the same cases of roofs with the previously presented differential equations solution.

Figure (7) presents a comparison of " N_x " values at crown for different ratios of (L/R) for both, solutions by the beam method and differential equations.

The same figure shows that at a ratio $L/R \approx 3.5$, the beam-method gives results close to the solution by the differential equations. Thus, for ratios $L/R > 3.5$, the approximate beam-method can be used.

It is emphasized here that the beam-method cannot be used for the third case of boundary conditions because the shell is supported along the four edges.

CHAPTER (IV)
EXPERIMENTAL VERIFICATION

An experimental program was undertaken with full scale shell roofs using the first two mentioned types of boundary conditions.

Figure (8-a) is a photograph of the shell model built in the Civil Engineering Laboratory at the University of Windsor. The parameters of the roof were as follows:

Radius of shell = 7.00 feet.

Span of shell = 20.00 feet.

Half the central angle (ϕ_e) = 41°

The shell was built of standard arc-and-tangent corrugated sheets with gauge 22, and was simply supported at the ends on steel trusses as shown in Figure (8-a).

A case of snow loading was simulated by suspending aluminum bars from the shell, as illustrated in Figure (8-b). In a cross-sectional view there were three levels of bars. The bars at the first level were suspended by aircraft wires, $\phi = \frac{1}{16}$ " , that were attached to some of the bolts which fastened the sheets together. These bolts had small holes drilled through their center-lines and the wires were inserted and attached to the heads of the bolts. Each bar was suspended by two wires. At the second level

each bar was suspended by two wires, each wire being attached to a separate first level bar. The third level consisted of a plywood platform on which weights were placed. The platform was suspended by two wires attached to separate bars at the second level.

The first two experiments were carried out for Case (I) of boundary conditions. Two longitudinal angles $2\frac{1}{2} \times 2\frac{1}{2} \times \frac{1}{4}$ were bolted at the valleys as longitudinal stiffeners.

The following page is a photocopy of the computer program output for the theoretical solution to this shell model.

Mechanical dials were used to measure the u-displacements at the support every 10° , Figure (9-c). The dials were located at points 6, 6' & 7, 7' & 8, 8' & 9, 9' and 10, 10'.

In the first experiment, the vertical deflection of the crown point at the mid-span " w_5 " was measured by a mechanical dial. In this test, only three increments of load were applied. The following are the analyses of this experiment.

This experimental analysis is based on the mechanical properties given in Equation (1), which were examined experimentally for the sheets used in these tests, in reference (8).

THEORETICAL SOLUTION OF THE SHELL ROOF TESTED IN THE LABORATORY.

BOUNDARY CONDITIONS

LONGITUDINAL STIFFENERS IN THE VALLEYS ONLY.

VALUES OF CONSTANTS

AN		BN		CN		DN		EN		FN		GN		HN	
-0.00450719		0.00738445		C.25814377		-0.13781982		-0.06569213		0.05200924		0.28535866		C.22756991	
RADIUS		SPAN		EDGE ANGLE		GAUGE THICKNESS									
84.00Inch		240.00Inch		41 DEGREE		22									
FIE	NX	MFIE	MFIE	MFIE	MXFIE	M	L	V							
0.01383	0.01283	-C.000007	2.31297586	C.56455566	C.000007	C.56455566	G.C004049	-0.338770							
C.067200	-1.02189	-C.188884	-0.120513	2.26349831	C.5017559	C.5017559	-C.C299037	-0.294881							
C.174500	-1.91532	-C.370413	-0.429531	2.12138081	C.4574052	C.4574052	-C.C560484	-0.251254							
0.261800	-2.66654	-C.537037	-0.849064	1.90033913	C.4513229	C.4513229	-C.C780313	-0.208083							
0.349000	-3.27672	-C.682500	-1.306693	1.61430359	C.4836256	C.4836256	-C.C958873	-0.165564							
0.426300	-3.74554	-0.802226	-1.740638	1.27597113	C.4746352	C.4746352	-C.1057234	-0.123729							
C.523400	-4.00662	-C.892263	-2.098656	0.89875233	C.4647672	C.4647672	-C.1155593	-0.082721							
C.610800	-4.25126	-C.945900	-2.341701	0.49605369	C.4544057	C.4544057	-C.1255757	-0.042645							
0.698100	-4.36630	-C.973668	-2.445520	0.07554103	C.4438067	C.4438067	-C.1277717	-0.003439							
0.715500	-4.36602	-C.874279	-2.448377	-0.00400196	C.4416808	C.4416808	-C.1277636	0.004264							

AREA OF EDGE STIFFENER
0.02209

TABLE (1)

Dial Readings for u-displacements at
left end of shell for experiment No. (1).

Load psf	u_6 inch	u_7	u_8	u_9	u_{10}
0.66	-0.007	-0.040	-0.071	-0.083	-0.090
1.1	-0.027	-0.063	-0.111	-0.140	-0.151
2.2	-0.0575	-0.132	-0.131	-0.320	-0.202

TABLE (2)

Dial Readings for u-displacement at
right end of shell for experiment No. (1).

Load psf	u'_6	u'_7	u'_8	u'_9	u'_{10}
0.66	-0.005	-0.045	-0.061	-0.077	-0.105
1.1	-0.009	-0.050	-0.102	-0.130	-0.142
2.2	-0.017	-0.139	-0.209	-0.266	-----

The average value of the displacement, u , of the two end trusses, was calculated. Then the equivalent displacement under unit load was computed for each load increment. Finally, the extrapolated value of the u-displacements under unit load were calculated. These are given as follows:

TABLE (3)

Extrapolated values of u-displacement in inches for Experiment No. (1) per unit load p (lb/ft)

Method	u_6	u_7	u_8	u_9	u_{10}
Experiment	-0.014p	-0.0585p	-0.0905p	-0.116p	-0.131p
Theory	-0.001p	-0.055p	-0.096p	-0.119p	-0.127p

Figure (10) shows the comparison between the theoretical and experimental u-displacements at the end support. Figure (11) shows the load-deflection curve for the crown-point of mid-span for this experiment.

In the second experiment, a trial was made to measure the vertical deflections of selected points (1,2,3 & 4) on the shell surface using a theodolite (Swiss Wild T16), [Figure (9)]. The theoretical values of these vertical deflections were computed from the following equation (21):

$$y_{\phi} = w_{\phi} \cos(\phi_e - \phi) - v_{\phi} \sin(\phi_e - \phi)$$

where y_{ϕ} is the vertical deflection at angle ϕ . Eight increments of load (one pound per square foot each) were applied. At the last two increments, the axial strain, ϵ_x , was measured on the longitudinal stiffeners at mid-span using electrical resistance strain gauges. [G.F. = 2.02, R = 120 ± 0.1Ω].

To calculate the axial strains, ϵ_x , and consequently, the stress-resultant " N_x ", two thin nails were soldered to the shell surface at points 2, 3, 4 and 5, so that the change in distance between the nails can be measured by a micrometer.

The analyses of this experiment are shown in Tables (4 to 7). Figures (12 to 19) show the comparison between the theoretical and experimental results.

Analysis of Experiment No. (2):

TABLE (4)

Average values of displacement "u" for
Experiment No. (2).

Load (psf)	u_6	u_7	u_8	u_9	u_{10}
1	0.016	0.058	0.099	0.122	0.134
2	0.0345	0.123	0.203	0.252	0.278
3	0.0545	0.199	0.314	0.396	0.477
4	0.076	0.253	0.429	0.531	0.583
5	0.101	0.333	0.559	0.690	0.688
6	0.126	0.410	0.691	0.857	0.832
8	0.191	0.568	-----	-----	1.130

TABLE (5)

Dial reading of vertical deflection of crown point at mid-span for Experiment (2).

Load (psf)	1	2	3	4	5	6
w_5 (in)	0.453	0.933	1.474	1.960	2.536	--(*)

TABLE (6)

Vertical deflections of points 1, 2, 3 & 4 measured by a Theodolite for Experiment (2).

Point Load	y_1 (in)	y_2	y_3	y_4
1	0.90	0.60	0.75	0.49
2	1.30	1.60	1.50	0.98
3	1.96	2.02	----	1.09
4	2.50	2.30	2.60	1.90
5	2.74	2.90	3.07	2.50
6	3.15	3.40	3.65	3.00
8	4.05	4.38	4.75	4.45

* dial went out of range.

TABLE (7)

Comparison between Experimental and Theoretical
 N_x -Distribution.

Method	N_{x1}	N_{x2}	N_{x3}	N_{x4}	N_{x5}
experimentally	+0.025p	-2.140p	-3.54p	-3.85p	-4.40p
theoretically	+0.0138p	-1.915p	-3.276p	-4.086p	-4.366p

(N_x in lb/in ξ p in psf)

The third experiment was conducted on a shell roof having the second type of boundary conditions. Two additional longitudinal angles $2\frac{1}{2} \times 2\frac{1}{2} \times \frac{1}{4}$ were attached back to back along the crown line of the shell.

The theoretical solution, as obtained from the computer, is shown in the following table.

In this experiment, 2 lbs. per square foot increments were applied up to 16 psf. The deflection of the crown point at mid-span as well as the u-displacements were recorded as before. The analysis of this experiment were done in a similar manner as explained in the first two experiments. Figures (20,21) show the comparison between the theoretical and experimental results of this experiment.

THEORETICAL SOLUTION OF THE SHELL ROOF TESTED IN THE LABORATORY.

BOUNDARY CONDITIONS

LONGITUDINAL STIFFENERS IN VALLEYS AND CROWN.

FIE	NX	NFIE	MFIE	NXFIE	W	L	V
0.0	0.01296	-0.000000	0.000001	1.84503174	-0.0213692	0.0004048	-0.0004737
0.087200	0.01129	-0.145650	-0.125087	1.84623623	-0.0120432	0.0003525	-0.0019181
0.174500	0.00636	-0.293301	-0.465883	1.84710884	-0.0043942	0.0001985	-0.0026193
0.261800	0.0020	-0.443644	-0.965653	1.84743690	0.0011910	0.0000063	-0.0027424
0.349000	-0.00567	-0.597265	-1.551865	1.84717846	0.0047274	-0.0001770	-0.0024595
0.436300	-0.01032	-0.755178	-2.137526	1.84641171	0.0065442	-0.0003222	-0.0019665
0.523600	-0.01324	-0.917756	-2.765619	1.84528065	0.0071554	-0.0004133	-0.0013626
0.610800	-0.01426	-1.085718	-3.210312	1.84396362	0.0071509	-0.0004451	-0.0007381
0.698100	-0.01337	-1.258229	-3.427391	1.84263802	0.0070438	-0.0004174	-0.0001218
0.715500	-0.01297	-1.293366	-3.434304	1.84238911	0.0070356	-0.0004048	-0.0000001

AREA CF EDGE STIFFENER 2.01762
 AREA OF TOP STIFFENER 0.01759

CHAPTER (V)

APPLICATIONS OF CYLINDRICAL SHELLS
MADE OF CORRUGATED SHEETS IN GRAIN BINSV.1. Simplified Differential Equation:

For grain bins, the loads are of the rotational type of symmetry since the filling is symmetrical along the circumferential perimeter. Thus, in this case, the following simplifications can be made:

$$P_{\phi} = N_{x\phi} = Q_{\phi} = \frac{\partial N_{\phi}}{\partial \phi} = \frac{\partial M_{\phi}}{\partial \phi} = M_{x\phi} = 0$$

Although the transversal shearing forces Q_x are negligible in the case of the standard type of corrugated sheets, they will be considered in the derivation. This would allow the use of the present solution for other types of corrugations (such as those of Chapter (VI)).

Assuming the radial loading, p_z , to be positive when acting inwards, and taking these simplifications into consideration, the equilibrium Equations (2-a,b,...), are reduced to the following:

$$N_x' = -p_x \quad (32-a)$$

$$N_{\phi} + RQ_x' = -Rp_z \quad (32-b)$$

$$M_x' = Q_x \quad (32-c)$$

Also, the elastic relationships, Equations (9-a...f), are reduced to:

$$N_{\phi} = - \frac{D_{\phi}}{R} w \quad (33-a)$$

$$N_x = D_x u' \quad (33-b)$$

$$M_x = -B_x w'' \quad (33-c)$$

Substituting for M_x from Equation (33-c) into Equation (32-c), then:

$$Q_x = -B_x w'''$$

$$\text{or } \frac{\partial Q_x}{\partial x} = -B_x w'''' \quad (34)$$

Substituting Equations (33-a) and (34) into Equation (32-b) results in:

$$B_x \frac{\partial^4 w}{\partial x^4} + \frac{D_{\phi}}{R^2} w = p_z \quad (35)$$

The radial loading, p_z , was suggested by the ACI⁽⁴⁾ as follows:

$$p_z = - \left[\frac{\gamma r}{u} \right] \left[1 - e^{-k \bar{u} x / r} \right] \quad (36)$$

where: r = the hydraulic radius, \bar{u} = the coefficient of friction between the bin's wall and filling material,
 $K = \frac{p_z}{p_x}$, γ = unit weight of filling material.

Thus, Equation (35) becomes:

$$B_x w'''' + \left(\frac{D_\phi}{R^2} \right) w = \left[(\gamma r) / \bar{u} \right] \left[e^{-K\bar{u}x/r} - 1 \right] \quad (37)$$

Equation (37) is the governing differential equation of grain bins.

V.2. Method of Solution:

Referring to Equation (37), the particular solution can be assumed as follows:

$$w_p = E^* e^{-K\bar{u}x/r} + F^* \quad (38)^*$$

Substituting for " w_p " into Equation (37):

$$\begin{aligned} B_x \left[-\frac{K\bar{u}}{r} \right]^4 \left[E^* e^{-K\bar{u}x/r} \right] + \left[\frac{D_\phi}{R^2} \right] \left[E^* e^{-K\bar{u}x/r} + F^* \right] \\ = \frac{\gamma r}{\bar{u}} \left(e^{-K\bar{u}x/r} \right) - \frac{\gamma r}{\bar{u}} \end{aligned} \quad (39)$$

Equating the coefficients in Equation (39):

$$E^* = \frac{\gamma r}{\bar{u}} \left[\frac{R^2 r^4}{B_x K^4 \bar{u}^4 R^2 + r^4 D_\phi} \right] \quad (40-a)$$

$$F^* = - \frac{R^2 \gamma r}{D_\phi \bar{u}} \quad (40-b)$$

The particular solution w_p becomes:

$$w_p = \frac{\gamma r}{\bar{u}} \left[\frac{R^2 r^4}{B_x K^4 u^4 R^2 + r^4 D_\phi} \right] e^{-K\bar{u}x/r} - \frac{\gamma r R^2}{D_\phi \bar{u}} \quad (41)$$

If the term expressing the load in Equation (37) is suppressed, the corresponding homogeneous equation reads:

$$B_x \frac{\partial^4 w}{\partial x^4} + \frac{D_\phi}{R^2} w = 0 \quad (42)$$

Assuming a homogeneous solution to be exponential in x , $w_H = K^* e^{\lambda x}$, where K^* is a constant; and substituting for w_H into Equation (42), it follows that:

$$B_x \lambda^4 + \frac{D_\phi}{R^2} = 0 \quad (43)$$

Equation (43) is the characteristic equation. The four roots of this equation can be obtained as follows:

$$\lambda^4 = - \frac{D_\phi}{B_x R^2}$$

$$\lambda = \pm \sqrt{\pm \sqrt{- \frac{D_\phi}{R^2 B_x}}} = \pm \sqrt{\pm i \sqrt{\frac{D_\phi}{R^2 B_x}}}$$

$$\text{Defining } s^2 = \frac{D_\phi}{B_x R^2}$$

$$\lambda = \pm \sqrt{\pm i s}$$

$$\text{Defining } s = z^2$$

$$\lambda = \pm z \sqrt{\pm i}$$

$$\text{or } \lambda = \pm \frac{z}{\sqrt{2}} \sqrt{\pm 2i}$$

Since $\pm 2i = (i \pm 1)^2$, then;

$$\lambda = \pm \frac{z}{\sqrt{2}} (i \pm 1)$$

Defining $\alpha = \frac{z}{\sqrt{2}}$ gives:

$$\lambda = \pm \alpha (i \pm 1) \tag{44}$$

Equation (44) gives the four roots $\lambda_{1,2,3,4}$.

Having obtained the roots, an explicit solution can be developed as follows:

$$w_H = K_1^* e^{\alpha x (i+1)} + K_2^* e^{-\alpha x (i+1)} + K_3^* e^{\alpha x (i-1)} + K_4^* e^{-\alpha x (i-1)}$$

or:

$$w_H = e^{-\alpha x} (K_2^* e^{-i\alpha x} + K_3^* e^{i\alpha x}) + e^{\alpha x} (K_1^* e^{i\alpha x} + K_4^* e^{-i\alpha x}) \tag{45}$$

where K_1^* , K_2^* , ... are arbitrary constants.

The terms multiplied by " $e^{-\alpha x}$ " represent the disturbance originating from the upper edge [Figure (22)]. The terms multiplied by " $e^{\alpha x}$ " represent the disturbance originating from the lower edge. Thus, a new independent variable, \bar{x} , is introduced such that:

$$\bar{x} = (h - x) \quad \text{where } h = \text{total height of bin.}$$

It follows that \bar{x} is the distance from the lower shell edge. The reason for this substitution will be made evident by the discussion of the solution later.

With the new notation, \bar{x} , Equation (45) can be written as:

$$\begin{aligned} w_H = & e^{-\alpha x} \left[(K_3^* + K_2^*) \cos \alpha x + i(K_3^* - K_2^*) \sin \alpha x \right] \\ & + e^{-\alpha \bar{x}} e^{\alpha h} \left[(K_1^* e^{i\alpha h} + K_4^* e^{-i\alpha h}) \cos \alpha x + i(K_4^* e^{-i\alpha h} \right. \\ & \left. - K_1^* e^{i\alpha h}) \sin \alpha \bar{x} \right] \end{aligned} \quad (46)$$

Introducing new constants C_1 , C_2 , C_3 and C_4 , then:

$$w_H = e^{-\alpha x} (C_1 \cos \alpha x + C_2 \sin \alpha x) + e^{-\alpha \bar{x}} (C_3 \cos \alpha \bar{x} + C_4 \sin \alpha \bar{x}) \quad (47)$$

Thus, the total solution is:

$$w = w_p + w_H \quad (48)$$

The constants C_1 , C_2 , C_3 and C_4 can be found by superimposing the particular and the homogeneous solutions to fulfill the requirements of the boundary conditions at the upper and lower edges of the bin.

V.3. Stress-Resultants:

Equation (48) can be written in a more expanded form as follows:

$$w = E^* e^{-K\bar{u}x/r} + F^* + e^{-\alpha x} (C_1 \cos \alpha x + C_2 \sin \alpha x) + e^{-\alpha(h-x)} (C_3 \cos(\alpha h - \alpha x) + C_4 \sin(\alpha h - \alpha x)) \quad (49)$$

where E^* and F^* are given by Equations (40-a,b) respectively.

$$\text{Since } N_\phi = \frac{-D_\phi}{R} w$$

$$N_\phi = -\frac{D_\phi}{R} \left[E^* e^{-K\bar{u}x/r} + F^* + e^{-\alpha x} (C_1 \cos \alpha x + C_2 \sin \alpha x) + e^{-\alpha(h-x)} (C_3 \cos(\alpha h - \alpha x) + C_4 \sin(\alpha h - \alpha x)) \right] \quad (50)$$

$$M_x = -B_x w''$$

$$M_x = -B_x \left\{ \frac{K^2 \bar{u}^2}{r^2} E^* (e^{-K\bar{u}x/r}) + e^{-\alpha x} \left[-2C_2 \alpha^2 \cos \alpha x \right. \right. \\ \left. \left. + 2\alpha^2 C_1 \sin \alpha x \right] + e^{-\alpha(h-x)} \left[-2\alpha^2 C_4 \cos (\alpha h - \alpha x) \right. \right. \\ \left. \left. + 2\alpha^2 C_3 \sin (\alpha h - \alpha x) \right] \right\} \quad (51)$$

$$Q_x = -B_x w'''$$

$$Q_x = -B_x \left\{ -\frac{K^3 \bar{u}^3}{r^3} E^* (e^{-K\bar{u}x/r}) + e^{-\alpha x} \left[2\alpha^3 (C_1 + C_2) \right. \right. \\ \left. \left. \cos \alpha x + 2\alpha^3 (C_2 - C_1) \sin \alpha x \right] + e^{-\alpha(h-x)} \left[-2\alpha^3 (C_3 + C_4) \right. \right. \\ \left. \left. \cos (\alpha h - \alpha x) + 2\alpha^3 (C_3 - C_4) \sin (\alpha h - \alpha x) \right] \right\} \quad (52)$$

From Equation (32-a), the stress-resultant " N_x " is expressed as:

$$N_x = \int -p_x dx$$

The stress-resultant, N_x , depends on the distribution of the frictional forces, p_x .

These frictional forces depend on: the angle of internal friction of the filling; the coefficient of friction between the grain and corrugated sheet wall; and the rigidity of the sheets. These parameters need further study.

V.4. Boundary Conditions:

The integration constants (C_1 , C_2 , C_3 and C_4) can be calculated by adding the particular and the homogeneous solutions to fulfill the boundary conditions that exist at the upper and lower edges of the bin.

Case (1): Fixed Bottom and Free Top:

This is practical for an extremely rigid ring at the base of a bin having a free upper edge. Referring to Figure (23-a), this condition requires that the displacement "w" of the lower edge, as well as its derivative with respect to x (slope), are equal to zero. The upper edge is free from moments and forces. Hence, at $x = 0$; $M_x = 0 \dots (i)$, $Q_x = 0 \dots (ii)$ and $x = h$, $w = 0 \dots (iii)$, $\dot{w} = 0 \dots (iv)$.

Case (2): Simply Supported at Top and Fixed at Bottom:

If there is a ring at the upper edge, the boundary conditions, (Figure 23-b), in this case would be:
at $x = 0$, $w = (w_{ring}) \dots (i)$, $M_x = 0 \dots (ii)$ at $x = h$
 $w = 0 \dots (iii)$, $\dot{w} = 0 \dots (iv)$. The extension of the ring (w_{ring}), is governed by the structure and loading of the cover, as well as the ring itself. In the following analysis, it is assumed that the cover is infinitely rigid in the plane of the ring and $w_{ring} \approx 0$.

Solving the boundary condition $w = 0$ at $\bar{x} = 0$ (or $x = h$) then:

$$w_{\bar{x}=0} = E^* e^{-K\bar{u}h/r} + F^* + e^{-\alpha h} (C_1 \cos \alpha h + C_2 \sin \alpha h) \\ + e^0 (C_3 \cos (0) + 0) = 0$$

or $E^* e^{-\bar{K}u\bar{h}/r} + F^* e^{-\alpha h} (C_1 \cosh\alpha + C_2 \sinh\alpha) + C_3 = 0$
 Because of the quick damping of $e^{-\alpha h}$, (which represents, at the lower edge, the rest of the disturbance originating from the upper edge), this part represents a very small value and can be neglected. Thus:

$$C_3 = E^* e^{-\bar{K}u\bar{h}/r} + F^* = w_p \quad (53-a)$$

Similarly, constants of an integration C_3 and C_4 can be neglected for the other boundary conditions (at $x = 0$). The significance of the introduction of the co-ordinate \bar{x} becomes evident in these expressions.

For the other three boundary conditions, the remaining constants are determined as follows:

$$C_4 = C_3 - \frac{\bar{K}uE^*}{\alpha r} e^{-\bar{K}u\bar{h}/r} \quad (53-b)$$

$$C_2 = \frac{K^2 u^2}{2\alpha^2 r^2} E^* \quad (53-c)$$

$$C_1 = \frac{K^3 u^3}{2r^3 \alpha^3} E^* - C_2 \quad (53-d)$$

Once the constants C_1 , C_2 , C_3 and C_4 have been evaluated, the complete solution is obtained, excepting for N_x -distribution, which can be evaluated if the frictional forces are known. The value of " N_x " is obtained by integrating the load p_x . Vertical stiffeners are necessary when the calculated value of N_x exceeds the

allowable value as given by the following equation:

$$N_x = 60 \times \frac{t}{0.035} \quad (54)$$

V.5. Effective Width:

For vertically stiffened bins, the longitudinal stress-resultants " N_x " are unequally distributed throughout its width, due to the shear strain in the sheets.

The stresses reach the maximum at the stiffener and decrease towards the minimum at the centre, Figure (24). In order to have a ready and precise method of calculating the maximum stresses and deformations in the bin, the actual width of the sheets is replaced by an imaginary width, λ_e , which is termed the "effective width". The longitudinal forces, N_x , are considered to be constant over the width, λ_e , and are equal to the maximum actual force which occurs at the stiffener, thus $\lambda_e = \frac{1}{(N_x)_{max.}} \cdot \int_{-\frac{b}{2}}^{+\frac{b}{2}} N_x R d\phi$.

Herein the forces " N_x " will be carried by the stiffeners together with the effective width of the corrugated sheets; and hence:

$$A_{total} = \left(\lambda_e \cdot t \cdot \frac{D_x}{D} + A \right) n$$

where: λ_e is the effective width of the corrugated sheets; n = the number of vertical stiffeners; and A is the cross-sectional area of each stiffener.

To determine the effective width, λ_e , the computer program, used for shell-roofs was utilized except that the membrane solution was replaced by the one for frictional forces, p_x , which are assumed to be distributed in a sine-wave.

Referring to Figure (24), the bin's height, h , is taken to be half the span of the corresponding shell roof, in which case the boundary conditions of either case (1) or Case (2) are fully satisfied. The mid-span of the shell represents the lower edge of the bin, which is fixed in both Cases (1) and (2). The end of the shell (at $x = L/2$), represents the upper edge of the bin (either simply supported (Case 2) or free (Case 1)). Thus, curves are prepared to determine the effective width, which depends on the spacing between the stiffeners, b_a , and the total height of the bin. It should be mentioned here that " λ_e " does not depend on the height at which it is to be calculated since " N_x " is distributed in a sine wave along the total height.

Figures (25,26) show the relation between (h/b_a) and (λ_e/b_a) ; and that between (h/b_a) and (λ_e/h) , respectively. From these curves, it is seen that the slip at sheet-to-sheet and sheet-to-frame connections, ρ , has a pronounced effect on the values of the effective width, λ_e . The reason for this is the shear deformation within the sheets.

CHAPTER (VI)

EFFECT OF GEOMETRY OF CORRUGATION
ON THE LOAD CAPACITY OF THE SHELL

It was noticed that although the first case of shell roofs, stiffened in valleys only, is the most practical one, there are excessive displacements imposing limitations on the applicability of the arc-and-tangent type of corrugations in this case. This is a result of the deficiency in the axial rigidity, D_x , due to the spring (accordion) action in the x-direction (the ratio of $\frac{D_x}{D_\phi} \simeq 0.004$). This axial rigidity can be improved in different ways.

In this chapter, some alternatives are shown for new shapes of corrugations, and the approximate results are estimated, and compared with the standard arc-and-tangent type of corrugation.

VI.1. Alternative No. (1):

A decrease in the depth of corrugation, $2f$, will increase the axial rigidity, D_x , since: $D_x = \frac{Et}{6(1-\mu^2)} \left(\frac{t}{f}\right)^2$.

For example, a value of $f = 0.125$ inch, (i.e. half the original value of the standard corrugation), leads to four times the rigidity D_x . The values obtained for the u-displacements with $f = 0.125$ inch are compared with those of $f = 0.25$ inch, and the results are shown in Figure (27), for the shell model tested in the laboratory.

On the other hand, any decrease in "f" will cause a decrease in the bending rigidity, B_ϕ , since $B_\phi = 0.522 f^2 \cdot t \cdot E$. Thus, the critical buckling load under shear will decrease ⁽¹⁾.

Further research is necessary to determine the optimum value of "f" that gives the best performance of sheets in elastic behaviour as well as elastic stability.

V.2. Second Alternative:

The author found a recent technique, developed by WESTEEL ROSCO LTD.-Toronto-Canada, to produce another modified shape of corrugation. A picture of this new dimpled shape is shown in Figure (28). Experiments on corrugated sheets with this new dimpled shape were conducted to determine the axial rigidity, D_x . The results are given in Figure (29). These experiments showed that the axial rigidity, D_x , was about 18 times greater than the value of the standard arc-and-tangent type.

The approximate structural rigidities of this suggested shape can be estimated as follows:

$$D_x = E_x \cdot t \quad (55-a)$$

$$D_\phi = E_\phi \cdot t \quad (55-b)$$

$$D_{x\phi} = \rho^* \frac{E \cdot t}{2(1+\mu)} \quad (55-c)$$

$$B_x = \frac{Et^3}{12(1-\mu^2)} \quad (55-d)$$

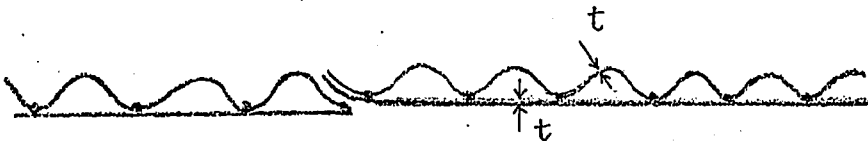
$$B_{\phi} = E_{\phi} I_{\phi} \quad (55-e)$$

$$B_{x\phi} = \frac{Et^3}{12(1+\mu)} \quad (55-f)$$

in which: $E_x = 0.145E$, $E_{\phi} \simeq E$, $\rho^* = 1.0$, $I_{\phi} = 0.522 f^2 t - (0.08)^2 t (0.044)$.

VI.3. Third Alternative:

A flat steel plate spot-welded to the corrugated sheets would increase the rigidity, D_x , appreciably.



A flat steel plate spot-welded
to the corrugated sheet.

Third Alternative

The membrane and bending rigidities can be estimated
as follows:

$$D_x = Et + \frac{Et}{6(1-\mu^2)} \left[\frac{t}{f} \right]^2 \quad (56-a)$$

$$D_{\phi} = E (2t) \quad (56-b)$$

$$D_{x\phi} = \rho_1 \frac{E(2t)}{2(1+\mu)}, \quad \rho_1 = 1.0 \quad (56-c)$$

$$B_x = \frac{1}{2} \left[\frac{E(2t)^3}{12(1-\mu^2)} + \frac{E \cdot 2t \cdot f^2}{(1-\mu^2)} \right] \quad (56-d)$$

$$B_\phi = E I_\phi, \quad I_\phi = 0.522f^2t + 2.04 \times 0.125^2t \quad (56-e)$$

$$B_{x\phi} = \frac{1.33Etf^2}{(1+\mu)} \quad (22) \quad (56-f)$$

In the case of the arc-and-tangent type of corrugation the ratios of the rigidities in the x-direction are small compared to those in the ϕ -direction. These ratios are considerably increased in the above alternatives. The effect of this change on the degree of accuracy of the roots obtained from the simplified Equation (23), is now examined.

Figure (30) shows the maximum percentage error in the roots vs. the ratio (L/R) , for the arc-and-tangent type $(\frac{D_x}{D_\phi} \simeq 0.004)$, alternative No. (3) $(\frac{D_x}{D_\phi} \simeq 0.5)$ and for an isotropic case with $\frac{D_x}{D_\phi} = 1.0$. This figure indicates that as the ratio of $(\frac{D_x}{D_\phi})$ increases, the accuracy of the simplified characteristic Equation (23), increases.

Furthermore, a comparison is made of the " N_x " values at the crown, for different (L/R) ratios as calculated by the beam-method, and the differential equations for Alternative (3). Figure (31) shows that, the beam-method gives results close to the solution of the differential equations when $L/R \geq 4$.

In order to show the effect of the alternative shapes of corrugation, a shell roof, having longitudinal stiffeners in valleys only, and with a radius, $R = 7.00$ feet, $\phi_e = 80^\circ$ and GAGE 18, is analysed utilizing:

- (a) The arc-and-tangent type of corrugation.
- (b) The dimpled shape.
- (c) The third alternative with GA 24 each
(Total $t = 0.5$ ").

For each case, the maximum span is determined such that the maximum deflection of the crown point at mid-span does not exceed $(1/100)$ of the span under an intensity of snow load of 50 p.s.f. The results are listed in the following table:

Corrugation Configuration	Span (Feet)
Arc-and-tangent	20
Dimpled Shape	50
Third Alternative	70

CHAPTER (VII)
OBSERVATIONS AND CONCLUSIONS

1. The experimental results showed a good agreement with those obtained theoretically, confirming that treating corrugated sheets as orthotropic shells is a valid approach. It also proves that the present solution is acceptable for design purposes.
2. The simplified equations, based on Donnell's assumptions, give acceptable results for short shells. For concrete shells the Donnell equations are being used with the ratio of $L/R < 1.6^{(21)}$ as an acceptable upper limit for the definition of short shells. A comparison of the error in the roots of the characteristic Equation (23) reveals that, at the same level of approximation used for concrete shells, corrugated sheet shells can be analysed with higher ratios of (L/R) .

Furthermore, it was found that, as the ratio of $\frac{D_x}{D_\phi}$ increases, the degree of accuracy improves.

It should be emphasized that the range of (L/R) within which the simplified characteristic equation can be used, depends on the type of boundary conditions along the straight edges. This is due to the fact that the bending solution is an edge disturbance effect.

3. The approximate beam-method can be applied, if the length of the shell reaches a limit at which the solution using the differential equations becomes unreliable.

Therefore, the present study offers methods of solution covering almost all lengths of shells, excepting barrels supported on four edges.

4. The slip due to shear at sheet-to-sheet and sheet-to-frame connections has an insignificant effect on the calculated stresses and deflections of the shell roof.

5. Since the geometry of corrugation has a considerable effect on the load capacity of the shell, other geometrical forms are suggested for better performance.

6. Theoretical solutions for stiffened and unstiffened grain bins made of corrugated sheets are obtained. Curves are presented for the determination of the effective width of corrugated sheets (stiffened by vertical ribs) under frictional forces. These curves can be used in the design of stiffened grain bins. The shear slip at sheet-to-sheet and sheet-to-frame connections, p , has a pronounced effect on the magnitude of the effective width.

FIGURES

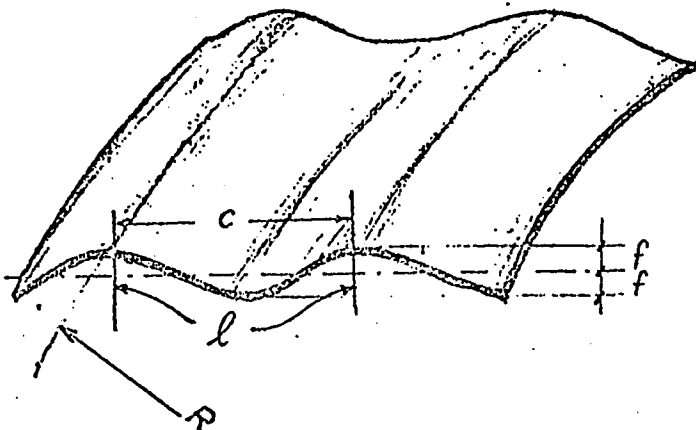


Figure (1)

(a) Stress resultants $N_x, N_\phi, N_{x\phi}$

(b) Moments $M_x, M_\phi, M_{x\phi}$

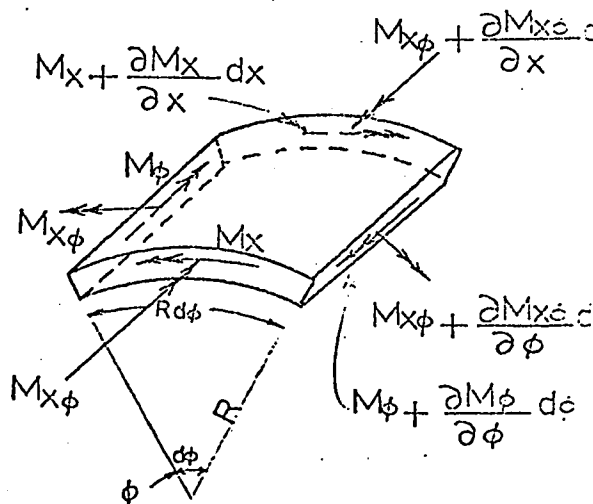
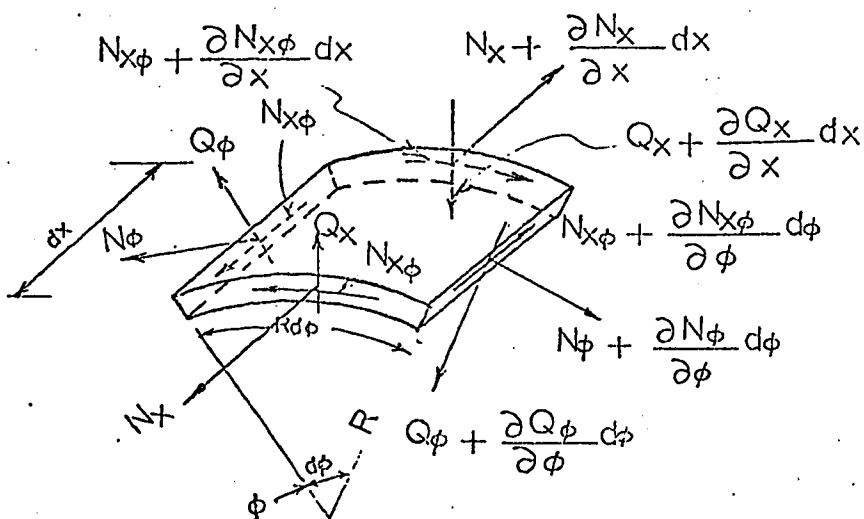


Figure (2)

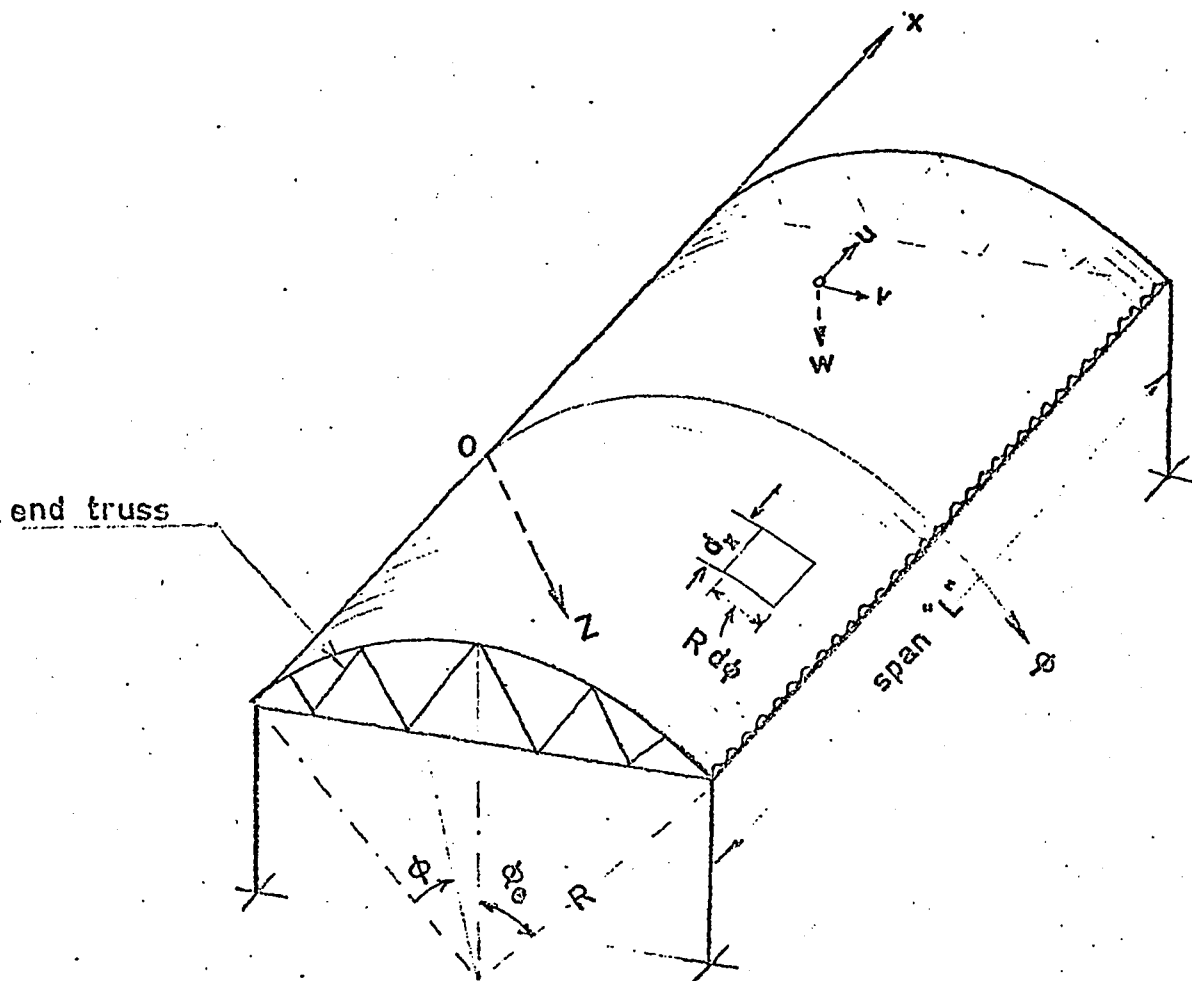
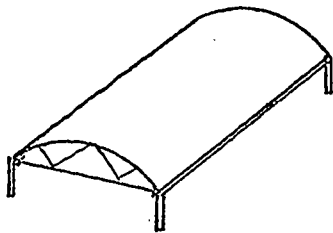
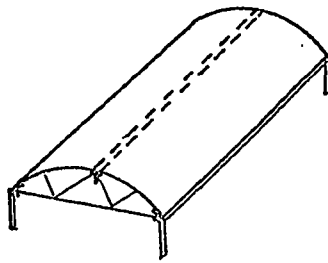


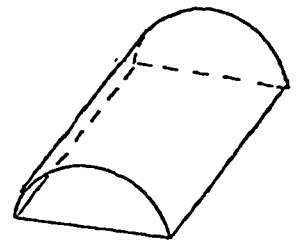
figure 3: COORDINATE SYSTEM.



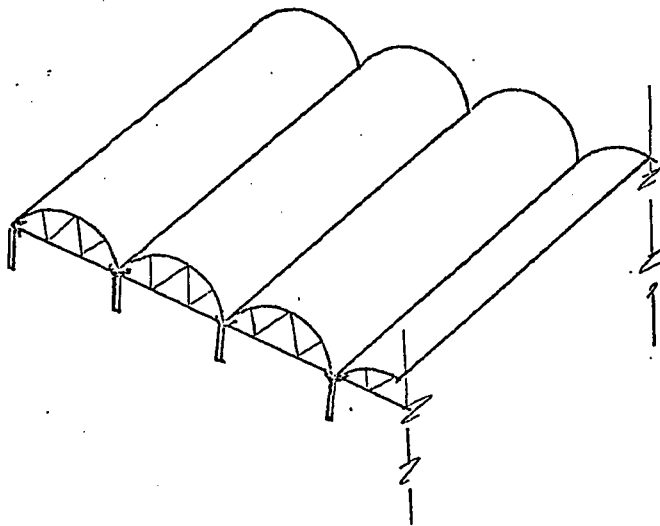
(a) case I



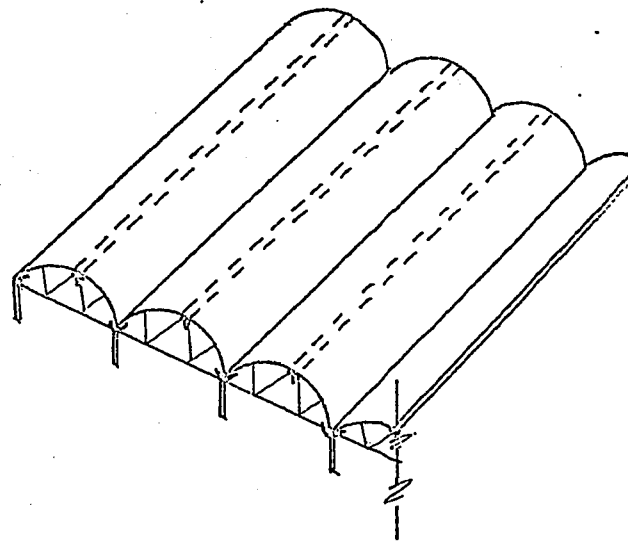
(b) case II



(c) case III

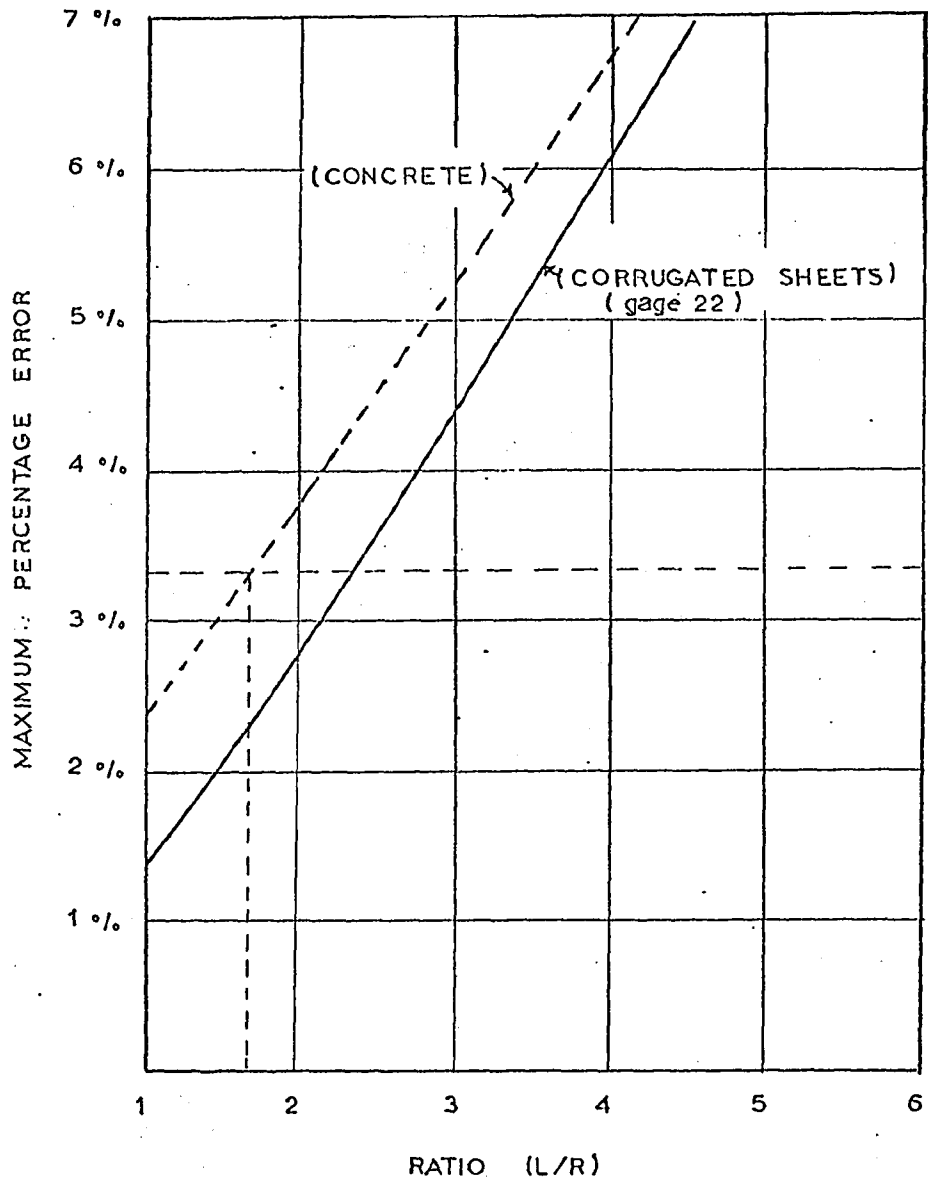


(d) case IV

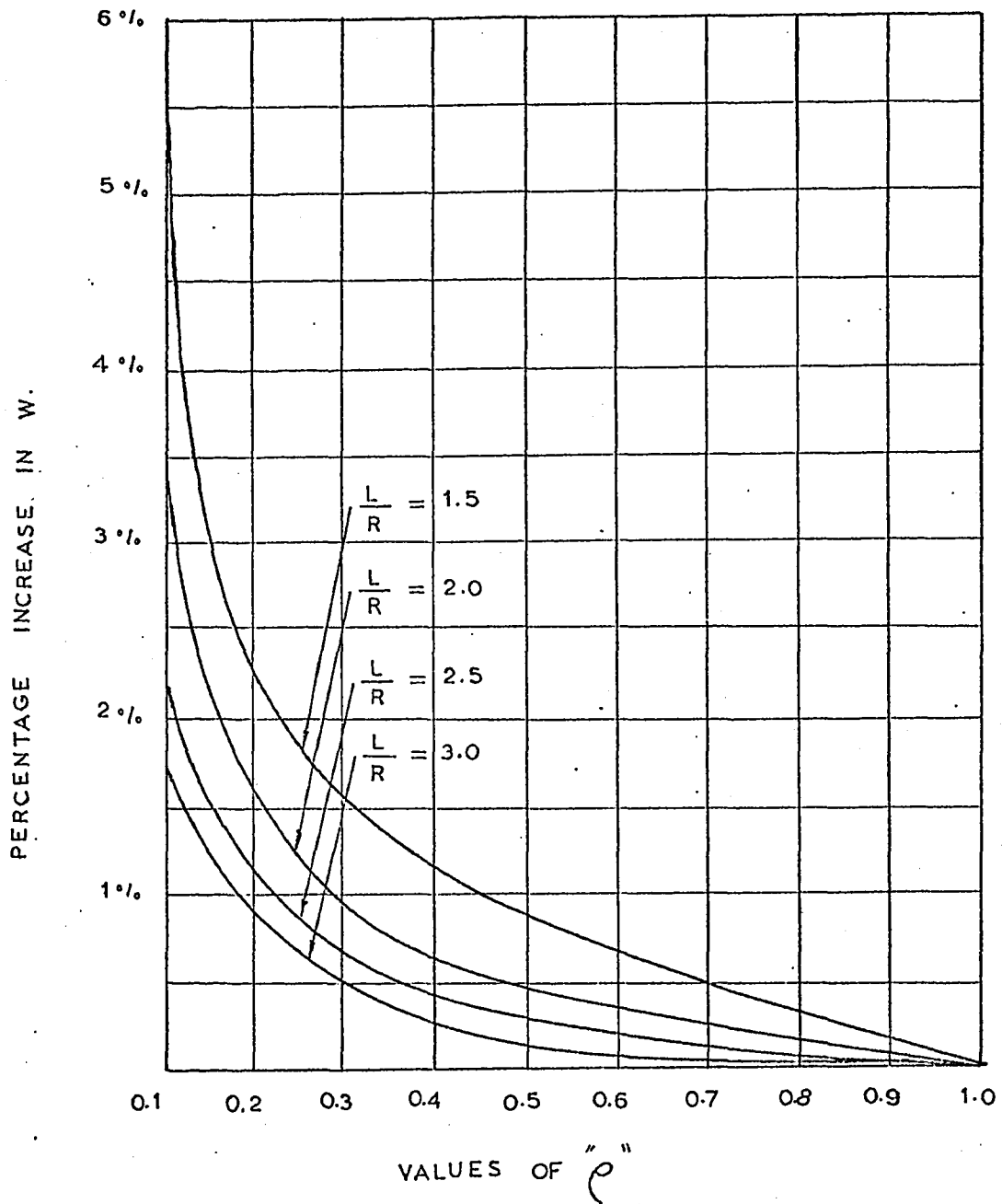


(e) case V

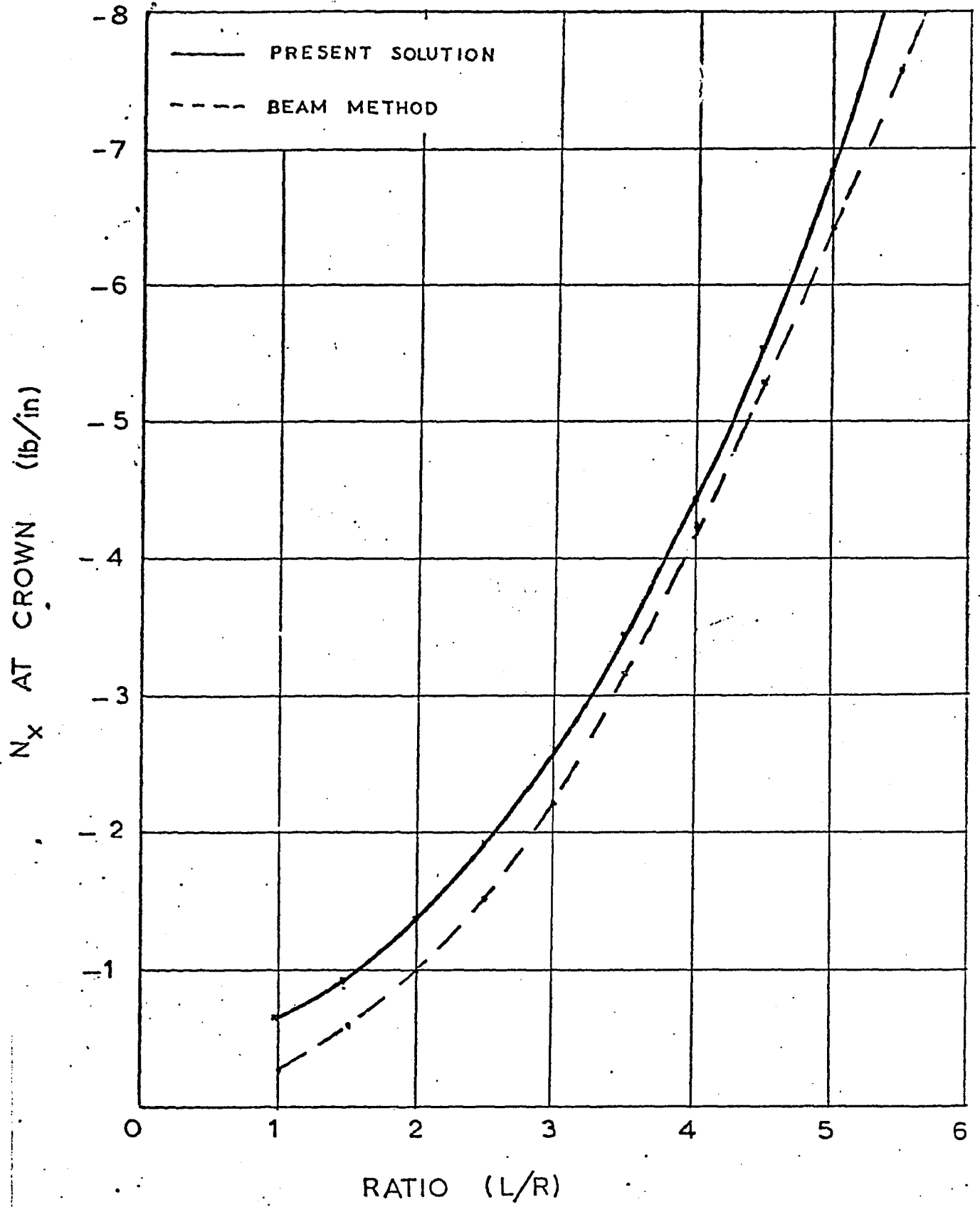
FIGURE 4 : PRACTICAL APPLICATIONS IN ROOFING.



FIGURE(5) COMPARISON BETWEEN MAXIMUM PERCENTAGE ERROR IN THE ROOTS FOR CONCRETE & CORRUGATED SHELLS.



FIGURE(6): EFFECT OF "e" ON SHELL ROOFS FOR DIFFERENT RATIOS ($\frac{L}{R}$).



FIGURE(7): COMPARISON BETWEEN PRESENT SOLUTION AND THE BEAM METHOD.

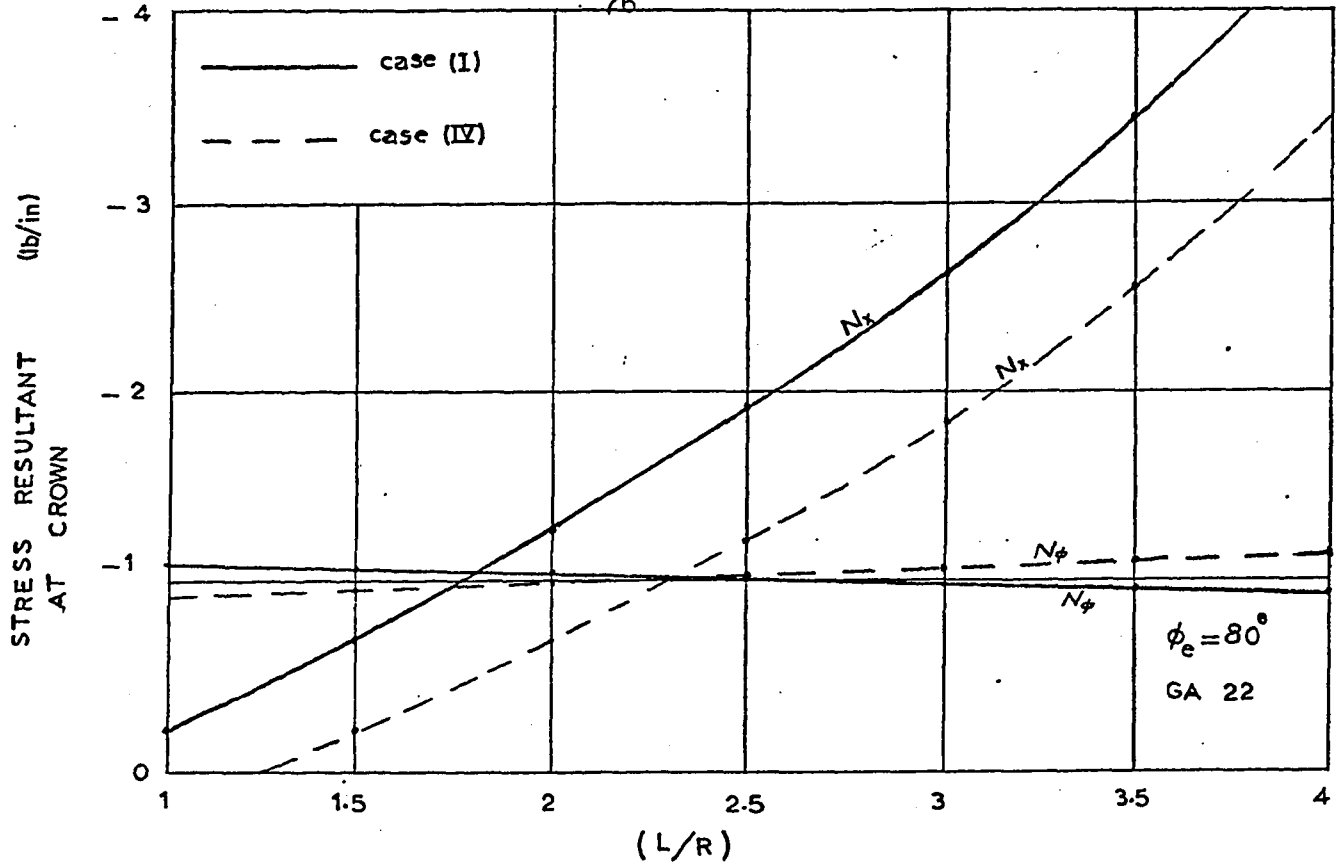


FIGURE (8-a)

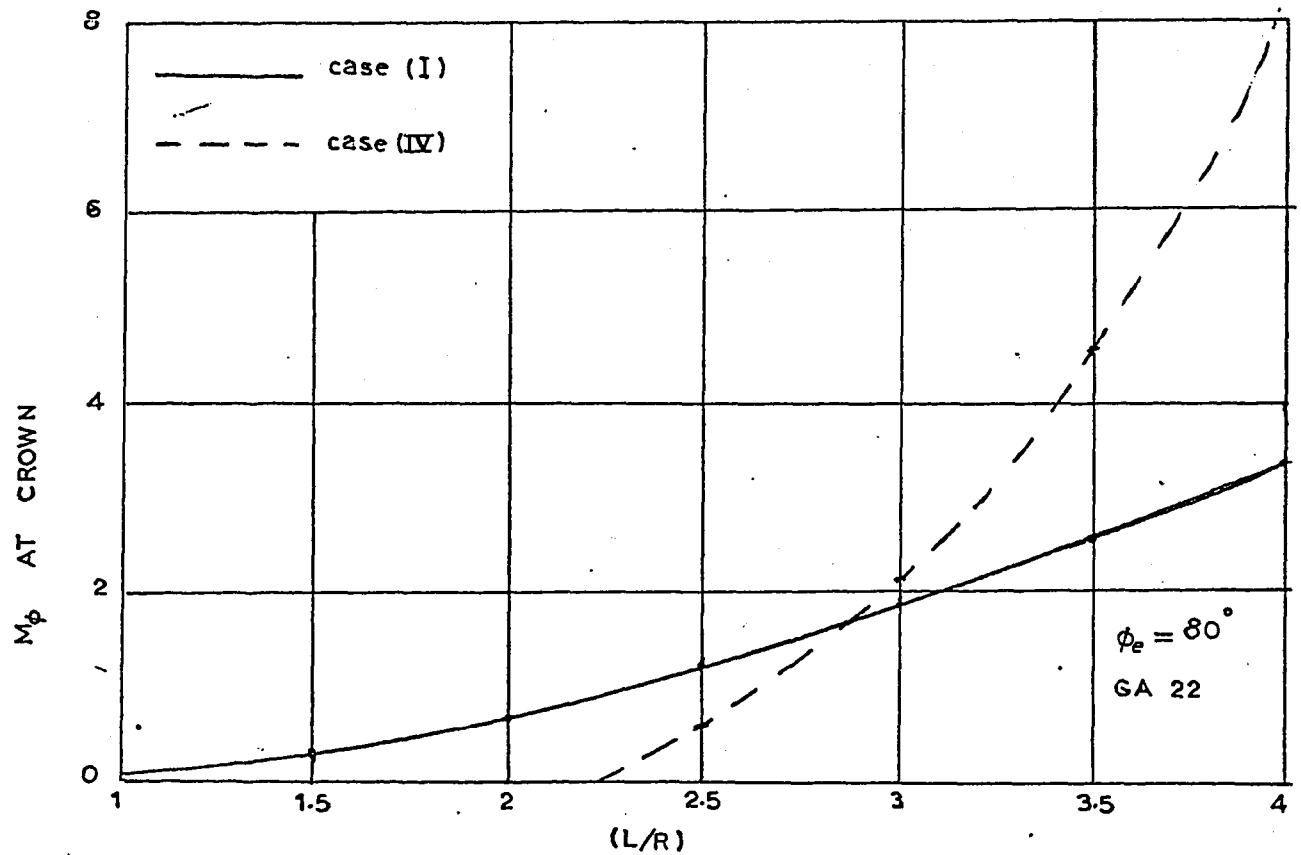


FIGURE (8-b)

COMPARISON BETWEEN CASE (I) & CASE (IV) OF BOUNDARY CONDITIONS.



FIGURE (9-a): A PICTURE OF THE SHELL MODEL.

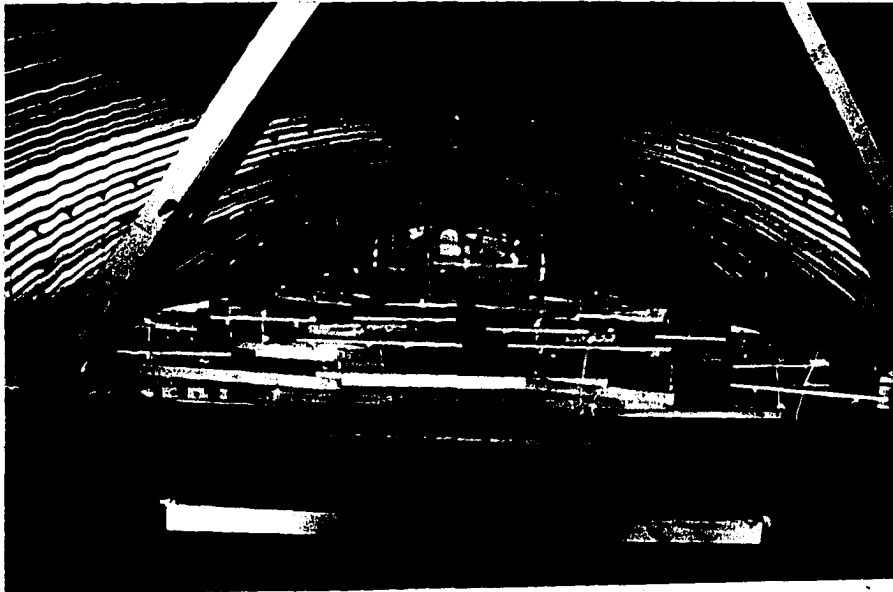
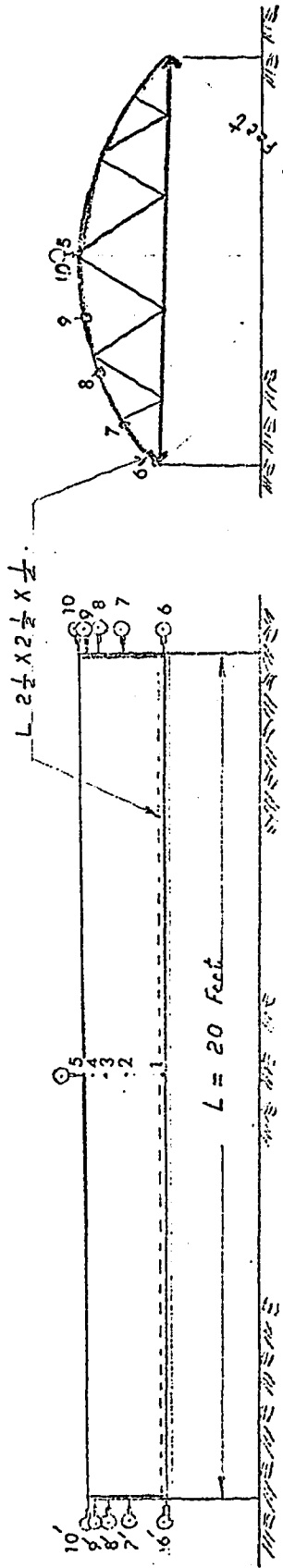


FIGURE (9-b): A PICTURE OF THE LOADING SYSTEM.

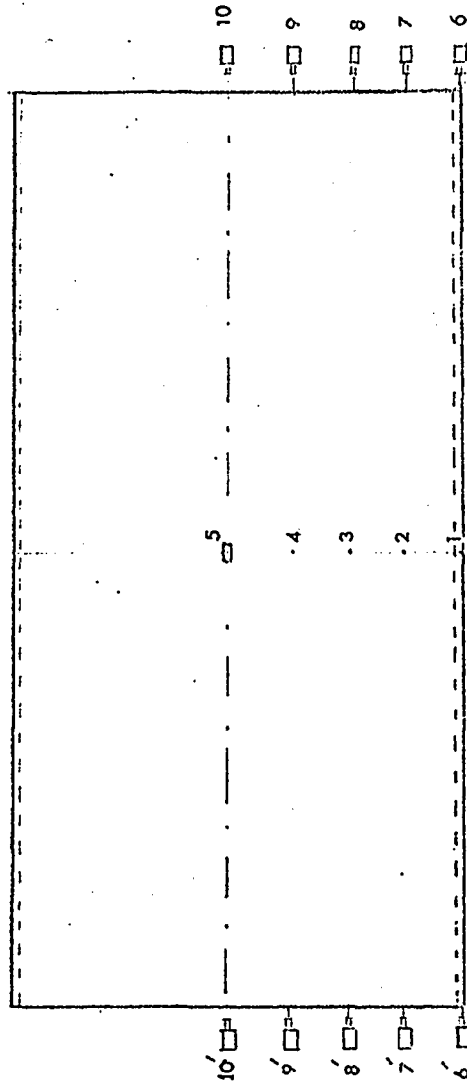


SIDE VIEW

ELEVATION

GENERAL ARRANGEMENT
OF ROOF.

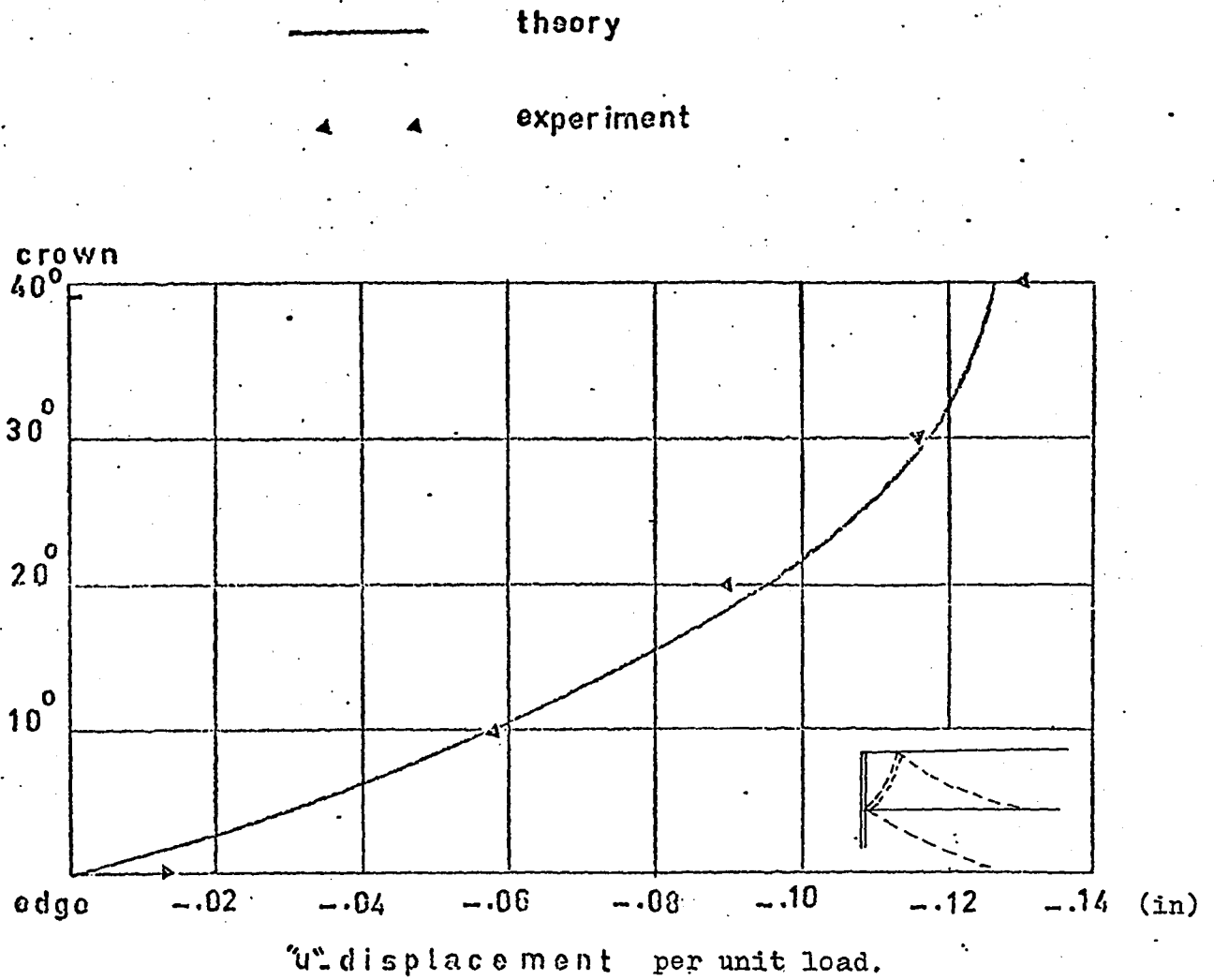
scale: 1:500



PLAN

FIGURE 9 - c

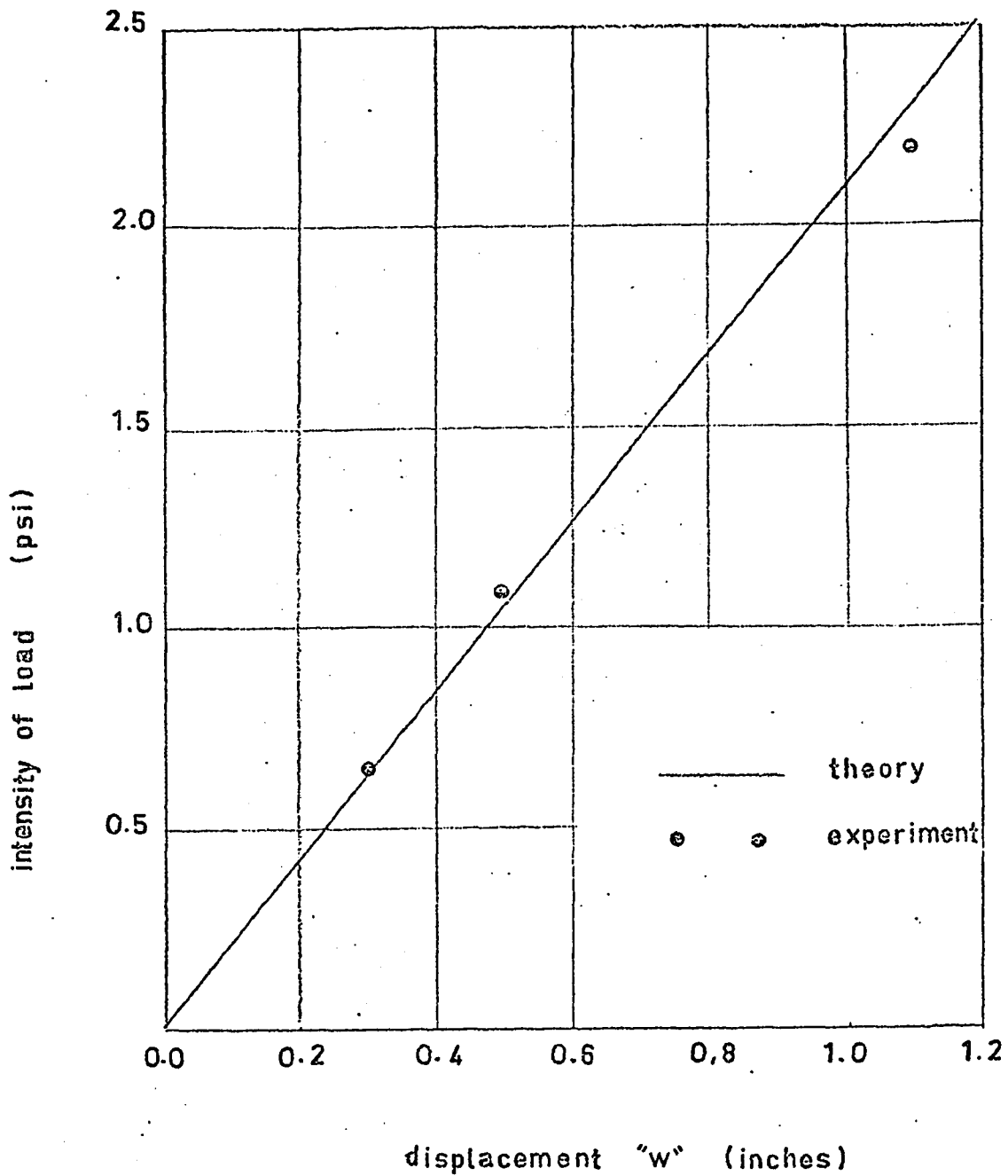
EXPERIMENT NO. 1



COMPARISON BETWEEN THEORETICAL AND EXPERIMENTAL VALUES
OF THE DISPLACEMENT "U" AT SUPPORT.

figure 10

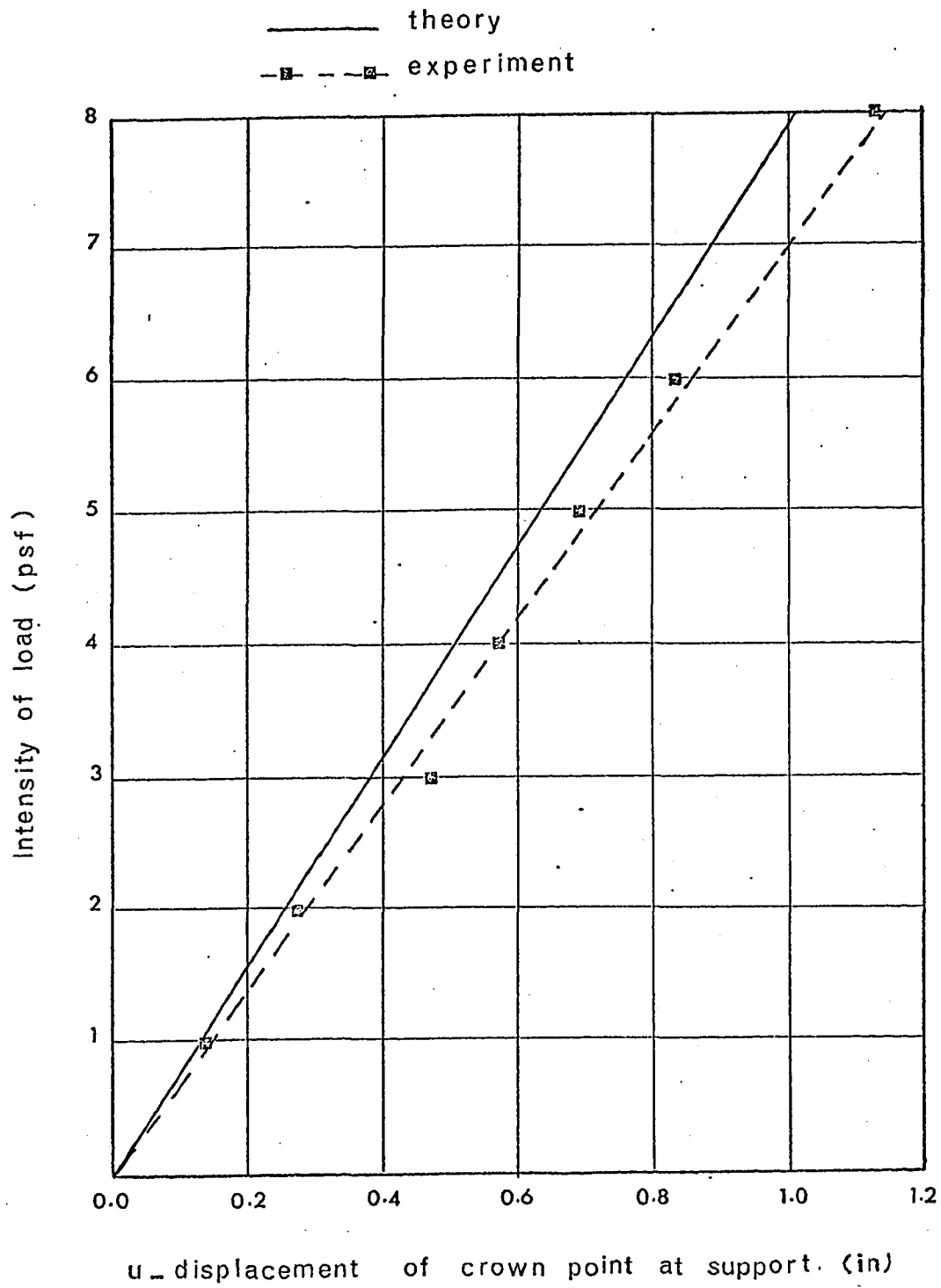
EXPERIMENT NO (1)



COMPARISON BETWEEN THEORETICAL AND EXPERIMENTAL
LOAD-DEFLECTION CURVES OF CROWN POINT AT MID-SPAN.

figure 11

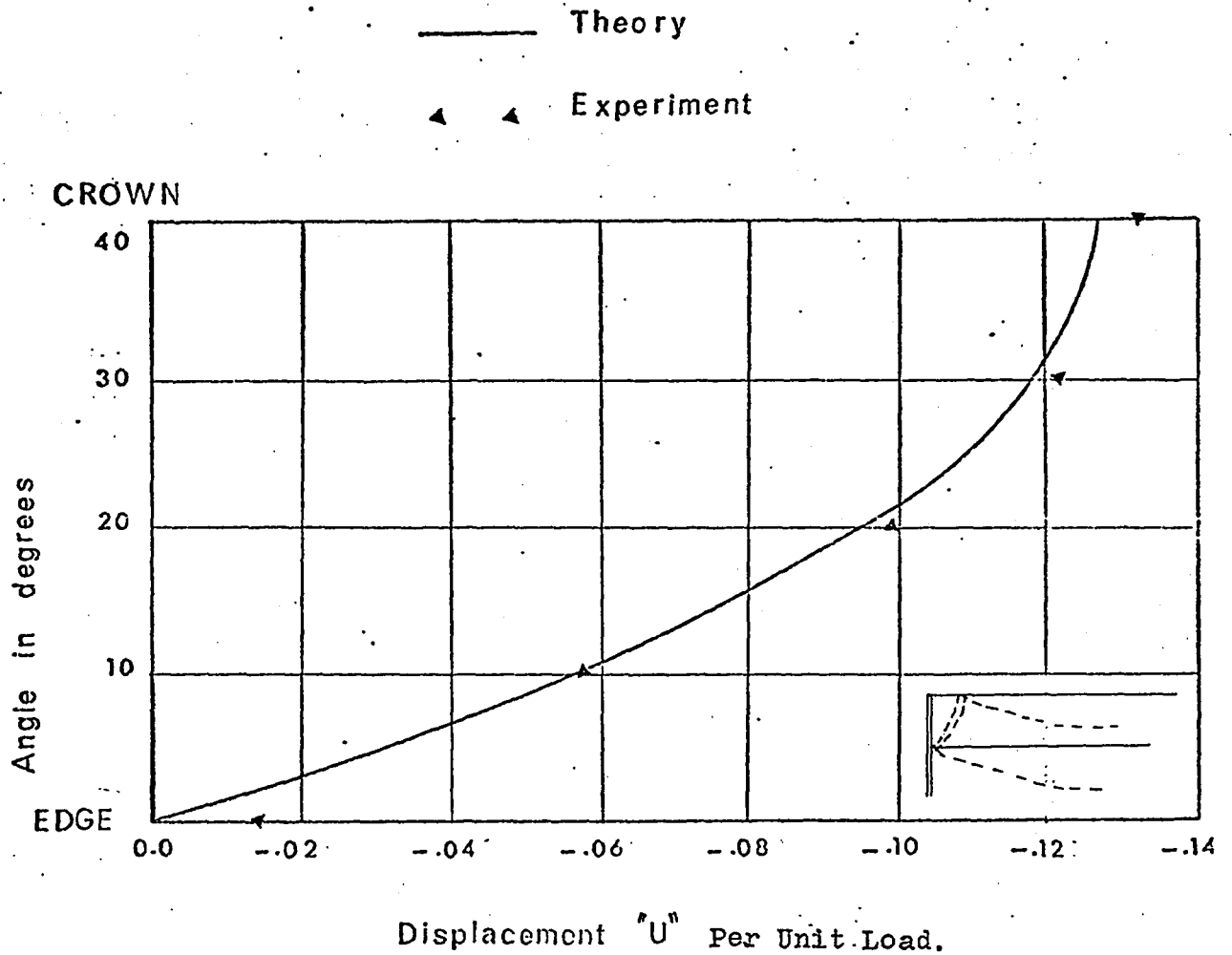
EXPERIMENT No 2



COMPARISON BETWEEN THEORETICAL AND EXPERIMENTAL VALUES OF "U"-DISPLACEMENT OF CROWN POINT AT SUPPORT.

Figure 12

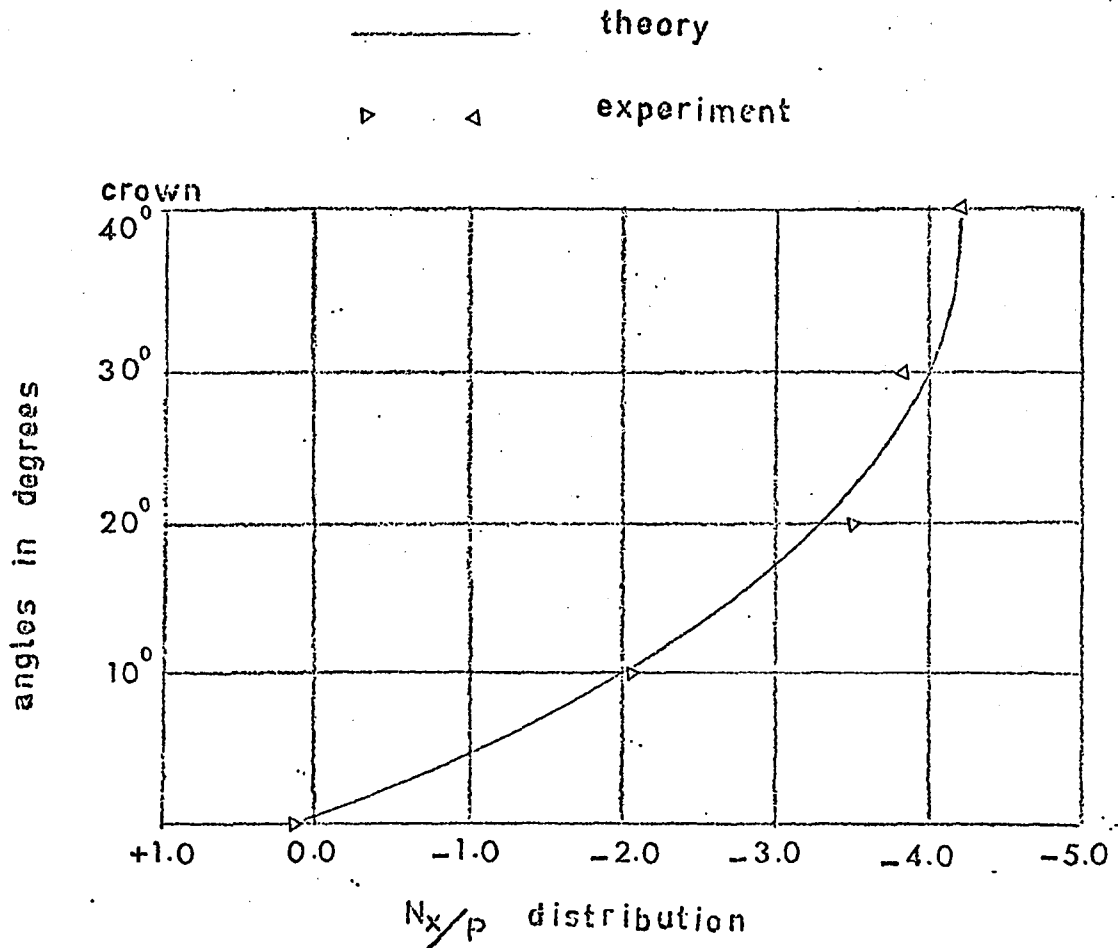
EXPERIMENT No 2



COMPARISON BETWEEN THEORETICAL AND EXPERIMENTAL
VALUES OF U-DISPLACEMENT AT SUPPORT

Figure 13

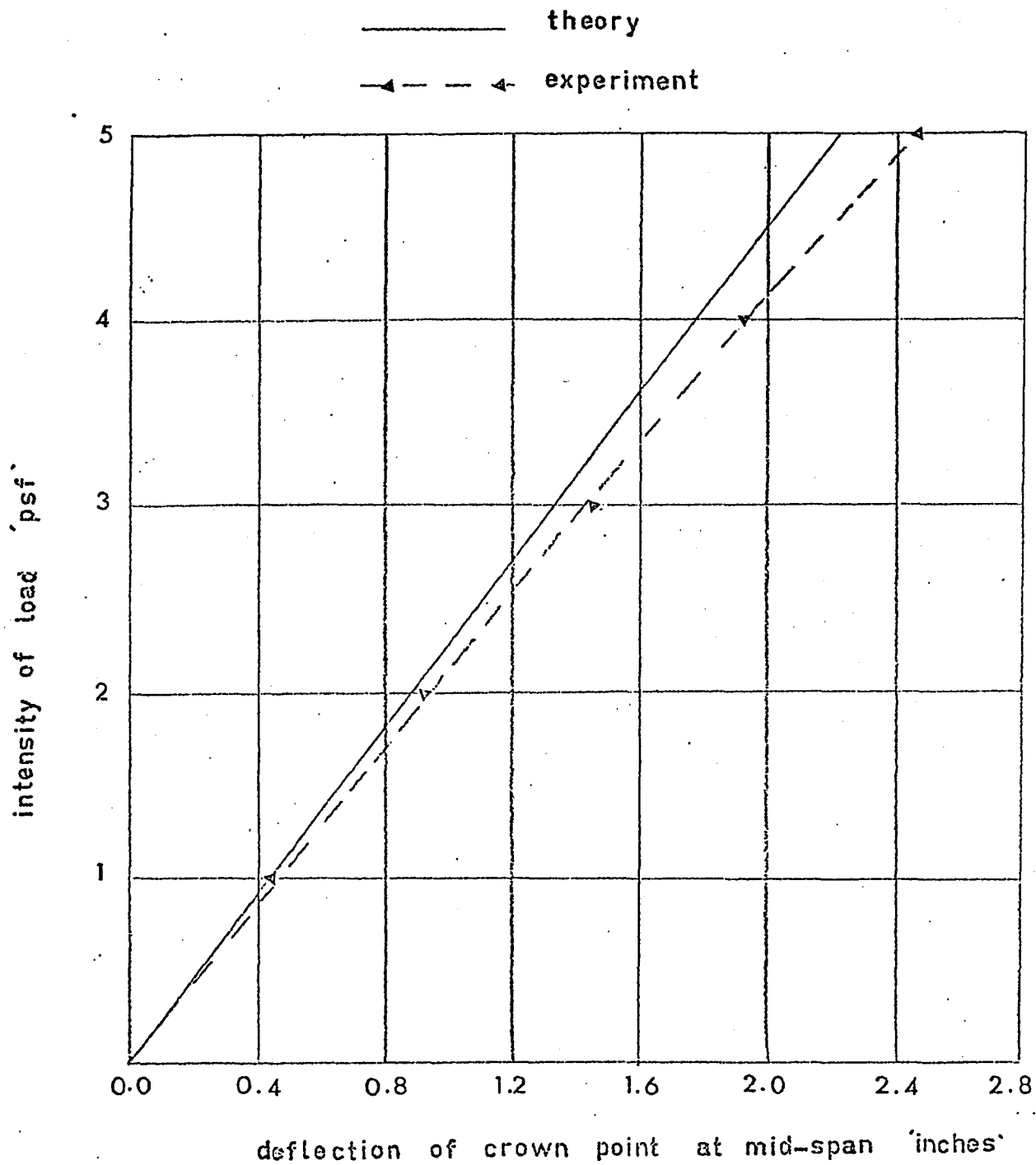
EXPERIMENT NO. 2



COMPARISON BETWEEN THEORETICAL AND EXPERIMENTAL
VALUES OF N_x -DISTRIBUTION AT MID-SPAN.

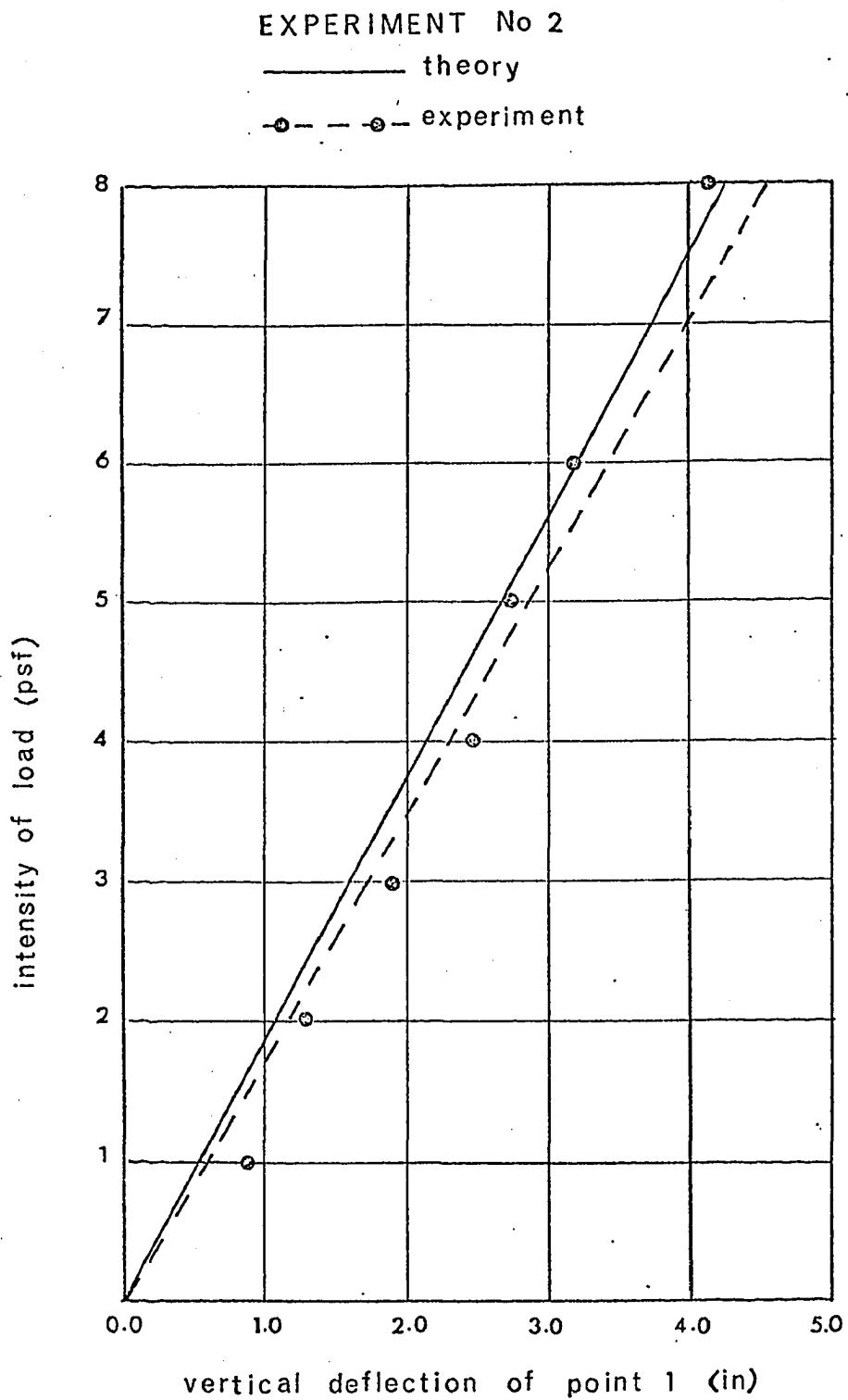
figure 14

EXPERIMENT NO. 2



COMPARISON BETWEEN THEORETICAL AND EXPERIMENTAL LOAD-
DEFLECTION CURVES OF CROWN POINT AT MID-SPAN.

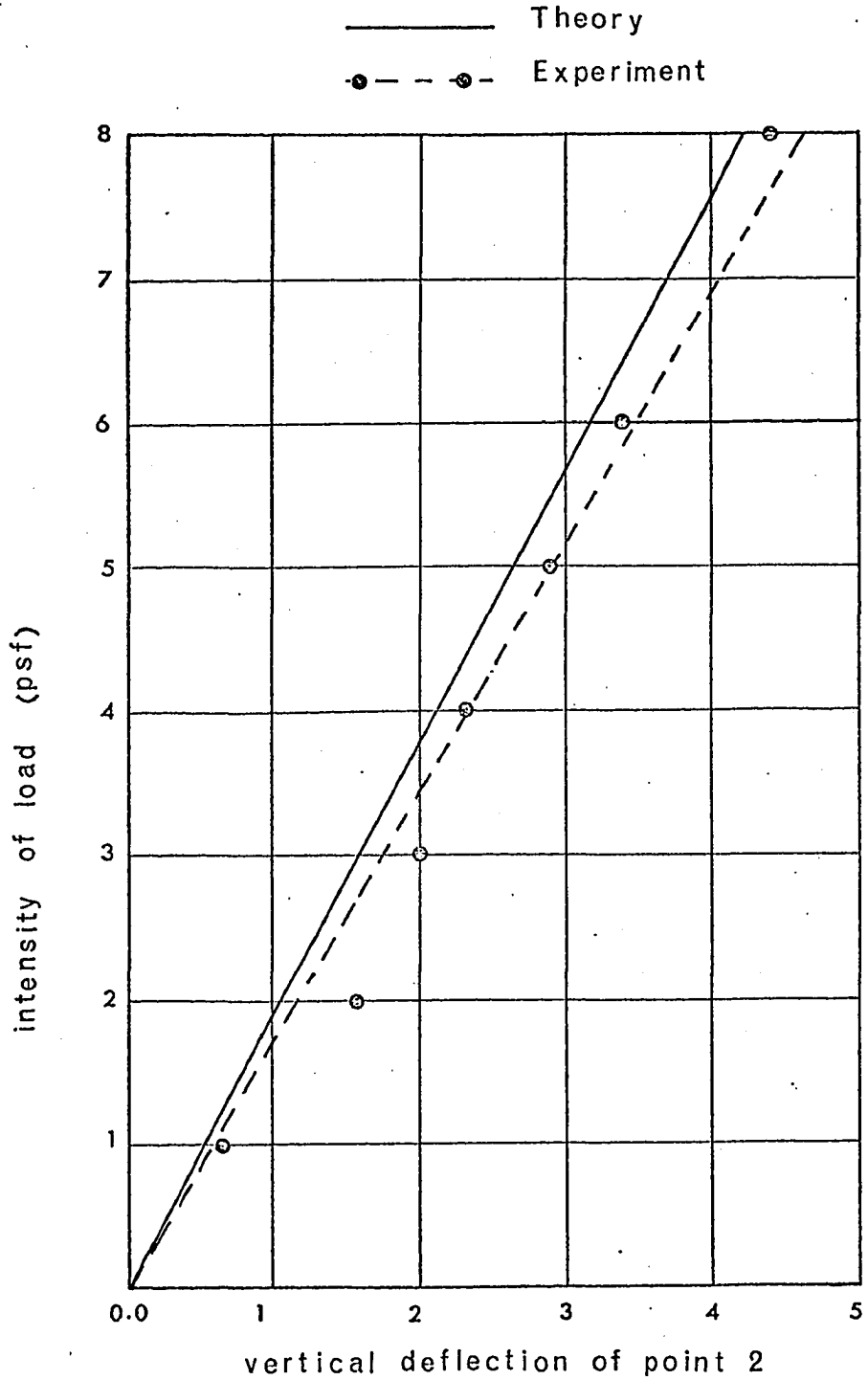
figure 15



COMPARISON BETWEEN THEORETICAL AND EXPERIMENTAL
LOAD-DEFLECTION CURVES FOR POINT 1

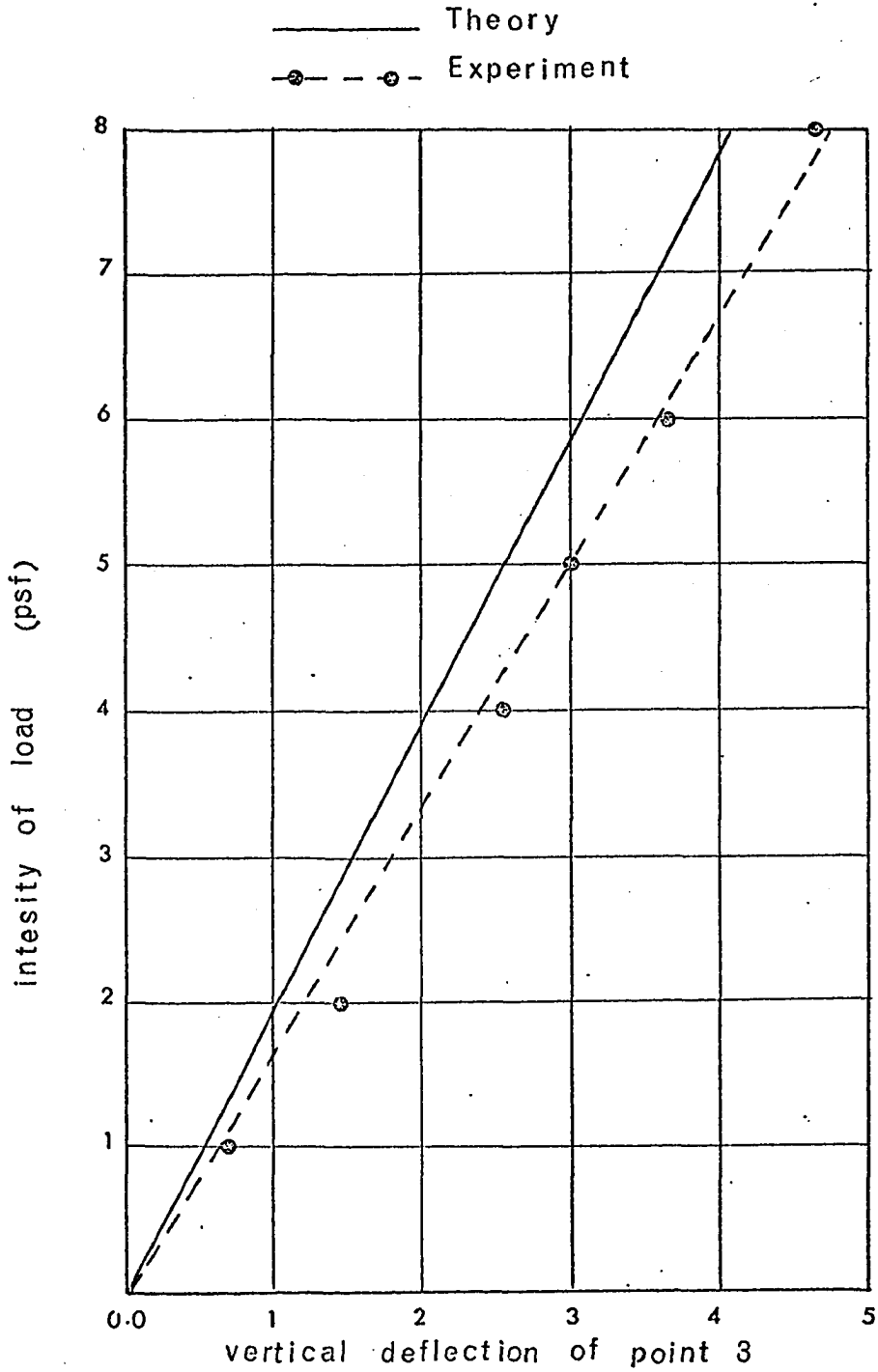
Figure 16

EXPERIMENT No. 2



COMPARISON BETWEEN THEORETICAL AND EXPERIMENTAL
LOAD-DEFLECTION CURVES FOR POINT 2

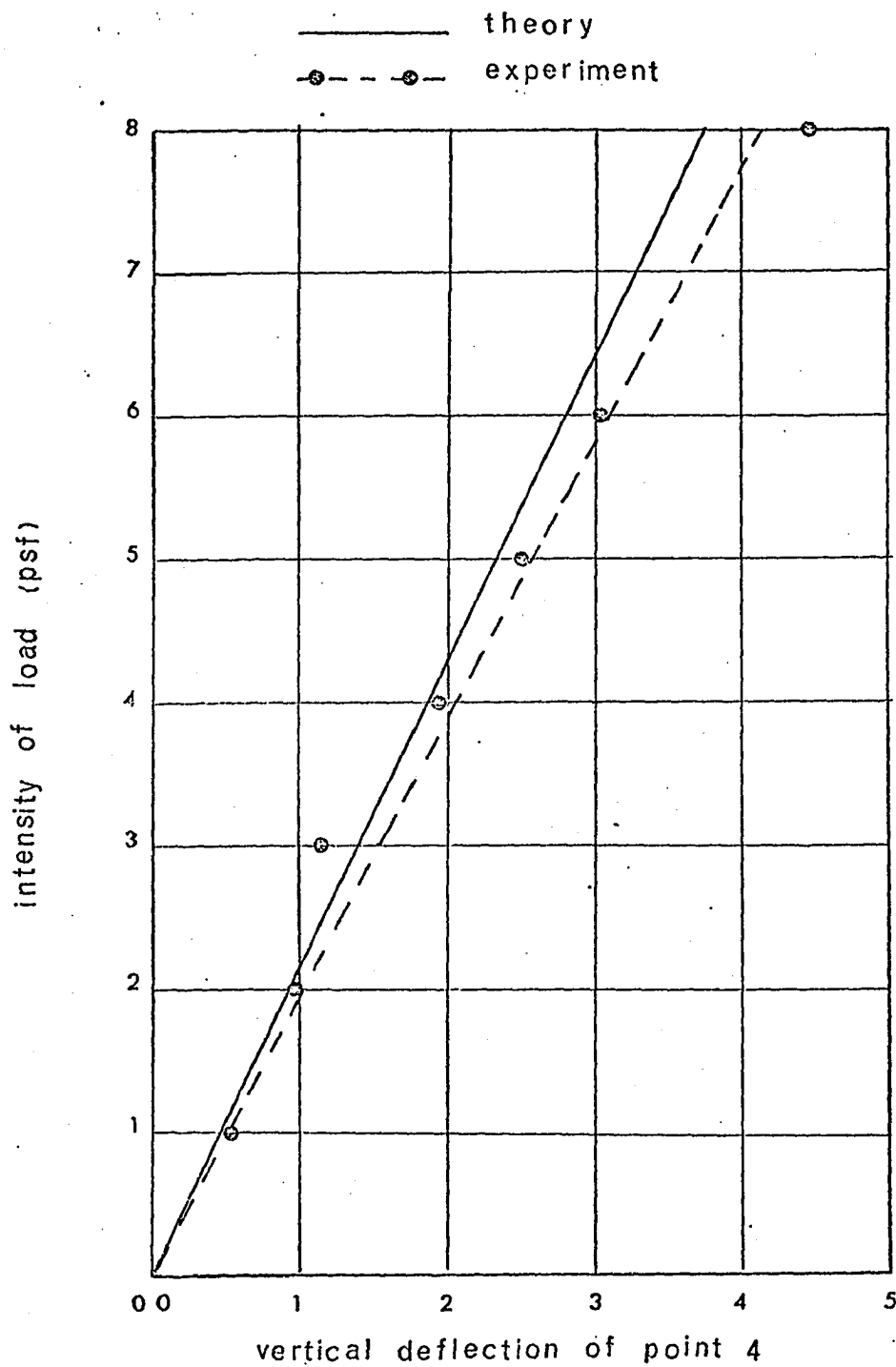
figure 17



COMPARISON BETWEEN THEORETICAL AND EXPERIMENTAL
LOAD-DEFLECTION CURVES FOR POINT 3

figure 18

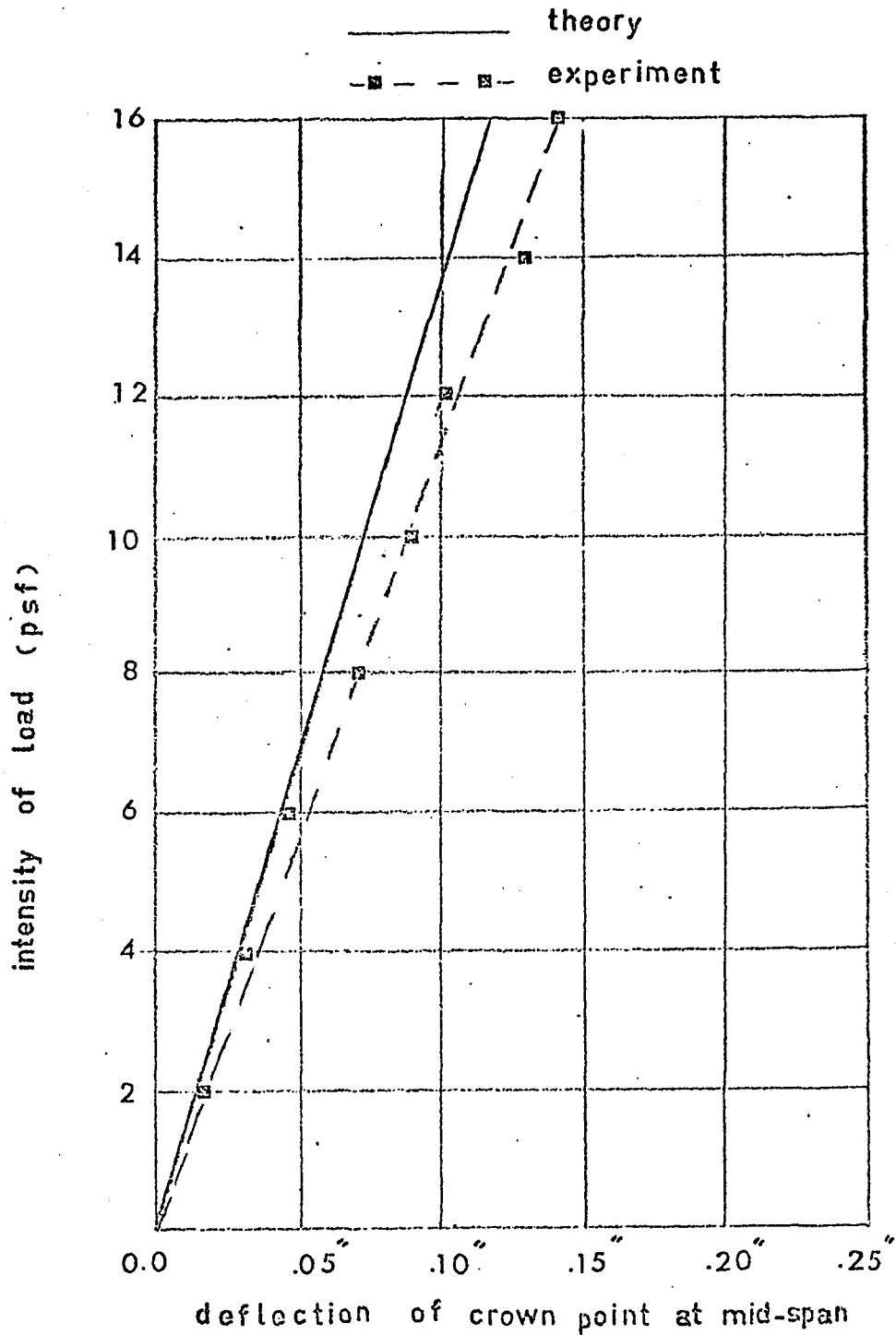
EXPERIMENT No 2



COMPARISON BETWEEN THEORETICAL AND EXPERIMENTAL
LOAD-DEFLECTION CURVES FOR POINT 4

figure 19

EXPERIMENT NO. 3



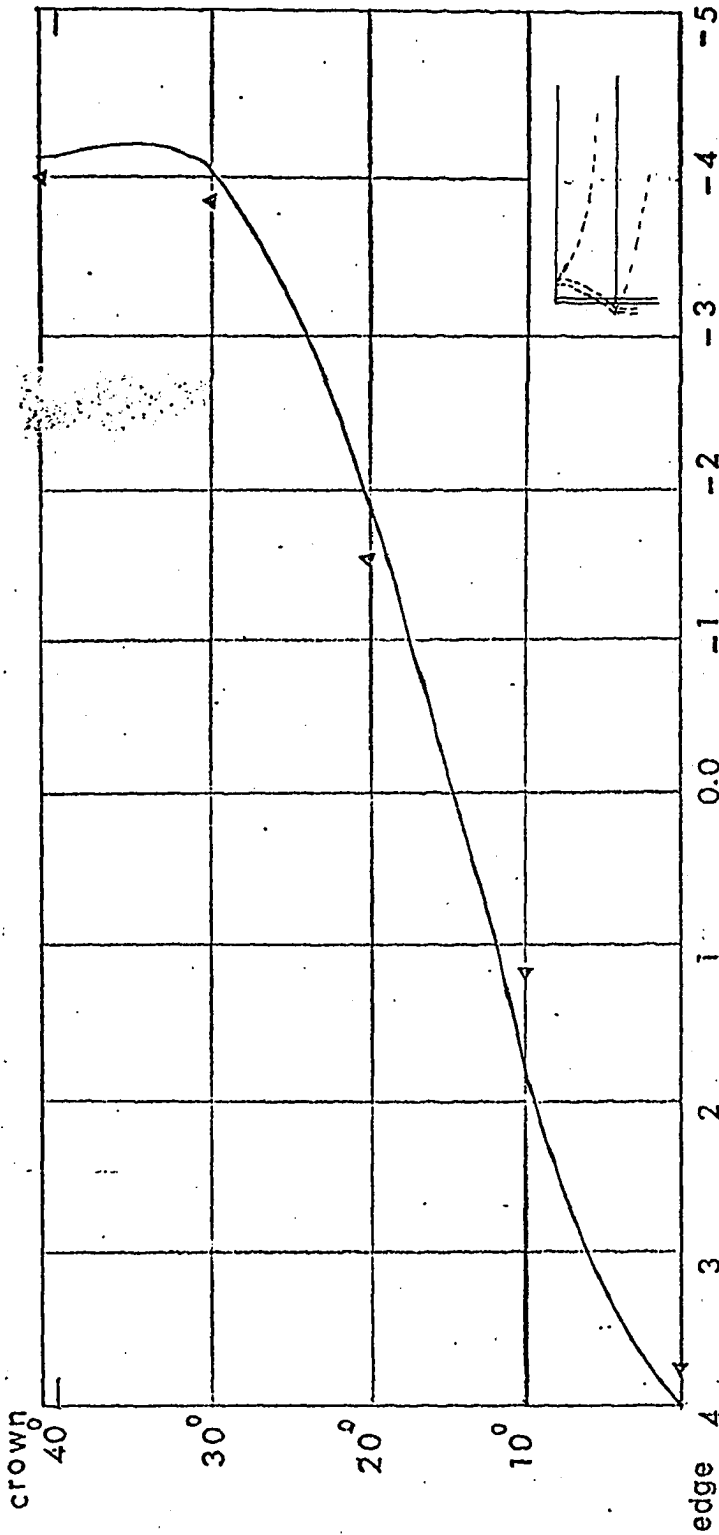
COMPARISON BETWEEN THEORETICAL AND EXPERIMENTAL LOAD-
DEFLECTION CURVES OF CROWN POINT AT MID-SPAN.

figure 20

EXPERIMENT NO. (3)

----- theory

△ experiment



"u" - displacement x 10⁴ (inches)
per unit load psf

COMPARISON BETWEEN THEORETICAL AND EXPERIMENTAL VALUES

OF THE DISPLACEMENT "U" AT SUPPORT.

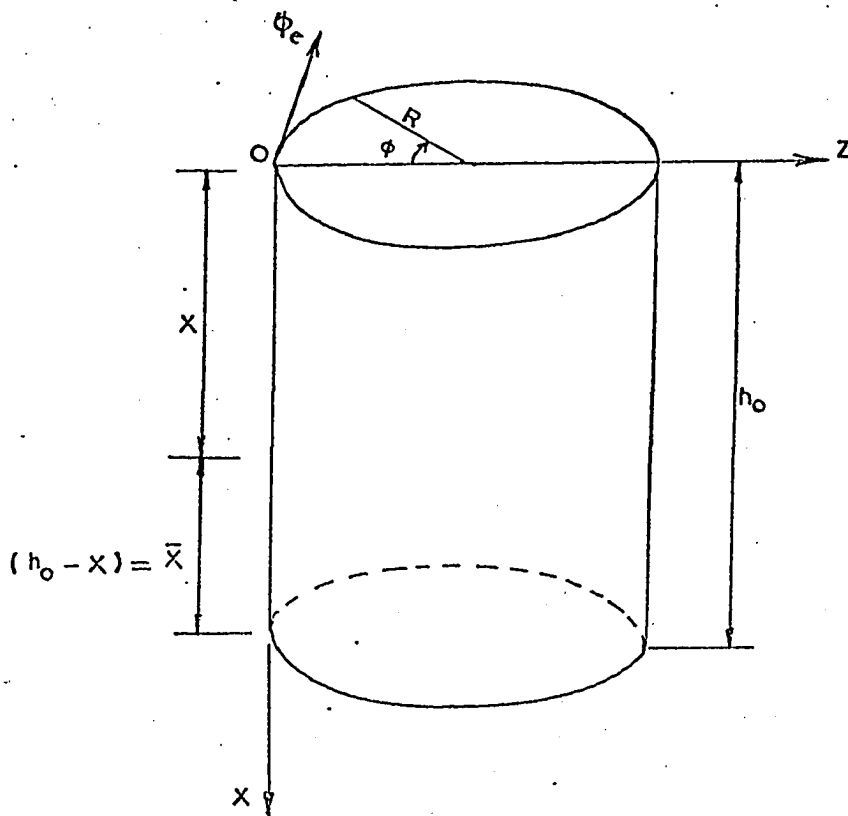


Figure (22): COORDINATE SYSTEM IN GRAIN BINS.

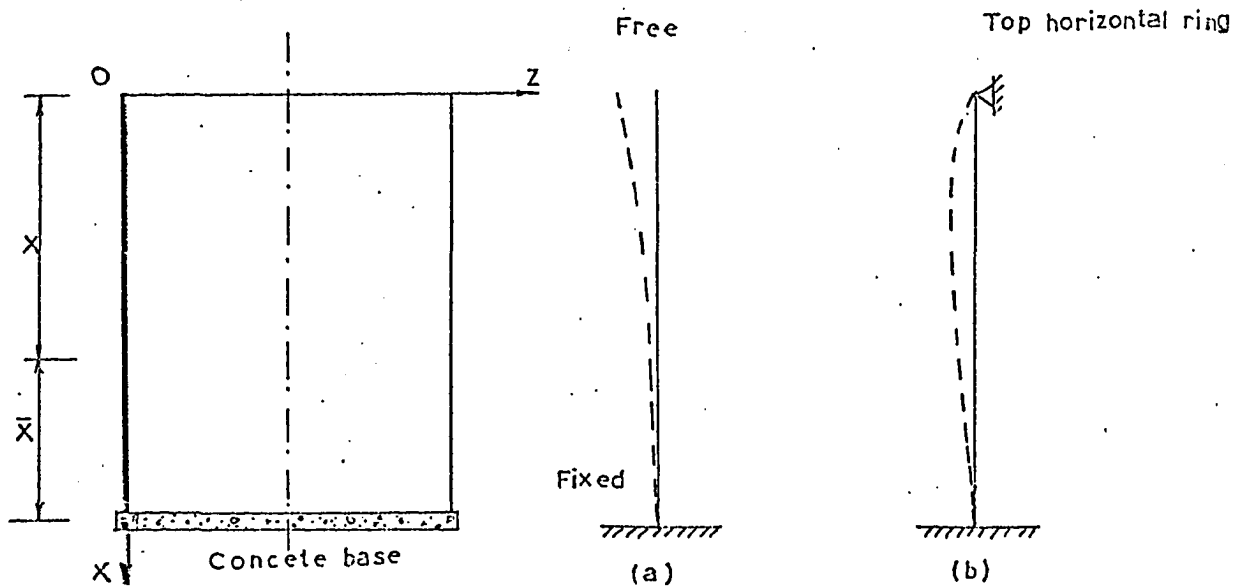
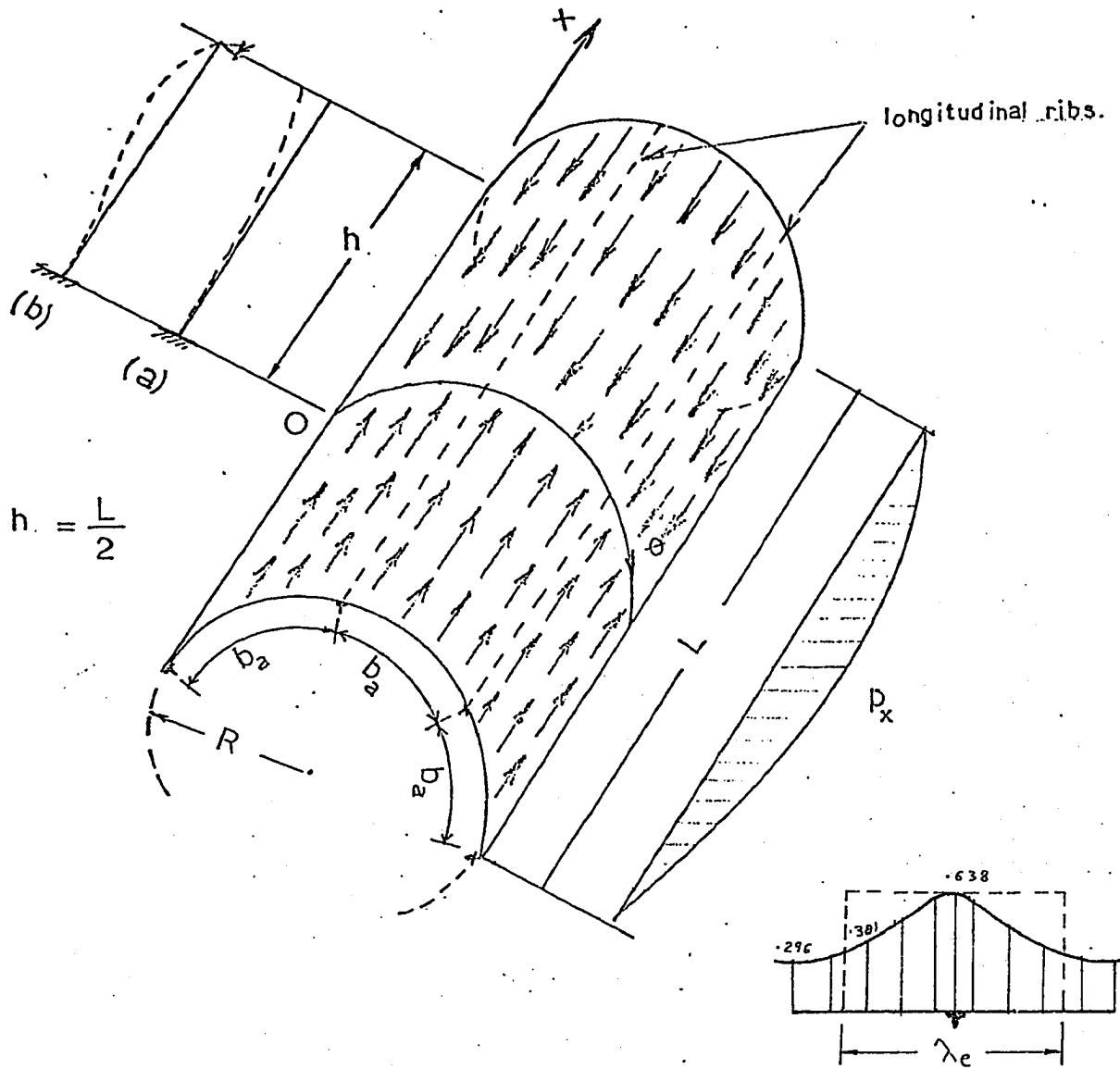


Figure (23): BOUNDARY CONDITIONS IN GRAIN BINS.



CIRCULAR BIN UNDER FRICTIONAL FORCES.

STIFFEND BY LONGITUDINAL RIBS.

FIGURE 24.

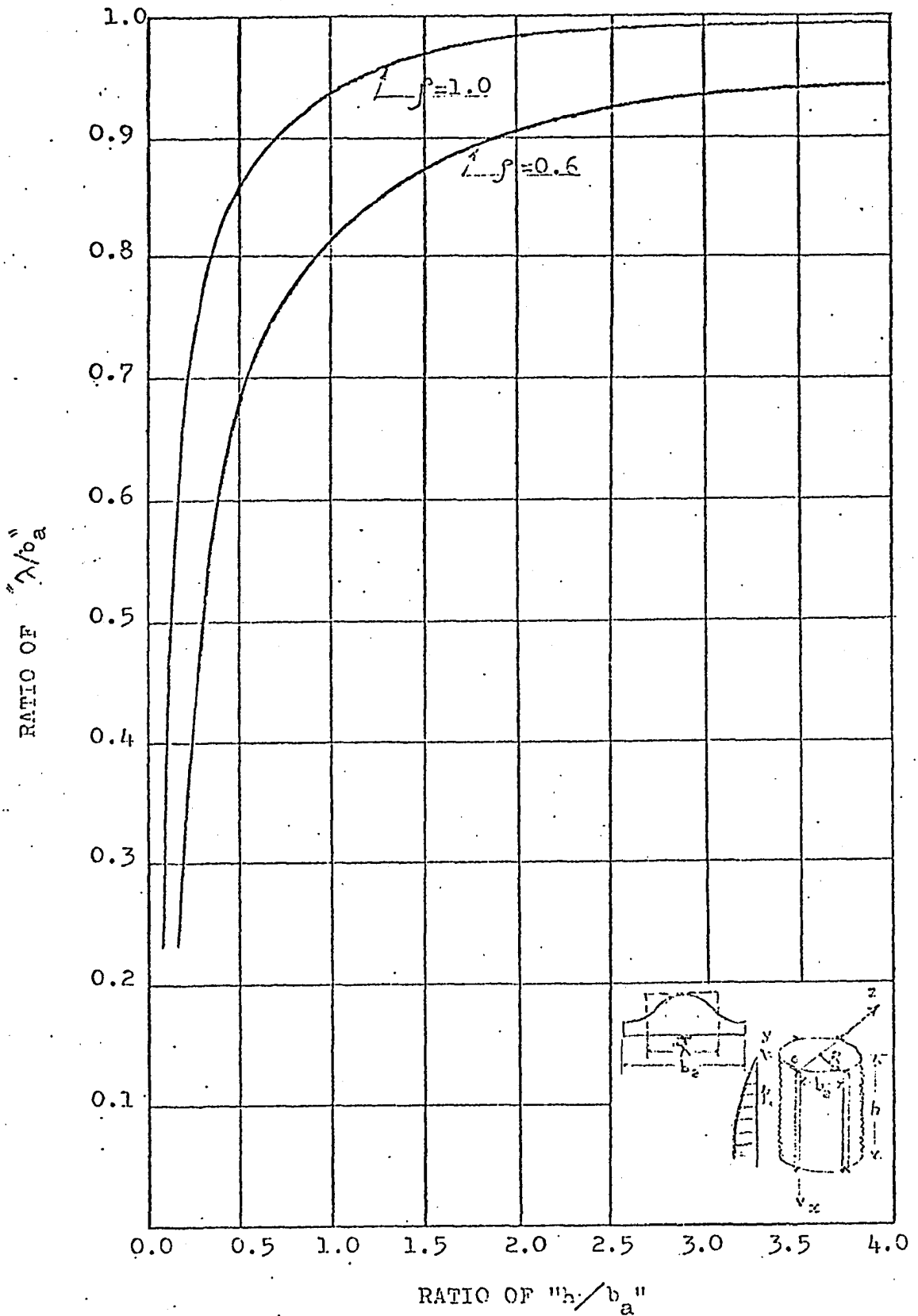


Fig. (25) - EFFECTIVE WIDTH OF CORRUGATED SHEETS.

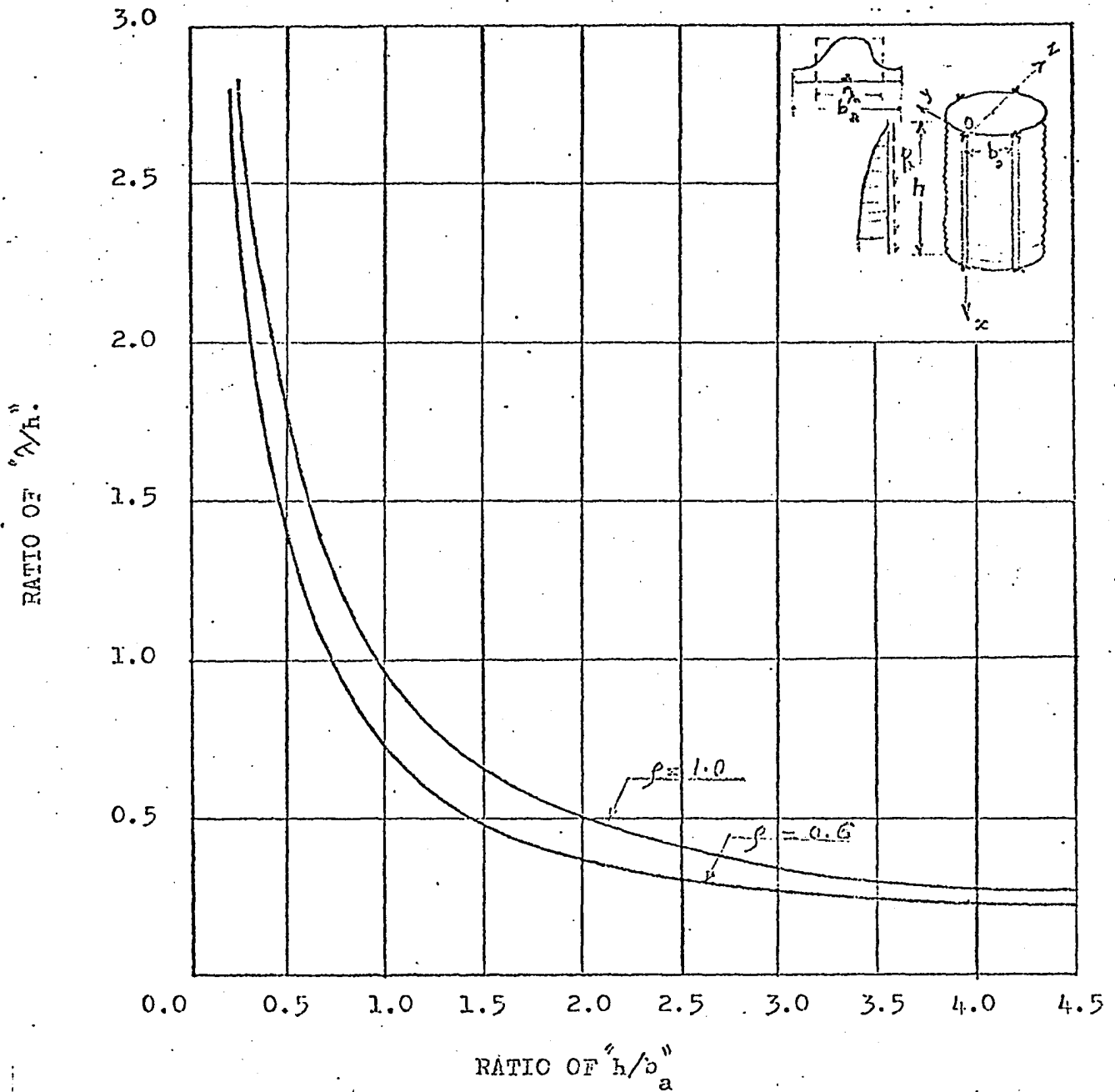


Fig. (26) - EFFECTIVE WIDTH OF CORRUGATED SHEETS.

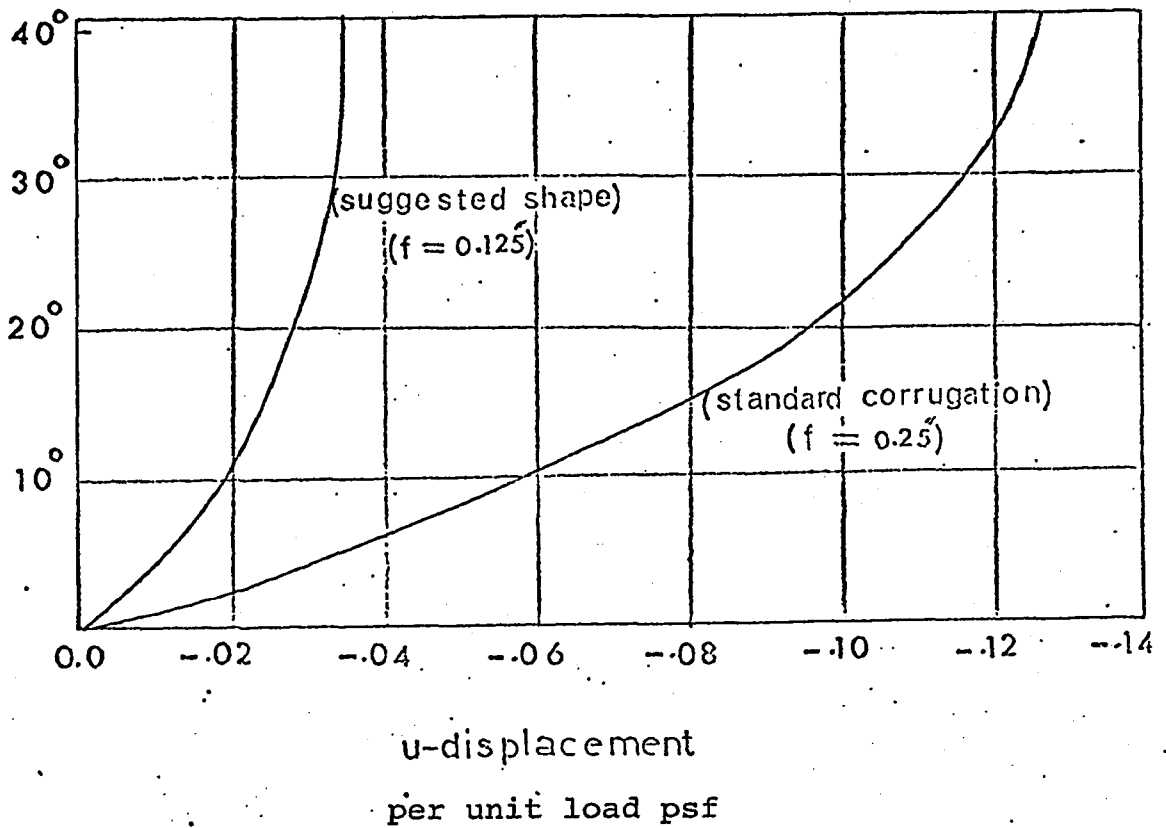


FIGURE 27

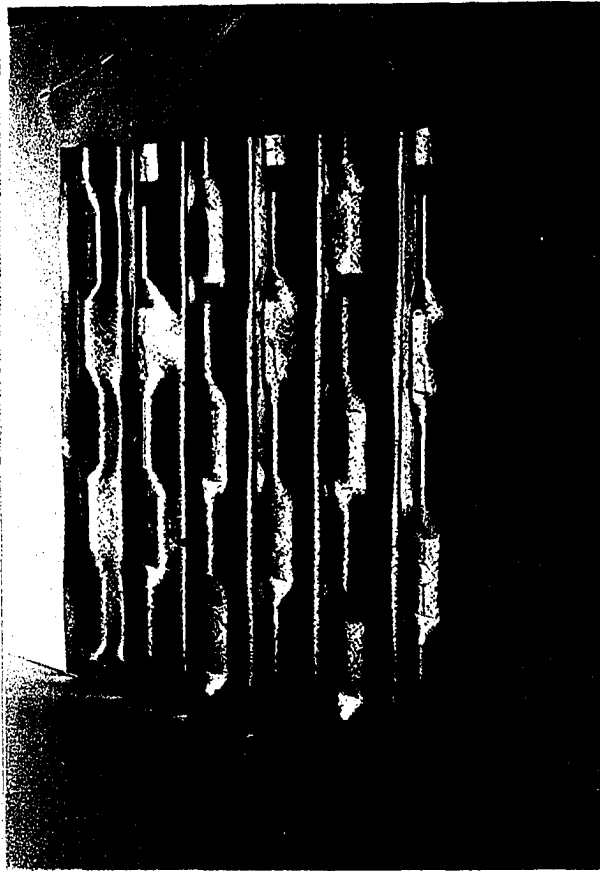


FIGURE (28): A PICTURE OF THE DIMPLED CORRUGATION.

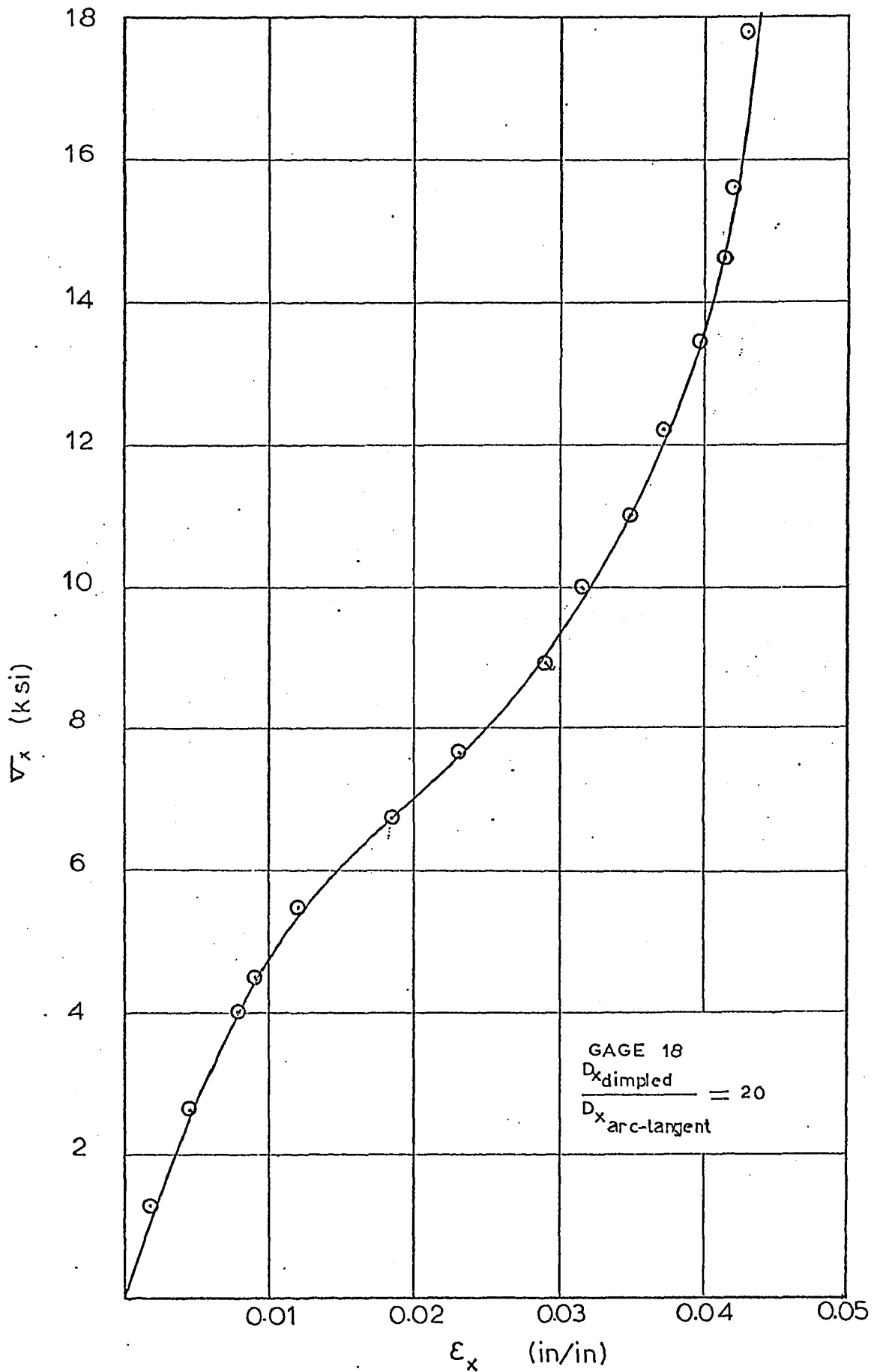


FIGURE (29-a) : STRESS-STRAIN CURVE OF DIMPLED SHAPE.

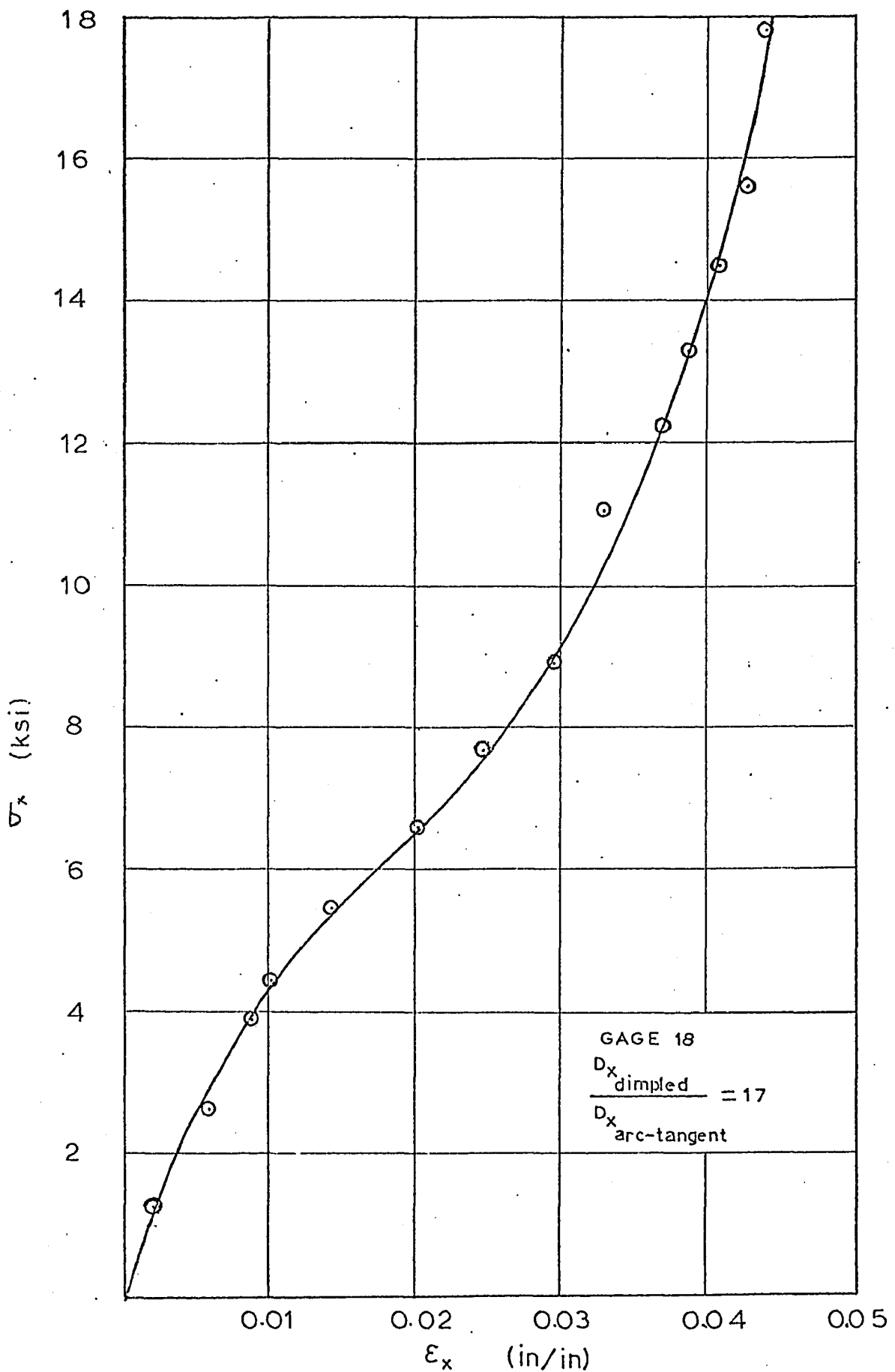


FIGURE (29-b): STRESS-STRAIN CURVE OF DIMPLED SHAPE

----- CONCRETE (t=4")

—————	$\frac{D_x}{D_\phi} = 0.004$	} GAGE 22
-----	$\frac{D_x}{D_\phi} = 0.5$	
- · - · -	$\frac{D_x}{D_\phi} = 1.0$	
- · - · -	$\frac{D_x}{D_\phi}$	

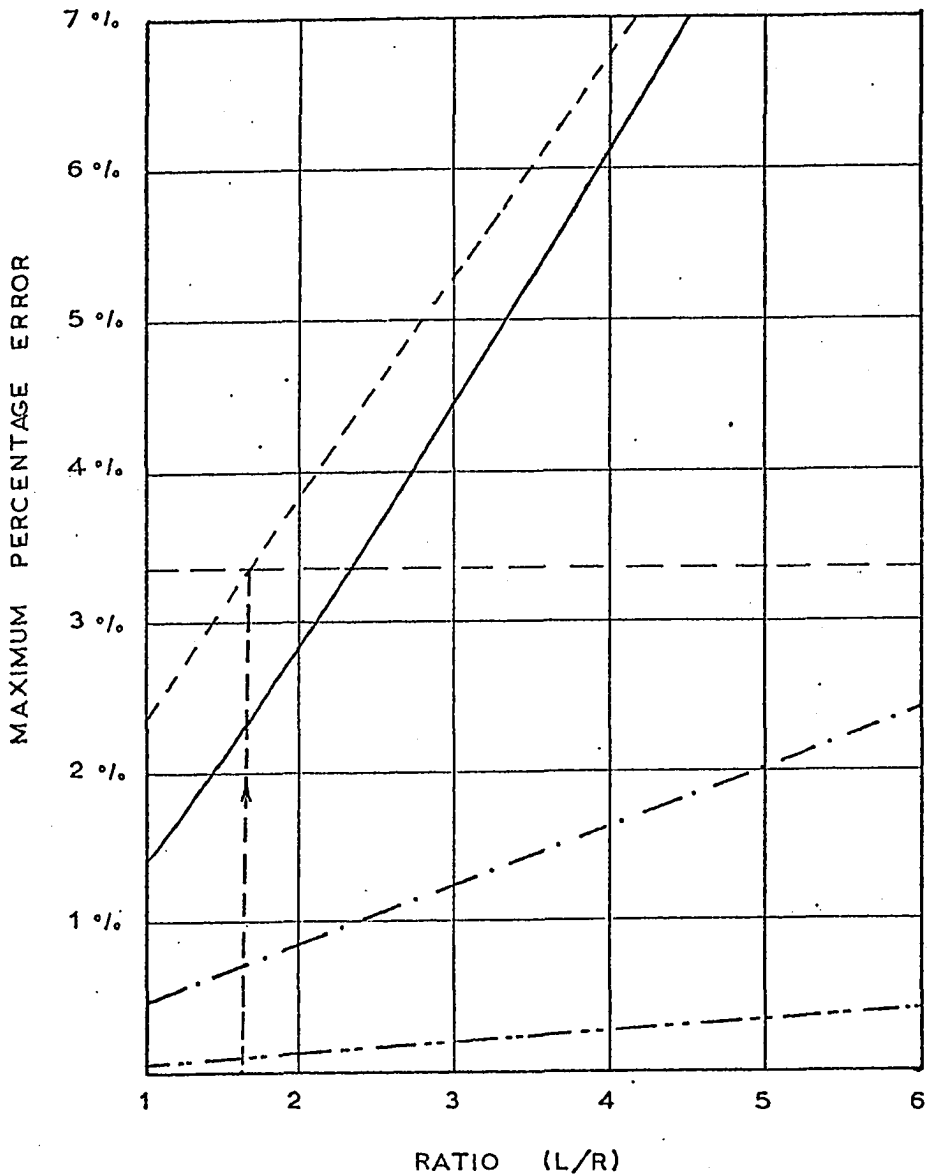
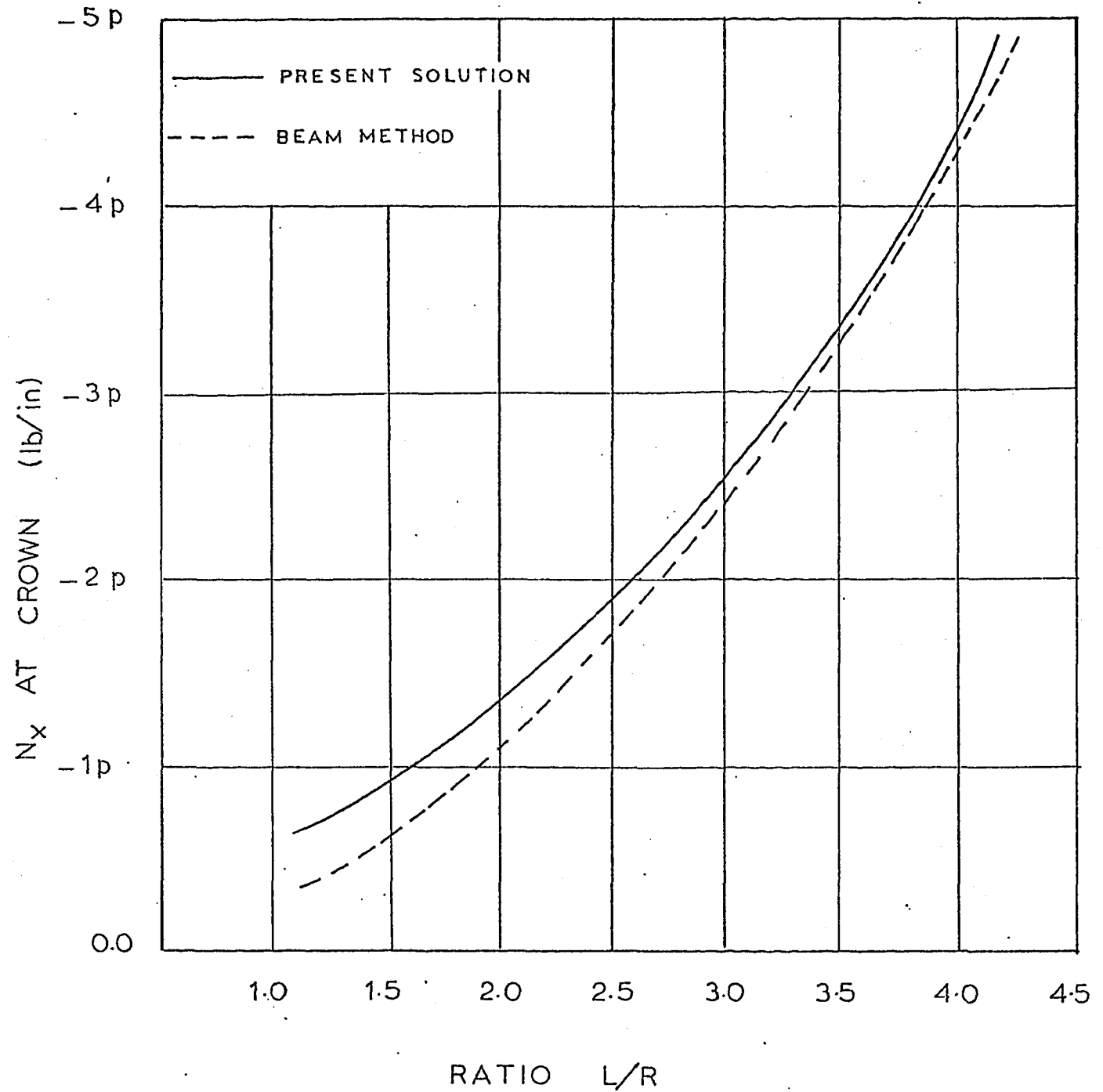


FIGURE (30) MAXIMUM PERCENTAGE ERROR IN THE ROOTS VS. RATIOS (L/R).



FIGURE(31): COMPARISON BETWEEN PRESENT SOLUTION AND THE BEAM METHOD FOR THIRD SUGGESTED FORM.

APPENDIX (I)

DERIVATION OF EXACT CHARACTERISTIC
EQUATION OF ORTHOTROPIC SHELLS

The governing differential equations, Eqn. (6-a, b, c), are rewritten as follows:

$$D_x \ddot{u} + \frac{B_x}{R} \ddot{w} + D_{x\phi} \left(\frac{\ddot{u}}{R^2} + \frac{\dot{v}}{R} \right) + \frac{B_{x\phi}}{2R^3} \left(\frac{\ddot{u}}{R} - \dot{w} \right) = 0 \quad (6-a)$$

$$D_\phi (\ddot{v} - \dot{w}) + D_{x\phi} (R \dot{u} + R^2 \ddot{v}) + \frac{3}{2} B_{x\phi} (\ddot{v} + \dot{w}) = 0 \quad (6-b)$$

$$D_\phi (\dot{v} - w) - \frac{B_\phi}{R^2} (\ddot{w} + 2\dot{w} + w) - B_x (R^2 \ddot{w} + R \dot{u}) - B_{x\phi} \left(2 \ddot{w} + \frac{3}{2} \dot{v} - \frac{1}{2R} \dot{u} \right) = 0 \quad (6-c)$$

Assuming a solution:

$$w = A^* e^{m\phi} \cos \frac{\lambda x}{R} \quad (i-a)$$

$$v = B^* e^{m\phi} \cos \frac{\lambda x}{R} \quad (i-b)$$

$$u = C^* e^{m\phi} \sin \frac{\lambda x}{R} \quad (i-c)$$

where $\lambda = \frac{\pi R}{L}$; A^* , B^* & C^* are constants.

Substituting equations (i-a, b, c) into the governing differential equations, Eqn. (6-a, b, c), the following three equations are obtained:

$$A^* \left[\frac{B_x}{R} \left(\frac{\lambda}{R} \right)^3 + \frac{m^2 B_{x\phi}}{2R^3} \left(\frac{\lambda}{R} \right) \right] - B^* \left[\frac{D_{x\phi}}{R} \left(\frac{\lambda}{R} \right) m \right] + C^* \left[\frac{D_{x\phi}}{R^2} m^2 - D_x \left(\frac{\lambda}{R} \right)^2 + \frac{B_{x\phi}}{2R^3} \frac{m^2}{R} \right] = 0 \quad (ii-a)$$

$$A^* \left[-D_\phi m - \frac{3B_{x\phi}}{2} m \left(\frac{\lambda}{R} \right)^2 \right] + B^* \left[D_\phi m^2 - D_{x\phi} R^2 \left(\frac{\lambda}{R} \right)^2 - \frac{3B_{x\phi}}{2} \left(\frac{\lambda}{R} \right)^2 \right] \\ + C^* \left[D_{x\phi} R m \left(\frac{\lambda}{R} \right) \right] = 0 \dots \dots \dots (ii-b)$$

$$A^* \left[-D_\phi - \frac{B_\phi}{R^2} m^4 - \frac{2B_\phi}{R^2} m^2 - \frac{B_\phi}{R^2} - B_x R^2 \left(\frac{\lambda}{R} \right)^4 + 2B_{x\phi} m^2 \left(\frac{\lambda}{R} \right)^2 \right] \\ + B^* \left[D_\phi m + \frac{3B_{x\phi}}{2} m \left(\frac{\lambda}{R} \right)^2 \right] + C^* \left[B_x R \left(\frac{\lambda}{R} \right)^3 + \frac{B_{x\phi}}{2R} m^2 \left(\frac{\lambda}{R} \right) \right] = \dots \dots \dots (ii-c)$$

Equations (ii-a, b, c) can be written in a matrix form as follows:

$$\begin{bmatrix}
 \left[\frac{B_x}{R} \left(\frac{A}{R} \right)^3 + \frac{m^2 B_{xp}}{2R^3} \left(\frac{A}{R} \right) \right] & \left[-\frac{D_{xp}}{R} m \left(\frac{A}{R} \right) \right] & \left[\frac{D_{xp}^2 m^2 - D_x^2 \left(\frac{A}{R} \right)^2 + \frac{B_{xp} m^2}{2R^4} \right] \\
 \left[-D_p m - \frac{3B_{xp} m}{2} \left(\frac{A}{R} \right)^2 \right] & \left[D_p m^2 - D_{xp}^2 \left(\frac{A}{R} \right)^2 - \frac{3B_{xp}}{2} \left(\frac{A}{R} \right)^3 \right] & \left[D_{xp} R m \left(\frac{A}{R} \right) \right] \\
 \left[-D_p - \frac{B_x}{R^2} m^4 - \frac{B_x}{R^2} 2m^2 - \frac{B_x}{R^2} - B_x^2 \left(\frac{A}{R} \right)^4 + 2B_{xp} m^2 \left(\frac{A}{R} \right)^2 \right] & \left[D_p m + \frac{3B_{xp}}{2} m \left(\frac{A}{R} \right)^2 \right] & \left[B_x R \left(\frac{A}{R} \right)^3 + \frac{B_{xp} m^2}{2R} \left(\frac{A}{R} \right) \right]
 \end{bmatrix}
 \begin{bmatrix}
 A \\
 B \\
 C
 \end{bmatrix}
 = \{0\}$$

$$\therefore [F] \cdot [A] = \{0\}$$

$$\therefore [F] = \{0\}$$

Thus the determinant of $[F]$ should equal to zero.

Expanding this determinant and equating to zero, the exact characteristic equation is obtained.

as follows:

$$\begin{aligned}
& m^8 \left[\frac{1}{R^4} \left(\frac{D_{x\phi} D_\phi B_\phi}{1} + \frac{B_{x\phi} D_\phi B_\phi}{2 R^2} \right) \right] + m^6 \left[\lambda^2 \left(\frac{D_\phi B_{x\phi}^2}{4 R^6} + \frac{D_{x\phi}^2 B_\phi}{R^4} \right. \right. \\
& - \frac{2 D_\phi D_{x\phi} B_{x\phi}}{R^4} - \frac{D_{x\phi}^2 B_\phi}{R^4} - \frac{3 D_{x\phi} B_\phi B_{x\phi}}{2 R^6} - \frac{D_x D_\phi B_\phi}{R^4} \\
& - \frac{D_\phi B_{x\phi}^2}{R^6} - \frac{D_{x\phi} B_\phi B_{x\phi}}{2 R^6} - \left. \frac{3 B_\phi B_{x\phi}^2}{4 R^8} \right) + \left(\frac{2 B_\phi D_\phi D_{x\phi}}{R^4} \right. \\
& + \left. \frac{D_\phi B_\phi B_{x\phi}}{R^6} \right) \Big] + m^4 \left[\lambda^4 \left(\frac{B_x B_{x\phi} D_\phi}{2 R^6} + \frac{B_{x\phi} B_x D_\phi}{2 R^6} - \frac{B_{x\phi}^2 D_{x\phi}}{4 R^6} \right. \right. \\
& - \frac{3 B_{x\phi}^3}{8 R^8} - \frac{3 B_{x\phi}^2 D_{x\phi}}{4 R^6} - \frac{3 D_{x\phi} B_{x\phi}^2}{4 R^6} - \frac{2 D_{x\phi}^2 B_{x\phi}}{R^4} - \frac{9 D_{x\phi} B_{x\phi}^2}{4 R^6} \\
& + \frac{D_\phi D_{x\phi} B_x}{R^4} + \frac{2 D_{x\phi}^2 B_{x\phi}}{R^4} + \frac{3 D_{x\phi} B_{x\phi}^2}{R^6} + \frac{2 D_x D_\phi B_{x\phi}}{R^4} \\
& + \frac{D_x D_{x\phi} B_\phi}{R^4} + \frac{3 D_x B_\phi B_{x\phi}}{2 R^6} - \frac{9 B_{x\phi}^3}{8 R^8} + \frac{B_x B_{x\phi} D_\phi}{2 R^6} + \frac{D_{x\phi} B_{x\phi}^2}{R^6} \\
& + \left. \frac{3 B_{x\phi}^3}{2 R^8} \right) + \lambda^2 \left(- \frac{D_\phi D_{x\phi} B_{x\phi}}{2 R^4} + \frac{2 B_\phi D_{x\phi}^2}{R^4} - \frac{3 D_\phi D_{x\phi} B_{x\phi}}{R^4} \right. \\
& - \frac{2 B_\phi D_{x\phi}^2}{R^4} - \frac{3 B_\phi B_{x\phi} D_{x\phi}}{R^6} - \frac{2 D_x D_\phi B_\phi}{R^4} - \frac{B_{x\phi} D_\phi D_{x\phi}}{2 R^4} \\
& - \left. \frac{3 D_\phi B_{x\phi}^2}{2 R^6} - \frac{B_\phi B_{x\phi} D_{x\phi}}{R^6} - \frac{3 B_{x\phi}^2 B_\phi}{2 R^6} \right) + \left(- \frac{D_{x\phi} D_\phi^2}{R^2} + \frac{D_{x\phi} D_\phi^2}{R^2} \right. \\
& + \frac{B_\phi D_\phi D_{x\phi}}{R^4} - \frac{B_{x\phi} D_\phi^2}{2 R^4} + \frac{B_{x\phi} D_\phi^2}{2 R^4} + \left. \frac{D_\phi B_{x\phi} B_\phi}{2 R^6} \right) \Big] + m^2 \left[\lambda^6 \left(\frac{D_\phi B_x^2}{R^6} \right. \right. \\
& - \frac{B_x B_{x\phi} D_{x\phi}}{2 R^6} - \frac{3 B_x B_{x\phi} D_{x\phi}}{2 R^6} - \frac{3 B_x B_{x\phi}^2}{4 R^8} - \frac{B_x B_{x\phi} D_{x\phi}}{2 R^6} - \frac{3 B_x B_{x\phi}^2}{4 R^8} \\
& - \frac{3 D_{x\phi} B_x B_{x\phi}}{2 R^6} - \frac{B_x D_{x\phi}^2}{R^4} - \frac{3 B_x B_{x\phi} D_{x\phi}}{2 R^6} + \frac{B_x D_{x\phi}^2}{R^4} + \frac{9 D_x B_{x\phi}}{4 R^6} \\
& - \frac{B_x D_x D_\phi}{R^4} - \frac{2 D_x D_{x\phi} B_{x\phi}}{R^4} - \frac{3 D_x B_{x\phi}^2}{R^6} - \frac{B_x B_{x\phi} D_{x\phi}}{2 R^6} - \left. \frac{3 B_x B_{x\phi}^2}{2 R^8} \right) \\
& + \lambda^4 \left(\frac{3 D_x B_\phi B_{x\phi}}{R^6} - \frac{2 B_x D_\phi D_{x\phi}}{R^4} + \frac{2 D_x D_{x\phi} B_\phi}{R^4} + \frac{3 D_x D_\phi B_{x\phi}}{R^4} \right) \\
& + \lambda^2 \left(\frac{D_\phi D_{x\phi}^2}{R^2} + \frac{B_\phi D_{x\phi}^2}{R^4} - \frac{D_\phi D_{x\phi}^2}{R^2} - \frac{B_\phi D_{x\phi}^2}{R^4} - \frac{3 D_\phi D_{x\phi} B_{x\phi}}{2 R^4} \right. \\
& - \left. \frac{3 B_\phi B_{x\phi} D_{x\phi}}{2 R^6} + \frac{D_x D_\phi^2}{R^2} - \frac{D_x D_\phi^2}{R^2} - \frac{D_x D_\phi B_\phi}{R^4} - \frac{D_\phi D_{x\phi} B_{x\phi}}{2 R^4} \right)
\end{aligned}$$

$$\begin{aligned}
& - \frac{B_\phi B_{x\phi} D_{x\phi}}{2R^6} - \frac{3D_{x\phi} B_{x\phi}^2}{4R^6} - \frac{3B_\phi B_{x\phi}^2}{2R^8} \Big] + \left[\lambda^8 \left(- \frac{B_{x\phi}^2 D_{x\phi}}{R^6} \right. \right. \\
& - \frac{3B_{x\phi}^2 B_{x\phi}}{2R^8} + \frac{D_x B_x D_{x\phi}}{R^4} + \frac{3D_x B_x B_{x\phi}}{2R^6} \Big) + \lambda^4 \left(\frac{D_x D_\phi D_{x\phi}}{R^2} \right. \\
& \left. \left. + \frac{D_x D_{x\phi} B_\phi}{R^4} + \frac{3D_x D_\phi B_{x\phi}}{2R^4} + \frac{3D_x B_\phi B_{x\phi}}{2R^6} \right) \right] = 0
\end{aligned}$$

Neglecting terms containing $\frac{1}{R^2}$ w.r.t. unity inside brackets after multiplying both sides by $\left(\frac{R^4}{D_{x\phi} D_\phi B_\phi} \right)$, the following equation is obtained:

$$\begin{aligned}
& m^8 + m^6 \left[\lambda^2 \left(- \frac{2B_{x\phi}}{B_\phi} - \frac{D_x}{D_{x\phi}} \right) + 2 \right] + m^4 \left[\lambda^4 \left(\frac{B_x}{B_\phi} + \frac{D_x}{D_\phi} \right. \right. \\
& \left. \left. + \frac{2D_x B_{x\phi}}{D_{x\phi} B_\phi} \right) + \lambda^2 \left(- \frac{4B_{x\phi}}{B_\phi} - \frac{2D_x}{D_{x\phi}} \right) + 1 \right] + m^2 \left[\lambda^6 \left(- \frac{B_x D_x}{B_\phi D_{x\phi}} \right. \right. \\
& \left. \left. - \frac{2D_x B_{x\phi}}{D_\phi B_\phi} \right) + \lambda^4 \left(\frac{2D_x}{D_\phi} + \frac{3D_x B_{x\phi}}{D_{x\phi} B_\phi} - \frac{2B_x}{B_\phi} \right) + \lambda^2 \left(- \frac{2B_{x\phi}}{B_\phi} - \frac{D_x}{D_{x\phi}} \right) \right] \\
& \left. + \left[\lambda^8 \left(\frac{D_x B_x}{D_\phi B_\phi} \right) + \lambda^4 \left(\frac{D_x R^2}{B_\phi} + \frac{3D_x B_{x\phi}}{2D_{x\phi} B_\phi} + \frac{D_x}{D_\phi} \right) \right] = 0 \dots \dots (25)
\end{aligned}$$

Equation (25) is the exact characteristic equation.

APPENDIX (II)

STRESS-RESULTANTS AND DISPLACEMENTS

DUE TO BENDING

1. LONGITUDINAL BENDING MOMENTS "M_x" :

$$M_x = B_x \left(\frac{\lambda}{R} \right)^2 \left[e^{\alpha_1 \phi} (A \cos \beta_1 \phi + B \sin \beta_1 \phi) + e^{-\alpha_1 \phi} (C \cos \beta_1 \phi + D \sin \beta_1 \phi) + e^{\alpha_2 \phi} (E \cos \beta_2 \phi + F \sin \beta_2 \phi) + e^{-\alpha_2 \phi} (G \cos \beta_2 \phi + H \sin \beta_2 \phi) \right] \cos \frac{\lambda x}{R} .$$

2. TRANSVERSAL BENDING MOMENTS "M_φ" :

$$M_\phi = - \frac{B_\phi}{R^2} \left[A (e^{\alpha_1 \phi} \{ (\alpha_1^2 - \beta_1^2) \cos \beta_1 \phi - 2 \alpha_1 \beta_1 \sin \beta_1 \phi \}) + B (e^{\alpha_1 \phi} \{ (\alpha_1^2 - \beta_1^2) \sin \beta_1 \phi + 2 \alpha_1 \beta_1 \cos \beta_1 \phi \}) + C (e^{-\alpha_1 \phi} \{ (\alpha_1^2 - \beta_1^2) \cos \beta_1 \phi + 2 \alpha_1 \beta_1 \sin \beta_1 \phi \}) + D (e^{-\alpha_1 \phi} \{ (\alpha_1^2 - \beta_1^2) \sin \beta_1 \phi - 2 \alpha_1 \beta_1 \cos \beta_1 \phi \}) + E (e^{\alpha_2 \phi} \{ (\alpha_2^2 - \beta_2^2) \cos \beta_2 \phi - 2 \alpha_2 \beta_2 \sin \beta_2 \phi \}) + F (e^{\alpha_2 \phi} \{ (\alpha_2^2 - \beta_2^2) \sin \beta_2 \phi + 2 \alpha_2 \beta_2 \cos \beta_2 \phi \}) + G (e^{-\alpha_2 \phi} \{ (\alpha_2^2 - \beta_2^2) \cos \beta_2 \phi + 2 \alpha_2 \beta_2 \sin \beta_2 \phi \}) + H (e^{-\alpha_2 \phi} \{ (\alpha_2^2 - \beta_2^2) \sin \beta_2 \phi - 2 \alpha_2 \beta_2 \cos \beta_2 \phi \}) \right] \cos \frac{\lambda x}{R} .$$

3. TWISTING MOMENTS "M_{xφ}" :

$$\begin{aligned}
 M_{x\phi} = & B_{x\phi} \frac{\lambda}{R^2} \left[A \left\{ e^{\alpha_1 \phi} (\alpha_1 \cos \beta_1 \phi - \beta_1 \sin \beta_1 \phi) \right\} \right. \\
 & + B \left\{ e^{\alpha_1 \phi} (\alpha_1 \sin \beta_1 \phi + \beta_1 \cos \beta_1 \phi) \right\} \\
 & + C \left\{ e^{-\alpha_1 \phi} (-\alpha_1 \cos \beta_1 \phi - \beta_1 \sin \beta_1 \phi) \right\} \\
 & + D \left\{ e^{-\alpha_1 \phi} (-\alpha_1 \sin \beta_1 \phi + \beta_1 \cos \beta_1 \phi) \right\} \\
 & + E \left\{ e^{\alpha_2 \phi} (\alpha_2 \cos \beta_2 \phi - \beta_2 \sin \beta_2 \phi) \right\} \\
 & + F \left\{ e^{\alpha_2 \phi} (\alpha_2 \sin \beta_2 \phi + \beta_2 \cos \beta_2 \phi) \right\} \\
 & + G \left\{ e^{-\alpha_2 \phi} (-\alpha_2 \cos \beta_2 \phi - \beta_2 \sin \beta_2 \phi) \right\} \\
 & \left. + H \left\{ e^{-\alpha_2 \phi} (-\alpha_2 \sin \beta_2 \phi + \beta_2 \cos \beta_2 \phi) \right\} \right] \sin \frac{\lambda x}{R}
 \end{aligned}$$

4. LONGITUDINAL SHEARING FORCES "Q_x" :

$$\begin{aligned}
 Q_x = & \frac{\lambda}{R^3} \left[A \left\{ e^{\alpha_1 \phi} (S_1 \cos \beta_1 \phi - 2 \alpha_1 \beta_1 B_{x\phi} \sin \beta_1 \phi) \right\} \right. \\
 & + B \left\{ e^{\alpha_1 \phi} (S_1 \sin \beta_1 \phi + 2 \alpha_1 \beta_1 B_{x\phi} \cos \beta_1 \phi) \right\} \\
 & + C \left\{ e^{-\alpha_1 \phi} (S_1 \cos \beta_1 \phi + 2 \alpha_1 \beta_1 B_{x\phi} \sin \beta_1 \phi) \right\} \\
 & + D \left\{ e^{-\alpha_1 \phi} (S_1 \sin \beta_1 \phi - 2 \alpha_1 \beta_1 B_{x\phi} \cos \beta_1 \phi) \right\} \\
 & + E \left\{ e^{\alpha_2 \phi} (S_2 \cos \beta_2 \phi - 2 \alpha_2 \beta_2 B_{x\phi} \sin \beta_2 \phi) \right\} \\
 & + F \left\{ e^{\alpha_2 \phi} (S_2 \sin \beta_2 \phi + 2 \alpha_2 \beta_2 B_{x\phi} \cos \beta_2 \phi) \right\} \\
 & + G \left\{ e^{-\alpha_2 \phi} (S_2 \cos \beta_2 \phi + 2 \alpha_2 \beta_2 B_{x\phi} \sin \beta_2 \phi) \right\} \\
 & \left. + H \left\{ e^{-\alpha_2 \phi} (S_2 \sin \beta_2 \phi - 2 \alpha_2 \beta_2 B_{x\phi} \cos \beta_2 \phi) \right\} \right]
 \end{aligned}$$

$$+ H \left\{ e^{-\alpha_2 \phi} (S_2 \sin \beta_2 \phi - 2 \alpha_2 \beta_2 B_{x\phi} \cos \beta_2 \phi) \right\} \cdot \sin \frac{\lambda x}{R}$$

$$\text{where: } S_1 = B_{x\phi} \alpha_1^2 - B_{x\phi} \beta_1^2 - B_x \lambda^2$$

$$\& S_2 = B_{x\phi} \alpha_2^2 - B_{x\phi} \beta_2^2 - B_x \lambda^2$$

5. TRANSVERSAL SHEARING FORCES "Q_φ" :

$$Q_\phi = \frac{1}{R^3} \left[A \left\{ e^{\alpha_1 \phi} \left((B_{x\phi} \alpha_1 \lambda^2 + 3 \alpha_1 \beta_1^2 B_\phi - \alpha_1^3 B_\phi) \cos \beta_1 \phi \right. \right. \right. \\ \left. \left. + (-B_{x\phi} \beta_1 \lambda^2 + 3 B_\phi \alpha_1^2 \beta_1 - B_\phi \beta_1^3) \sin \beta_1 \phi \right) \right\} + B \left\{ e^{\alpha_1 \phi} \right. \\ \left. \left((B_{x\phi} \beta_1 \lambda^2 - 3 B_\phi \alpha_1^2 \beta_1 + B_\phi \beta_1^3) \cos \beta_1 \phi + (B_{x\phi} \lambda^2 \alpha_1 \right. \right. \\ \left. \left. - B_\phi \alpha_1^3 + 3 B_\phi \alpha_1 \beta_1^2) \sin \beta_1 \phi \right) \right\} + C \left\{ e^{-\alpha_1 \phi} \right. \\ \left. \left((-\alpha_1 B_{x\phi} \lambda^2 + B_\phi \alpha_1^3 - 3 B_\phi \alpha_1 \beta_1^2) \cos \beta_1 \phi + (-B_{x\phi} \beta_1 \lambda^2 \right. \right. \\ \left. \left. + 3 B_\phi \alpha_1^2 \beta_1 - B_\phi \beta_1^3) \sin \beta_1 \phi \right) \right\} + D \left\{ e^{-\alpha_1 \phi} \right. \\ \left. \left((\beta_1 B_{x\phi} \lambda^2 - 3 \alpha_1^2 B_\phi \beta_1 + B_\phi \beta_1^3) \cos \beta_1 \phi + (-\alpha_1 B_{x\phi} \lambda^2 \right. \right. \\ \left. \left. + B_\phi \alpha_1^3 - 3 B_\phi \alpha_1 \beta_1^2) \sin \beta_1 \phi \right) \right\} + E \left\{ e^{-\alpha_2 \phi} \left((B_{x\phi} \lambda^2 \alpha_2 \right. \right. \right. \\ \left. \left. - B_\phi \alpha_2^3 + 3 B_\phi \alpha_2 \beta_2^2) \cos \beta_2 \phi + (-B_{x\phi} \lambda^2 \beta_2 + 3 B_\phi \alpha_2^2 \beta_2 \right. \right. \\ \left. \left. - B_\phi \beta_2^3) \sin \beta_2 \phi \right) \right\} + F \left\{ e^{\alpha_2 \phi} \left((B_{x\phi} \lambda^2 \beta_2 + B_\phi \beta_2^3 \right. \right. \right. \\ \left. \left. - 3 B_\phi \alpha_2^2 \beta_2) \cos \beta_2 \phi + (B_{x\phi} \lambda^2 \alpha_2 + 3 B_\phi \alpha_2 \beta_2^2 - B_\phi \alpha_2^3) \right. \right. \\ \left. \left. \sin \beta_2 \phi \right) \right\} + G \left\{ e^{-\alpha_2 \phi} \left((-B_{x\phi} \lambda^2 \alpha_2 + B_\phi \alpha_2^3 - 3 B_\phi \alpha_2 \beta_2^2) \right. \right. \right.$$

$$\cos \beta_2 \phi + (-B_{x\phi} \lambda^2 \beta_2 + 3 B_{\phi} \alpha_2^2 \beta_2 - B_{\phi} \beta_2^3) \sin \beta_2 \phi \} + H \{ e^{-\alpha_2 \phi} \{ (B_{x\phi} \lambda^2 \beta_2 - 3 B_{\phi} \alpha_2^2 \beta_2 + B_{\phi} \beta_2^3) \cos \beta_2 \phi + (-B_{x\phi} \lambda^2 \alpha_2 + B_{\phi} \alpha_2^3 - 3 B_{\phi} \alpha_2 \beta_2^2) \sin \beta_2 \phi \} \} \cos \frac{\lambda x}{R} .$$

6. DIRECT TRANSVERSAL FORCES "N_φ" :

$$\begin{aligned} N_{\phi} = \frac{1}{R^3} [& A (e^{\alpha_1 \phi} \{ (B_x \lambda^4 - 2 B_{x\phi} \lambda^2 \alpha_1^2 + 2 B_{x\phi} \lambda^2 \beta_1^2 \\ & + B_{\phi} \alpha_1^4 - 6 B_{\phi} \alpha_1^2 \beta_1^2 + B_{\phi} \beta_1^4) \cos \beta_1 \phi + (4 B_{x\phi} \lambda^2 \alpha_1 \beta_1 \\ & - 4 B_{\phi} \alpha_1^3 \beta_1 + 4 B_{\phi} \alpha_1 \beta_1^3) \sin \beta_1 \phi \}) + B (e^{\alpha_1 \phi} \\ & \{ (-4 B_{x\phi} \lambda^2 \alpha_1 \beta_1 + 4 B_{\phi} \alpha_1^3 \beta_1 - 4 B_{\phi} \alpha_1 \beta_1^3) \cos \beta_1 \phi \\ & + (B_x \lambda^4 - 2 B_{x\phi} \lambda^2 \alpha_1^2 + 2 B_{x\phi} \lambda^2 \beta_1^2 + B_{\phi} \alpha_1^4 \\ & - 6 B_{\phi} \alpha_1^2 \beta_1^2 + B_{\phi} \beta_1^4) \sin \beta_1 \phi \}) + C (e^{-\alpha_1 \phi} \\ & \{ (\lambda^4 B_x - 2 B_{x\phi} \lambda^2 \alpha_1^2 + 2 B_{x\phi} \lambda^2 \beta_1^2 + B_{\phi} \alpha_1^4 \\ & - 6 B_{\phi} \alpha_1^2 \beta_1^2 + B_{\phi} \beta_1^4) \cos \beta_1 \phi + (-4 B_{x\phi} \lambda^2 \alpha_1 \beta_1 \\ & + 4 B_{\phi} \alpha_1^3 \beta_1 - 4 B_{\phi} \alpha_1 \beta_1^3) \sin \beta_1 \phi \}) + D (e^{-\alpha_1 \phi} \\ & \{ (4 B_{x\phi} \lambda^2 \alpha_1 \beta_1 - 4 B_{\phi} \alpha_1^3 \beta_1 + 4 B_{\phi} \alpha_1 \beta_1^3) \cos \beta_1 \phi + \\ & (\lambda^4 B_x - 2 \lambda^2 B_{x\phi} \alpha_1^2 + 2 \lambda^2 B_{x\phi} \beta_1^2 + B_{\phi} \alpha_1^4 - 6 B_{\phi} \alpha_1^2 \beta_1^2 \\ & + B_{\phi} \beta_1^4) \sin \beta_1 \phi \}) + E (e^{\alpha_2 \phi} \{ (\lambda^4 B_x - 2 B_{x\phi} \lambda^2 \alpha_2^2 \\ & + 2 B_{x\phi} \lambda^2 \beta_2^2 + B_{\phi} \alpha_2^4 - 6 B_{\phi} \alpha_2^2 \beta_2^2 + B_{\phi} \beta_2^4) \cos \beta_2 \phi \}) \end{aligned}$$

$$\begin{aligned}
& + (4 B_{x\phi} \lambda^2 \alpha_2 \beta_2 - 4 B_\phi \alpha_2^3 \beta_2 + 4 B_\phi \alpha_2 \beta_2^3) \sin \beta_2 \phi \} + F \\
& (e^{\alpha_2 \phi} \{ (-4 B_{x\phi} \lambda^2 \alpha_2 \beta_2 + 4 B_\phi \alpha_2^3 \beta_2 - 4 B_\phi \alpha_2 \beta_2^3) \cos \beta_2 \phi \\
& + (B_x \lambda^4 - 2 \lambda^2 B_{x\phi} \alpha_2^2 + 2 B_{x\phi} \lambda^2 \beta_2^2 + B_\phi \alpha_2^4 - 6 B_\phi \alpha_2^2 \beta_2^2 \\
& + B_\phi \beta_2^4) \sin \beta_2 \phi \}) + G (e^{-\alpha_2 \phi} \{ (B_x \lambda^4 - 2 B_{x\phi} \lambda^2 \alpha_2^2 \\
& + 2 B_{x\phi} \lambda^2 \beta_2^2 + B_\phi \alpha_2^4 - 6 B_\phi \alpha_2^2 \beta_2^2 + B_\phi \beta_2^4) \cos \beta_2 \phi \\
& + (-4 B_{x\phi} \lambda^2 \alpha_2 \beta_2 + 4 B_\phi \alpha_2^3 \beta_2 - 4 B_\phi \alpha_2 \beta_2^3) \sin \beta_2 \phi \}) \\
& + H (e^{-\alpha_2 \phi} \{ (4 \lambda^2 B_{x\phi} \alpha_2 \beta_2 - 4 B_\phi \alpha_2^3 \beta_2 + 4 B_\phi \alpha_2 \beta_2^3) \\
& \cos \beta_2 \phi + (\lambda^4 B_x - 2 \lambda^2 \alpha_2^2 B_{x\phi} + 2 \lambda^2 B_{x\phi} \beta_2^2 + B_\phi \alpha_2^4 \\
& - 6 B_\phi \alpha_2^2 \beta_2^2 + B_\phi \beta_2^4) \sin \beta_2 \phi \})] \cos \frac{\lambda x}{R} .
\end{aligned}$$

7. MEMBRANE SHEARING FORCES " $N_{x\phi}$ ":

$$\begin{aligned}
N_{x\phi} = & - \left(\frac{1}{R^3 \lambda} \right) [A (e^{\alpha_1 \phi} \{ (\lambda^4 B_x \alpha_1 - 2 B_x \lambda^2 \alpha_1^3 + 6 B_{x\phi} \lambda^2 \alpha_1 \beta_1^2 \\
& + B_\phi \alpha_1^5 - 10 B_\phi \alpha_1^3 \beta_1^2 + 5 B_\phi \alpha_1 \beta_1^4) \cos \beta_1 \phi + (-\lambda^2 B_x \beta_1 \\
& + 6 B_{x\phi} \lambda^2 \alpha_1^2 \beta_1 - 2 B_{x\phi} \lambda^2 \beta_1^3 - 5 B_\phi \alpha_1^4 \beta_1 + 10 \alpha_1^2 \beta_1^3 B_\phi \\
& - B_\phi \beta_1^5) \sin \beta_1 \phi \}) + B (e^{\alpha_1 \phi} \{ (\lambda^4 B_x \beta_1 - 6 \lambda^2 B_{x\phi} \alpha_1^2 \beta_1 \\
& + 2 \lambda^2 B_{x\phi} \beta_1^3 + 5 B_\phi \alpha_1^4 \beta_1 - 10 B_\phi \alpha_1^2 \beta_1^3 + B_\phi \beta_1^5) \cos \beta_1 \phi \\
& + (\lambda^4 B_x \alpha_1 - 2 \lambda^2 B_{x\phi} \alpha_1^3 + 6 \lambda^2 B_{x\phi} \alpha_1 \beta_1^2 + B_\phi \alpha_1^5
\end{aligned}$$

$$\begin{aligned}
& -10 B_{\phi} \alpha_1^3 \beta_1^2 + 5 B_{\phi} \alpha_1 \beta_1^4) \sin \beta_1 \phi \} + C (e^{-\alpha_1 \phi} \\
& \{ (-\lambda^4 \alpha_1 B_x + 10 B_{\phi} \alpha_1^3 \beta_1^2 + 2 B_{x\phi} \lambda^2 \alpha_1^3 - 6 B_{x\phi} \lambda^2 \alpha_1 \beta_1^2 \\
& - B_{\phi} \alpha_1^5 - 5 B_{\phi} \alpha_1 \beta_1^4) \cos \beta_1 \phi + (-\lambda^4 B_x \beta_1 + 6 B_{x\phi} \lambda^2 \alpha_1^2 \beta_1 \\
& - 2 B_{x\phi} \lambda^2 \beta_1^3 - 5 B_{\phi} \alpha_1^4 \beta_1 + 10 B_{\phi} \alpha_1^2 \beta_1^3 - B_{\phi} \beta_1^5) \sin \beta_1 \phi \}) \\
& + D (e^{-\alpha_1 \phi} \{ (\lambda^4 B_x \beta_1 - 6 \lambda^2 B_{x\phi} \alpha_1^2 \beta_1 + 2 \lambda^2 B_{x\phi} \beta_1^3 \\
& + 5 B_{\phi} \alpha_1^4 \beta_1 - 10 B_{\phi} \alpha_1^2 \beta_1^3 + B_{\phi} \beta_1^5) \cos \beta_1 \phi + (-\lambda^4 B_x \alpha_1 \\
& + 2 \lambda^2 B_{x\phi} \alpha_1^3 - 6 B_{x\phi} \lambda^2 \alpha_1 \beta_1^2 - B_{\phi} \alpha_1^5 + 10 B_{\phi} \alpha_1^3 \beta_1^2 \\
& - 5 B_{\phi} \alpha_1 \beta_1^4) \sin \beta_1 \phi \}) + E (e^{\alpha_2 \phi} \{ (\lambda^4 B_x \alpha_2 - 2 B_{x\phi} \lambda^2 \alpha_2^3 \\
& + 6 \lambda^2 B_{x\phi} \alpha_2 \beta_2^2 + B_{\phi} \alpha_2^5 - 10 B_{\phi} \alpha_2^3 \beta_2^2 + 5 B_{\phi} \alpha_2 \beta_2^4) \cos \beta_2 \phi \\
& + (-B_x \lambda^4 \beta_2 + 6 \lambda^2 B_{x\phi} \alpha_2^2 \beta_2 - 2 B_{x\phi} \lambda^2 \beta_2^3 - 3 B_{\phi} \alpha_2^4 \beta_2 \\
& + 10 B_{\phi} \alpha_2^2 \beta_2^3 - B_{\phi} \beta_2^5) \sin \beta_2 \phi \}) + F (e^{\alpha_2 \phi} \{ (\lambda^4 B_x \beta_2 \\
& - 6 \lambda^2 B_{x\phi} \alpha_2^2 \beta_2 + 2 \lambda^2 B_{x\phi} \beta_2^3 + 5 B_{\phi} \alpha_2^4 \beta_2 - 10 B_{\phi} \alpha_2^2 \beta_2^3 \\
& + B_{\phi} \beta_2^5) \cos \beta_2 \phi + (\lambda^4 \alpha_2 B_x - 2 B_{x\phi} \lambda^2 \alpha_2^3 + 6 \lambda^2 B_{x\phi} \alpha_2 \beta_2^2 \\
& + B_{\phi} \alpha_2^5 - 10 B_{\phi} \alpha_2^3 \beta_2^2 + 5 B_{\phi} \alpha_2 \beta_2^4) \sin \beta_2 \phi \}) + G (e^{-\alpha_2 \phi} \\
& \{ (-\lambda^4 \alpha_2 B_x + 2 \lambda^2 B_{x\phi} \alpha_2^3 - 6 \lambda^2 B_{x\phi} \alpha_2 \beta_2^2 - B_{\phi} \alpha_2^5 + 10 B_{\phi} \alpha_2^3 \beta_2^2 \\
& - 5 B_{\phi} \alpha_2 \beta_2^4) \cos \beta_2 \phi + (-\lambda^4 B_x \beta_2 + 6 \lambda^2 B_{x\phi} \alpha_2^2 \beta_2 - 2 \lambda^2 B_{x\phi} \beta_2^3 \\
& - 5 B_{\phi} \alpha_2^4 \beta_2 + 10 B_{\phi} \alpha_2^2 \beta_2^3 - B_{\phi} \beta_2^5) \sin \beta_2 \phi \}) + H (e^{-\alpha_2 \phi}
\end{aligned}$$

$$\left\{ \left(\lambda^4 B_x \beta_2 - 6 \lambda^2 B_{x\phi} \alpha_2^2 \beta_2 + 2 \lambda^2 B_{x\phi} \beta_2^3 + 5 B_\phi \alpha_2^4 \beta_2 - 10 B_\phi \alpha_2^2 \beta_2^3 + B_\phi \beta_2^5 \right) \cos \beta_2 \phi + \left(-\lambda^4 B_x \alpha_2 + 2 \lambda^2 \alpha_2^3 B_{x\phi} - 6 \lambda^2 B_{x\phi} \alpha_2 \beta_2^2 - B_\phi \alpha_2^5 + 10 B_\phi \alpha_2^3 \beta_2^2 - 5 B_\phi \alpha_2 \beta_2^4 \right) \sin \beta_2 \phi \right\} \sin \frac{\lambda x}{R}$$

8. DIRECT LONGITUDINAL FORCES " N_x ":

$$\begin{aligned} N_x = & - \left[\frac{1}{R^3 \lambda^2} \right] \left[A \left(e^{\alpha_1 \phi} \left\{ \left(\lambda^4 B_x \alpha_1^2 - 2 B_{x\phi} \lambda^2 \alpha_1^4 - B_x \lambda^4 \beta_1^2 + 12 B_{x\phi} \lambda^2 \alpha_1^2 \beta_1^2 + B_\phi \alpha_1^6 - 2 B_{x\phi} \lambda^2 \beta_1^4 - 15 B_\phi \alpha_1^4 \beta_1^2 + 15 B_\phi \alpha_1^2 \beta_1^4 - B_\phi \beta_1^6 \right) \cos \beta_1 \phi + \left(-2 \lambda^4 B_x \alpha_1 \beta_1 + 8 B_{x\phi} \lambda^2 \alpha_1^3 \beta_1 - 8 B_{x\phi} \lambda^2 \alpha_1 \beta_1^3 - 6 B_\phi \alpha_1^5 \beta_1 + 20 B_\phi \alpha_1^3 \beta_1^3 - 6 B_\phi \alpha_1 \beta_1^5 \right) \sin \beta_1 \phi \right\} \right) + B \left(e^{\alpha_1 \phi} \left\{ \left(2 \lambda^4 B_x \alpha_1 \beta_1 - 8 \lambda^2 B_{x\phi} \alpha_1^3 \beta_1 + 8 \lambda^2 B_{x\phi} \beta_1^3 \alpha_1 + 6 B_\phi \alpha_1^5 \beta_1 - 20 B_\phi \alpha_1^3 \beta_1^3 + 6 B_\phi \alpha_1 \beta_1^5 \right) \cos \beta_1 \phi + \left(\lambda^4 B_x \alpha_1^2 - 2 \lambda^2 B_{x\phi} \alpha_1^4 + 12 \lambda^2 B_{x\phi} \alpha_1^2 \beta_1^2 + B_\phi \alpha_1^6 - 15 B_\phi \alpha_1^4 \beta_1^2 + 15 B_\phi \alpha_1^2 \beta_1^4 - \lambda^4 B_x \beta_1^2 - 2 \lambda^2 B_{x\phi} \beta_1^4 - B_\phi \beta_1^6 \right) \sin \beta_1 \phi \right\} \right) + C \left(e^{-\alpha_1 \phi} \left\{ \left(\lambda^4 B_x \alpha_1^2 - \lambda^4 B_x \beta_1 - 15 B_\phi \alpha_1^4 \beta_1^2 - 2 B_{x\phi} \lambda^2 \alpha_1^4 + 12 B_{x\phi} \lambda^2 \alpha_1^2 \beta_1^2 + B_\phi \alpha_1^6 + 15 B_\phi \alpha_1^2 \beta_1^4 - 2 B_{x\phi} \lambda^2 \beta_1^4 - B_\phi \beta_1^6 \right) \cos \beta_1 \phi + \left(2 \lambda^4 B_x \alpha_1 \beta_1 - 8 B_{x\phi} \lambda^2 \alpha_1^3 \beta_1 + 8 B_{x\phi} \lambda^2 \alpha_1 \beta_1^3 + 6 B_\phi \alpha_1^5 \beta_1 - 20 B_\phi \alpha_1^3 \beta_1^3 + 6 B_\phi \alpha_1 \beta_1^5 \right) \sin \beta_1 \phi \right\} \right) \right] \end{aligned}$$

$$\begin{aligned}
& \sin \beta_1 \phi \} + D (e^{-\alpha_1 \phi} \{ (-2 \lambda^2 B_x \alpha_1 \beta_1 + 8 \lambda^2 B_{x\phi} \alpha_1^3 \beta_1 \\
& - 8 \lambda^2 B_{x\phi} \alpha_1 \beta_1^3 - 6 B_{\phi} \alpha_1^5 \beta_1 + 20 B_{\phi} \alpha_1^3 \beta_1^3 - 6 B_{\phi} \alpha_1 \beta_1^5) \\
& \cos \beta_1 \phi + (\lambda^4 B_x \alpha_1^2 - \lambda^4 B_x \beta_1^2 - 2 \lambda^2 B_{x\phi} \alpha_1^4 + B_{\phi} \alpha_1^6 \\
& + 12 B_{x\phi} \lambda^2 \alpha_1^2 \beta_1^2 + 15 B_{\phi} \alpha_1^2 \beta_1^4 - 15 B_{\phi} \alpha_1^4 \beta_1^2 - B_{\phi} \beta_1^6 \\
& - 2 \lambda^2 B_{x\phi} \beta_1^4) \sin \beta_1 \phi \} + E (e^{\alpha_2 \phi} \{ (\lambda^4 B_x \alpha_2^2 \\
& - 2 B_{x\phi} \lambda^2 \alpha_2^4 - \lambda^4 B_x \beta_2^2 + 12 B_{x\phi} \lambda^2 \alpha_2^2 \beta_2^2 + B_{\phi} \alpha_2^6 \\
& - 2 B_{x\phi} \lambda^2 \beta_2^4 - 15 B_{\phi} \alpha_2^4 \beta_2^2 + 15 B_{\phi} \alpha_2^2 \beta_2^4 - B_{\phi} \beta_2^6) \\
& \cos \beta_2 \phi + (-2 \lambda^4 B_x \alpha_2 \beta_2 + 8 B_{x\phi} \lambda^2 \alpha_2^3 \beta_2 - 6 B_{\phi} \alpha_2^5 \beta_2 \\
& - 8 B_{x\phi} \lambda^2 \alpha_2 \beta_2^3 + 20 B_{\phi} \alpha_2^3 \beta_2^3 - 6 B_{\phi} \alpha_2 \beta_2^5) \sin \beta_2 \phi \} \\
& + F (e^{-\alpha_2 \phi} \{ (2 \lambda^4 B_x \alpha_2 \beta_2 - 8 \lambda^2 B_{x\phi} \alpha_2^3 \beta_2 + 6 B_{\phi} \alpha_2^5 \beta_2 \\
& + 8 \lambda^2 B_{x\phi} \alpha_2 \beta_2^3 - 20 B_{\phi} \alpha_2^3 \beta_2^3 + 6 B_{\phi} \alpha_2 \beta_2^5) \cos \beta_2 \phi \\
& + (\lambda^4 B_x \alpha_2^2 - 2 \lambda^2 B_{x\phi} \alpha_2^4 + 12 \lambda^2 B_{x\phi} \alpha_2^2 \beta_2^2 + B_{\phi} \alpha_2^6 \\
& - 15 B_{\phi} \alpha_2^4 \beta_2^2 + 15 B_{\phi} \alpha_2^2 \beta_2^4 - \lambda^4 B_x \beta_2^2 - 2 \lambda^2 B_{x\phi} \beta_2^4 - B_{\phi} \beta_2^6) \\
& \sin \beta_2 \phi \} + G (e^{-\alpha_2 \phi} \{ (\lambda^4 B_x \alpha_2^2 - \lambda^4 B_x \beta_2^2 \\
& - 15 B_{\phi} \alpha_2^4 \beta_2^2 - 2 B_{x\phi} \lambda^2 \alpha_2^4 + 12 B_{x\phi} \lambda^2 \alpha_2^2 \beta_2^2 + B_{\phi} \alpha_2^6 \\
& + 15 B_{\phi} \alpha_2^2 \beta_2^4 - 2 B_{x\phi} \lambda^2 \beta_2^4 - B_{\phi} \beta_2^6) \cos \beta_2 \phi + \\
& (2 \lambda^4 B_x \alpha_2 \beta_2 - 8 B_{x\phi} \lambda^2 \alpha_2^3 \beta_2 + 8 B_{x\phi} \lambda^2 \alpha_2 \beta_2^3 + 6 B_{\phi} \alpha_2^5 \beta_2 \\
& - 20 B_{\phi} \alpha_2^3 \beta_2^3 + 6 B_{\phi} \alpha_2 \beta_2^5) \sin \beta_2 \phi \} + H (e^{-\alpha_2 \phi}
\end{aligned}$$

$$\left\{ \begin{aligned} & (-2 \lambda^4 B_x \alpha_2 \beta_2 + 8 \lambda^2 B_{x\phi} \alpha_2^3 \beta_2 - 8 \lambda^2 B_{x\phi} \alpha_2 \beta_2^3 - 6 B_\phi \alpha_2^5 \beta_2 \\ & + 20 B_\phi \alpha_2^3 \beta_2^3 - 6 B_\phi \alpha_2 \beta_2^5) \cos \beta_2 \phi + (\lambda^4 B_x \alpha_2^2 - \lambda^4 B_x \beta_2^2 \\ & - 2 \lambda^2 B_{x\phi} \alpha_2^4 + 12 B_{x\phi} \lambda^2 \alpha_2^2 \beta_2^2 + B_\phi \alpha_2^6 + 15 B_\phi \alpha_2^2 \beta_2^4 \\ & - 15 B_\phi \alpha_2^4 \beta_2^2 - B_\phi \beta_2^6 - 2 \lambda^2 B_{x\phi} \beta_2^4) \sin \beta_2 \phi \end{aligned} \right\} \cos \frac{\lambda x}{R}$$

9. THE LONGITUDINAL DISPLACEMENT "u" IN THE X-DIRECTION:

$$u = \int \frac{N_x}{D_x} dx$$

$$u = - \left[\frac{1}{R^2 \lambda^3 D_x} \right] \left[f_{(N_x)}(\phi) \right] \sin \frac{\lambda x}{R}$$

where " $f_{(N_x)}(\phi)$ " is the function in ϕ only appearing in Equation of N_x between brackets [].

10. TANGENTIAL DISPLACEMENT "v" :

$$\begin{aligned} v = & \left[A \left\{ \left(\frac{1}{\lambda^2 R^2 D_{x\phi}} \right) \left(e^{\alpha_1 \phi} \left((\lambda^2 B_x \alpha_1 - 2 B_{x\phi} \lambda^2 \alpha_1^3 + 6 B_{x\phi} \lambda^2 \alpha_1 \beta_1^2 \right. \right. \right. \right. \\ & + B_\phi \alpha_1^5 - 10 B_\phi \alpha_1^3 \beta_1^2 + 5 B_\phi \alpha_1 \beta_1^4) \cos \beta_1 \phi + (-\lambda^4 B_x \beta_1 \\ & + 6 B_{x\phi} \lambda^2 \alpha_1^2 \beta_1 - 2 B_{x\phi} \lambda^2 \beta_1^3 - 5 B_\phi \alpha_1^4 \beta_1 + 10 B_\phi \alpha_1^2 \beta_1^3 - B_\phi \beta_1^5) \\ & \left. \left. \left. \left. \sin \beta_1 \phi \right) \right) - \left(\frac{1}{D_x R^2 \lambda^4} \right) \left(e^{\alpha_1 \phi} \left((\lambda^4 B_x \alpha_1^3 - 2 B_{x\phi} \lambda^2 \alpha_1^5 \right. \right. \right. \right. \right. \end{aligned}$$

$$\begin{aligned}
& -3 \lambda^4 B_x \alpha_1 \beta_1^2 + 20 B_{x\phi} \lambda^2 \alpha_1^3 \beta_1^2 + B_\phi \alpha_1^7 - 10 B_{x\phi} \lambda^2 \alpha_1 \beta_1^4 \\
& - 21 B_\phi \alpha_1^5 \beta_1^2 + 35 B_\phi \alpha_1^3 \beta_1^4 - 7 B_\phi \alpha_1 \beta_1^6) \cos \beta_1 \phi + \\
& (-3 \lambda^4 B_x \alpha_1^2 \beta_1 + 10 B_{x\phi} \lambda^2 \alpha_1^4 \beta_1 + \lambda^4 B_x \beta_1^3 - 20 B_{x\phi} \lambda^2 \alpha_1^2 \beta_1^3 \\
& - 7 B_\phi \alpha_1^6 \beta_1 + 2 B_{x\phi} \lambda^2 \beta_1^5 + 35 B_\phi \alpha_1^4 \beta_1^3 - 21 B_\phi \alpha_1^2 \beta_1^5 \\
& + B_\phi \beta_1^7) \sin \beta_1 \phi) \} + B \left\{ \left(\frac{1}{\lambda^2 R^2 D_{x\phi}} \right) (e^{\alpha_1 \phi} ((\lambda^4 B_x \beta_1 \right. \\
& - 6 \lambda^2 B_{x\phi} \alpha_1^2 \beta_1 + 2 \lambda^2 B_{x\phi} \beta_1^3 + 5 B_\phi \alpha_1^4 \beta_1 - 10 B_\phi \alpha_1^2 \beta_1^3 \\
& + B_\phi \beta_1^5) \cos \beta_1 \phi + (\lambda^4 B_x \alpha_1 - 2 \lambda^2 B_{x\phi} \alpha_1^3 + 6 \lambda^2 B_{x\phi} \alpha_1 \beta_1^2 \\
& + B_\phi \alpha_1^5 - 10 B_\phi \alpha_1^3 \beta_1^2 + 5 B_\phi \alpha_1 \beta_1^4) \sin \beta_1 \phi) \right) - \left(\frac{1}{D_x R^2 \lambda^2} \right) \\
& (e^{\alpha_1 \phi} ((3 \lambda^4 B_x \alpha_1^2 \beta_1 - 10 \lambda^2 B_{x\phi} \alpha_1^4 \beta_1 + 20 \lambda^2 B_{x\phi} \alpha_1^2 \beta_1^3 \\
& + 7 B_\phi \alpha_1^6 \beta_1 - 35 B_\phi \alpha_1^4 \beta_1^3 + 21 B_\phi \alpha_1^2 \beta_1^5 - \lambda^4 B_x \beta_1^3 \\
& - 2 \lambda^2 B_{x\phi} \beta_1^5 - B_\phi \beta_1^7) \cos \beta_1 \phi + (-3 \lambda^4 B_x \alpha_1 \beta_1^2 \\
& + 20 \lambda^2 B_{x\phi} \alpha_1^3 \beta_1^2 - 10 \lambda^2 B_{x\phi} \alpha_1 \beta_1^4 - 21 B_\phi \alpha_1^5 \beta_1^2 \\
& + 35 B_\phi \alpha_1^3 \beta_1^4 - 7 B_\phi \alpha_1 \beta_1^6 + \lambda^4 B_x \alpha_1^3 - 2 \lambda^2 B_{x\phi} \alpha_1^5 \\
& + B_\phi \alpha_1^7) \sin \beta_1 \phi) \right) \} + C \left\{ \left(\frac{1}{\lambda^2 R^2 D_{x\phi}} \right) (e^{-\alpha_1 \phi} \right. \\
& ((-B_x \alpha_1 \lambda^4 + 10 B_\phi \alpha_1^3 \beta_1^2 + 2 B_{x\phi} \lambda^2 \alpha_1^3 - 6 B_{x\phi} \lambda^2 \alpha_1 \beta_1^2 \\
& - B_\phi \alpha_1^5 - 5 B_\phi \alpha_1 \beta_1^4) \cos \beta_1 \phi + (-\lambda^4 B_x \beta_1 + 6 B_{x\phi} \lambda^2 \alpha_1^2 \beta_1 \\
& - 2 B_{x\phi} \lambda^2 \beta_1^3 - 5 B_\phi \alpha_1^4 \beta_1 + 10 B_\phi \alpha_1^2 \beta_1^3 - B_\phi \beta_1^5)
\end{aligned}$$

$$\begin{aligned}
& \sin \beta_1 \phi) - \left(\frac{1}{D_x R^2 \lambda^4} \right) \left(e^{-\alpha_1 \phi} \left((-\lambda^4 B_x \alpha_1^3 + 3 \lambda^4 B_x \alpha_1 \beta_1^2 \right. \right. \\
& + 21 B_\phi \alpha_1^5 \beta_1^2 + 2 B_{x\phi} \lambda^2 \alpha_1^5 - 20 B_{x\phi} \lambda^2 \alpha_1^3 \beta_1^2 - B_\phi \beta_1^7 - 35 B_\phi \alpha_1^3 \beta_1^4 \\
& + 10 B_{x\phi} \lambda^2 \alpha_1 \beta_1^4 + 7 B_\phi \alpha_1 \beta_1^6) \cos \beta_1 \phi + (-3 \lambda^4 \alpha_1^2 B_x \beta_1 \\
& + \lambda^4 B_x \beta_1^3 + 35 B_\phi \alpha_1^4 \beta_1^3 + 10 B_{x\phi} \lambda^2 \alpha_1^4 \beta_1 - 20 B_{x\phi} \lambda^2 \alpha_1^2 \beta_1^3 \\
& - 7 B_\phi \alpha_1^6 \beta_1 - 21 B_\phi \alpha_1^2 \beta_1^5 + 2 B_{x\phi} \lambda^2 \beta_1^5 + B_\phi \beta_1^7) \sin \beta_1 \phi) \left. \right\} \\
& + D \left\{ \left(\frac{1}{\lambda^2 R^2 D_{x\phi}} \right) \left(e^{-\alpha_1 \phi} \left((\lambda^4 B_x \beta_1 - 6 \lambda^2 B_{x\phi} \alpha_1^2 \beta_1 \right. \right. \right. \\
& + 2 \lambda^2 B_{x\phi} \beta_1^3 + 5 B_\phi \alpha_1^4 \beta_1 - 10 B_\phi \alpha_1^2 \beta_1^3 + B_\phi \beta_1^5) \cos \beta_1 \phi \\
& + (-\lambda^4 B_x \alpha_1 + 2 \lambda^2 B_{x\phi} \alpha_1^3 - 6 B_{x\phi} \lambda^2 \alpha_1 \beta_1^2 - B_\phi \alpha_1^5 \\
& + 10 B_\phi \alpha_1^3 \beta_1^2 - 5 B_\phi \alpha_1 \beta_1^4) \sin \beta_1 \phi) \left. \right\} - \left(\frac{1}{D_x R^2 \lambda^4} \right) \\
& \left(e^{-\alpha_1 \phi} \left((3 \lambda^4 B_x \alpha_1^2 \beta_1 + 20 B_{x\phi} \lambda^2 \alpha_1^2 \beta_1^3 - 10 \lambda^2 B_{x\phi} \alpha_1^4 \beta_1 \right. \right. \right. \\
& + 7 B_{x\phi} \alpha_1^6 \beta_1 - 35 B_\phi \alpha_1^4 \beta_1^3 + 21 B_\phi \alpha_1^2 \beta_1^5 - \lambda^4 B_x \beta_1^3 \\
& - B_\phi \beta_1^7 - 2 \lambda^2 B_{x\phi} \beta_1^5) \cos \beta_1 \phi + (3 \lambda^4 B_x \alpha_1 \beta_1^2 \\
& - 20 \lambda^2 B_{x\phi} \alpha_1^3 \beta_1^2 + 10 \lambda^2 B_{x\phi} \alpha_1 \beta_1^4 + 21 B_\phi \alpha_1^5 \beta_1^2 \\
& - 35 B_\phi \alpha_1^3 \beta_1^4 + 7 B_\phi \alpha_1 \beta_1^6 - \lambda^4 B_x \alpha_1^3 + 2 \lambda^2 B_{x\phi} \alpha_1^5 \\
& - B_\phi \alpha_1^7) \sin \beta_1 \phi) \left. \right\} + E \left\{ \left(\frac{1}{\lambda^2 R^2 D_{x\phi}} \right) \left(e^{\alpha_2 \phi} \right. \right. \\
& \left((\lambda^4 B_x \alpha_2 - 2 B_{x\phi} \lambda^2 \alpha_2^3 + 6 \lambda^2 B_{x\phi} \alpha_2 \beta_2^2 + B_\phi \alpha_2^5 - 10 B_\phi \alpha_2^3 \beta_2^2 \right. \\
& + 5 B_\phi \alpha_2 \beta_2^4) \cos \beta_2 \phi + (-\lambda^4 B_x \beta_2 + 6 \lambda^2 B_{x\phi} \alpha_2^2 \beta_2 \\
& - 2 B_{x\phi} \lambda^2 \beta_2^3 - 5 B_\phi \alpha_2^4 \beta_2 + 10 B_\phi \alpha_2^2 \beta_2^3 - B_\phi \beta_2^5)
\end{aligned}$$

$$\begin{aligned}
& \sin \beta_2 \phi) - \left(\frac{1}{D_x R^2 \lambda^4} \right) \left(e^{\alpha_2 \phi} \left((\lambda^4 B_x \alpha_2^3 - 2 B_{x\phi} \lambda^2 \alpha_2^5 \right. \right. \\
& - 3 \lambda^4 B_x \alpha_2 \beta_2^2 + 20 B_{x\phi} \lambda^2 \alpha_2^3 \beta_2^2 + B_\phi \alpha_2^7 - 10 B_{x\phi} \lambda^2 \alpha_2 \beta_2^4 \\
& - 21 B_\phi \alpha_2^5 \beta_2^2 + 35 B_\phi \alpha_2^3 \beta_2^4 - 7 B_\phi \alpha_2 \beta_2^6) \cos \beta_2 \phi + \\
& (-3 \lambda^4 B_x \alpha_2^2 \beta_2 + 10 B_{x\phi} \lambda^2 \alpha_2^4 \beta_2 + \lambda^4 B_x \beta_2^3 - 20 B_{x\phi} \lambda^2 \alpha_2^2 \beta_2^3 \\
& - 7 B_\phi \alpha_2^6 \beta_2 + 2 B_{x\phi} \lambda^2 \beta_2^5 + 35 B_\phi \alpha_2^4 \beta_2^3 - 21 B_\phi \alpha_2^2 \beta_2^5 \\
& + B_\phi \beta_2^7) \sin \beta_2 \phi) \Big) \Big\} + F \left\{ \left(\frac{1}{\lambda^2 R^2 D_{x\phi}} \right) \left(e^{\alpha_2 \phi} \left((\lambda^4 B_x \beta_2 \right. \right. \right. \\
& - 6 \lambda^2 B_{x\phi} \alpha_2^2 \beta_2 + 2 \lambda^2 B_{x\phi} \beta_2^3 + 5 B_\phi \alpha_2^4 \beta_2 - 10 B_\phi \alpha_2^2 \beta_2^3 \\
& + B_\phi \beta_2^5) \cos \beta_2 \phi + (\lambda^4 \alpha_2 B_x - 2 B_{x\phi} \lambda^2 \alpha_2^3 + 6 \lambda^2 B_{x\phi} \alpha_2 \beta_2^2 \\
& + B_\phi \alpha_2^5 - 10 B_\phi \alpha_2^3 \beta_2^2 + 5 B_\phi \alpha_2 \beta_2^4) \sin \beta_2 \phi) \Big) - \left(\frac{1}{D_x R^2 \lambda^4} \right) \\
& \left(e^{\alpha_2 \phi} \left((3 \lambda^4 B_x \alpha_2^2 \beta_2 - 10 \lambda^2 B_{x\phi} \alpha_2^4 \beta_2 + 20 B_{x\phi} \lambda^2 \alpha_2^2 \beta_2^3 \right. \right. \\
& + 7 B_\phi \alpha_2^6 \beta_2 - 35 B_\phi \alpha_2^4 \beta_2^3 + 21 B_\phi \alpha_2^2 \beta_2^5 - \lambda^4 B_x \beta_2^3 \\
& - 2 \lambda^2 B_{x\phi} \beta_2^5 - B_\phi \beta_2^7) \cos \beta_2 \phi + (-3 \lambda^4 B_x \alpha_2 \beta_2^2 \\
& + 20 B_{x\phi} \lambda^2 \alpha_2^3 \beta_2^2 - 10 \lambda^2 B_{x\phi} \alpha_2 \beta_2^4 - 21 B_\phi \alpha_2^5 \beta_2^2 \\
& + 35 B_\phi \alpha_2^3 \beta_2^4 - 7 B_\phi \alpha_2 \beta_2^6 + \lambda^4 B_x \alpha_2^3 + B_\phi \alpha_2^7 \\
& - 2 \lambda^2 B_{x\phi} \alpha_2^5) \sin \beta_2 \phi) \Big) \Big\} + G \left\{ \left(\frac{1}{\lambda^2 R^2 D_{x\phi}} \right) \left(e^{-\alpha_2 \phi} \right. \right. \\
& \left((-\lambda^4 B_x \alpha_2 + 2 \lambda^2 B_{x\phi} \alpha_2^3 - 6 \lambda^2 B_{x\phi} \alpha_2 \beta_2^2 - B_\phi \alpha_2^5 \right. \\
& + 10 B_\phi \alpha_2^3 \beta_2^2 - 5 B_\phi \alpha_2 \beta_2^4) \cos \beta_2 \phi + (-\lambda^4 B_x \beta_2 \\
& + 6 B_{x\phi} \lambda^2 \alpha_2^2 \beta_2 - 2 B_{x\phi} \lambda^2 \beta_2^3 - 5 B_\phi \alpha_2^4 \beta_2 + 10 B_\phi \alpha_2^2 \beta_2^3
\end{aligned}$$

$$\begin{aligned}
& -B_{\phi} \beta_2^5) \sin \beta_2 \phi)) - \left(\frac{1}{D_x R^2 \lambda^4} \right) \left(e^{-\alpha_2 \phi} \left((-\lambda^4 \alpha_2^3 B_x \right. \right. \\
& + 3 \lambda^4 B_x \alpha_2 \beta_2^2 + 21 B_{\phi} \alpha_2^5 \beta_2^2 + 2 B_{x\phi} \lambda^2 \alpha_2^5 - 20 B_{x\phi} \lambda^2 \alpha_2^3 \beta_2^2 \\
& - B_{\phi} \alpha_2^7 - 35 B_{\phi} \alpha_2^3 \beta_2^4 + 10 B_{x\phi} \lambda^2 \alpha_2 \beta_2^4 + 7 B_{\phi} \alpha_2 \beta_2^6) \\
& \cos \beta_2 \phi + (-3 \lambda^4 B_x \alpha_2^2 \beta_2 + \lambda^4 B_x \beta_2^3 + 35 B_{\phi} \alpha_2^4 \beta_2^3 \\
& + 10 B_{x\phi} \lambda^2 \alpha_2^4 \beta_2 - 20 B_{x\phi} \lambda^2 \alpha_2^2 \beta_2^3 - 7 B_{\phi} \alpha_2^6 \beta_2 \\
& - 21 B_{\phi} \alpha_2^2 \beta_2^5 + 2 B_{x\phi} \lambda^2 \beta_2^5 + B_{\phi} \beta_2^7) \sin \beta_2 \phi) \Big\} + \\
& H \left\{ \left(\frac{1}{\lambda^2 R^2 D_{x\phi}} \right) \left(e^{-\alpha_2 \phi} \left((\lambda^4 B_x \beta_2 - 6 \lambda^2 B_{x\phi} \alpha_2^2 \beta_2 \right. \right. \right. \\
& + 2 \lambda^2 B_{x\phi} \beta_2^3 + 5 B_{\phi} \alpha_2^4 \beta_2 - 10 B_{\phi} \alpha_2^2 \beta_2^3 + B_{\phi} \beta_2^5) \\
& \cos \beta_2 \phi + (-\lambda^4 B_x \alpha_2 + 2 \lambda^2 \alpha_2^3 B_{x\phi} - 6 \lambda^2 B_{x\phi} \alpha_2 \beta_2^2 \\
& - B_{\phi} \alpha_2^5 + 10 B_{\phi} \alpha_2^3 \beta_2^2 - 5 B_{\phi} \alpha_2 \beta_2^4) \sin \beta_2 \phi) \Big\} \\
& - \left(\frac{1}{D_x R^2 \lambda^4} \right) \left(e^{-\alpha_2 \phi} \left((3 \lambda^4 B_x \alpha_2^2 \beta_2 - 10 \lambda^2 B_{x\phi} \alpha_2^4 \beta_2 \right. \right. \\
& + 20 \lambda^2 B_{x\phi} \alpha_2^2 \beta_2^3 + 7 B_{\phi} \alpha_2^6 \beta_2 - 35 B_{\phi} \alpha_2^4 \beta_2^3 + 21 B_{\phi} \alpha_2^2 \beta_2^5 \\
& - B_{\phi} \beta_2^7 - \lambda^4 B_x \beta_2^3 - 2 \lambda^2 B_{x\phi} \beta_2^5) \cos \beta_2 \phi + (-\lambda^4 B_x \alpha_2^3 \\
& + 3 \lambda^4 B_x \alpha_2 \beta_2^2 - 20 \lambda^2 B_{x\phi} \alpha_2^3 \beta_2^2 + 10 \lambda^2 B_{x\phi} \alpha_2 \beta_2^4 \\
& + 21 B_{\phi} \alpha_2^5 \beta_2^2 - 35 B_{\phi} \alpha_2^3 \beta_2^4 + 7 B_{\phi} \alpha_2 \beta_2^6 - B_{\phi} \alpha_2^7 \\
& + 2 B_{x\phi} \lambda^2 \alpha_2^5) \sin \beta_2 \phi) \Big\} \Big] \cos \frac{\lambda x}{R} .
\end{aligned}$$

11. ROTATION OF THE TANGENT " θ ":

Since $\theta = \frac{1}{R}(\nu + \dot{\omega})$, then substituting for ν & $\dot{\omega}$, the rotation of the tangent at any point on the shell surface can be obtained.

APPENDIX (III)

SAMPLES OF SIMPLIFIED FORMULAE AND DESIGN TABLES FOR
SHELL ROOFS MADE OF CORRUGATED
SHEETS

SIMPLIFIED FORMULAE:

$$N_x = \bar{N}_x \cdot p \cdot \cos \frac{\pi x}{L} \quad (\text{lb/in})$$

$$N_\phi = \bar{N}_\phi \cdot p \cdot \cos \frac{\pi x}{L} \quad (\text{lb/in})$$

$$N_{x\phi} = \bar{N}_{x\phi} \cdot p \cdot \sin \frac{\pi x}{L} \quad (\text{lb/in})$$

$$M_\phi = \bar{M}_\phi \cdot p \cdot \cos \frac{\pi x}{L} \quad (\text{lb/in})$$

where p = Intensity of snow load in (p.s.f.).

$$\text{Area of edge stiffener} = \frac{L}{\pi} (N_{x\phi})_{\text{valley}} \cdot \frac{P}{20000} \quad (\text{in}^2).$$

The following design tables are based on the following structural properties:

$$E = 30 \times 10^6 \text{ psi}, \quad \mu = 0.3, \quad \rho = 1.0, \quad t = 0.029$$

$$D_\phi = \left(\frac{L}{c}\right) \cdot t \cdot E$$

$$D_x = \frac{E \cdot t}{6(1-\mu^2)} \left(\frac{t}{f}\right)^2$$

$$D_{x\phi} = \rho \frac{E \cdot t}{2(1+\mu)} \left(\frac{c}{L}\right)$$

$$B_\phi = 0.522 E \cdot t \cdot f^2$$

$$B_x = \frac{E \cdot t^3}{12(1-\mu^2)} \left(\frac{c}{L}\right)$$

$$B_{x\phi} = \frac{E \cdot t^3}{12(1+\mu)} \left(\frac{L}{c}\right)$$

BOUNDARY CONDITIONS: CASE (I).

HALF CENTRAL ANGLE $\phi_e = 80^\circ$, GA 22.

RADIUS	SPAN	ϕ/ϕ_e	\bar{N}_x	\bar{N}_ϕ	$\bar{N}_{x\phi}$	\bar{M}_ϕ
10	15	VALLEY	0.0311	0.0	0.4722	0.0
		$\frac{1}{4}$	0.2737	-0.2777	0.6335	-0.0140
		$\frac{1}{2}$	-0.0760	-0.6137	0.7274	+0.1139
		$\frac{3}{4}$	-0.5428	-0.9254	0.4946	0.1979
		CROWN	-0.7461	-1.0537	0.0	0.2084
10	20	VALLEY	0.0311	0.0	0.6565	0.0
		$\frac{1}{4}$	0.4355	-0.2864	0.8471	0.0148
		$\frac{1}{2}$	-0.1539	-0.6172	0.9516	0.2803
		$\frac{3}{4}$	-0.9443	-0.9182	0.6424	0.5458
		CROWN	-1.2901	-1.0414	0.0	0.6395
10	25	VALLEY	0.0311	0.0	0.8645	0.0
		$\frac{1}{4}$	0.5658	-0.2990	1.0655	0.0553
		$\frac{1}{2}$	-0.2918	-0.6228	1.1562	0.5197
		$\frac{3}{4}$	-1.4279	-0.9076	0.7696	1.0552
		CROWN	-1.9247	-1.0228	0.0	1.2748
10	30	VALLEY	0.0311	0.0	1.0908	0.0
		$\frac{1}{4}$	0.6431	-0.3121	1.2874	0.0971
		$\frac{1}{2}$	-0.4999	-0.6288	1.3458	0.7683
		$\frac{3}{4}$	-1.9848	-0.8966	0.8812	1.5860
		CROWN	-2.6324	-1.0032	0.0	1.9375
10	35	VALLEY	0.0311	0.0	1.3232	0.0
		$\frac{1}{4}$	0.6841	-0.3228	1.5106	0.1314
		$\frac{1}{2}$	-0.7701	-0.6338	1.5303	0.9720
		$\frac{3}{4}$	-2.6219	-0.8875	0.9874	2.0214
		CROWN	-3.4269	-0.9872	0.0	2.4813
15	30	VALLEY	0.0311	0.0	0.9604	0.0
		$\frac{1}{4}$	0.7129	-0.4196	1.2651	-0.0110
		$\frac{1}{2}$	-0.2022	-0.9209	1.4490	0.3527
		$\frac{3}{4}$	-1.4414	-1.3858	0.9857	0.6256
		CROWN	-1.9831	-1.5773	0.0	0.6844

BOUNDARY CONDITIONS: CASE (II)

HALF CENTRAL ANGLE $\phi_e = 80^\circ$, GA 22.

RADIUS	SPAN	ϕ/ϕ_e	\bar{N}_x	\bar{N}_ϕ	$\bar{N}_{x\phi}$	\bar{M}_ϕ
10	15	VALLEY	0.03113	0.0	0.5263	0.0
		$\frac{1}{4}$	0.1076	-0.2904	0.5942	0.0603
		$\frac{1}{2}$	0.0181	-0.5693	0.6430	0.3491
		$\frac{3}{4}$	-0.0353	-0.8814	0.6313	0.0097
		CROWN	-0.0311	-1.2719	0.6062	-0.7211
10	20	VALLEY	0.0311	0.0	0.7041	0.0
		$\frac{1}{4}$	0.1791	-0.2861	0.7759	0.0575
		$\frac{1}{2}$	1.1023	-0.558	0.8587	0.2772
		$\frac{3}{4}$	-0.0002	-0.8831	0.8842	-0.2613
		CROWN	-0.0311	-1.3037	0.8723	-1.1447
10	25	VALLEY	0.0311	0.0	0.8553	0.0
		$\frac{1}{4}$	0.3376	-0.2760	0.9543	0.0312
		$\frac{1}{2}$	0.2497	-0.5490	1.0927	0.0902
		$\frac{3}{4}$	0.0526	-0.8897	1.1579	-0.7319
		CROWN	-0.0311	-1.3369	1.1564	-1.7898
10	30	VALLEY	0.0311	0.0	0.9811	0.0
		$\frac{1}{4}$	0.6180	-0.2628	1.1267	0.0065
		$\frac{1}{2}$	0.4925	-0.5384	1.3447	-0.1586
		$\frac{3}{4}$	0.1352	-0.8988	1.4589	-1.3245
		CROWN	-0.0311	-1.3740	1.4681	-2.5828
10	35	VALLEY	0.03113	0.0	1.0900	0.0
		$\frac{1}{4}$	1.0278	-0.2495	1.2946	-0.0453
		$\frac{1}{2}$	0.8392	-0.5285	1.6087	-0.4085
		$\frac{3}{4}$	0.2510	-0.9081	1.7793	-1.9111
		CROWN	-0.0311	-1.4094	1.7997	-3.3630
15	30	VALLEY	0.0311	0.0	1.0675	0.0
		$\frac{1}{4}$	0.2597	-0.4356	1.1760	0.1505
		$\frac{1}{2}$	0.0938	-0.8469	1.2795	0.8006
		$\frac{3}{4}$	-0.0291	-1.3202	1.2896	-0.0938
		CROWN	-0.0311	-1.9297	1.2712	-1.8760

BOUNDARY CONDITIONS: CASE (III).

HALF CENTRAL ANGLE $\phi_e = 90^\circ$, GA 22.

RADIUS	SPAN	ϕ/ϕ_e	\bar{N}_x	\bar{N}_ϕ	$\bar{N}_{x\phi}$	\bar{M}_ϕ
15	20	VALLEY	0.0	0.6266	0.9488	0.0
		$\frac{1}{4}$	0.0189	-0.2349	0.9572	0.3090
		$\frac{1}{2}$	-0.1150	-0.8446	0.9379	-0.5288
		$\frac{3}{4}$	-0.5410	-1.3353	0.6484	0.0300
		CROWN	-0.7996	-1.5457	0.0	0.4009
15	30	VALLEY	0.0	0.6249	1.5698	0.0
		$\frac{1}{4}$	-0.0669	-0.2232	1.5592	0.1333
		$\frac{1}{2}$	-0.4880	-0.8756	1.4101	-1.0022
		$\frac{3}{4}$	-1.2009	-1.3352	0.8941	-0.2254
		CROWN	-1.5857	-1.5166	0.0	0.4740
15	40	VALLEY	0.0	0.6254	2.1207	0.0
		$\frac{1}{4}$	-0.1677	-0.2343	2.0983	-0.3162
		$\frac{1}{2}$	-0.9609	-0.8877	1.8560	-1.6653
		$\frac{3}{4}$	-2.0895	-1.2543	1.557	-0.7841
		CROWN	-2.6738	-1.5060	0.0	-0.0444
15	50	VALLEY	0.0	0.5878	2.6367	0.0
		$\frac{1}{4}$	-0.2876	-0.2754	2.5904	-1.4963
		$\frac{1}{2}$	-1.5696	-0.9098	2.2888	-3.1625
		$\frac{3}{4}$	-2.0896	-1.3318	1.1557	-0.7841
		CROWN	-4.0909	-1.4903	0.0	-0.8726
10	30	VALLEY	0.0	0.3627	1.5577	0.0
		$\frac{1}{4}$	-0.1580	-0.1967	1.5388	-1.0970
		$\frac{1}{2}$	-0.8476	-0.6156	1.3481	-1.9030
		$\frac{3}{4}$	-1.7533	-0.8896	0.8109	-1.3011
		CROWN	-2.1629	-0.9858	0.0	-0.7163
10	40	VALLEY	0.0	0.2752	1.9836	0.0
		$\frac{1}{4}$	-0.2756	-0.2553	1.9583	-3.0369
		$\frac{1}{2}$	-1.4396	-0.6464	1.7136	-4.7427
		$\frac{3}{4}$	-2.9390	-0.8993	1.0349	-4.4591
		CROWN	-3.6331	-0.9904	0.0	-3.9870

BOUNDARY CONDITIONS: CASE (IV).

HALF CENTRAL ANGLE $\phi_e = 80^\circ$, GA 22.

RADIUS	SPAN	ϕ/ϕ_e	\bar{N}_x	\bar{N}_ϕ	$\bar{N}_{x\phi}$	\bar{M}_ϕ
10	30	VALLEY	0.0324	-0.0268	1.5751	6.7248
		$\frac{1}{4}$	-0.5604	-0.4754	1.4778	1.0455
		$\frac{1}{2}$	-1.1438	-0.7876	1.1660	-1.8590
		$\frac{3}{4}$	-1.6447	-0.9691	0.6507	-2.3995
		CROWN	-1.8509	-1.0287	0.0	-2.2944
10	35	VALLEY	0.0324	-0.0394	1.9272	11.0031
		$\frac{1}{4}$	-0.8459	-0.5142	1.7980	2.4818
		$\frac{1}{2}$	-1.6593	-0.8449	1.4034	-2.7070
		$\frac{3}{4}$	-2.3056	-1.0354	0.7750	-4.7057
		CROWN	-2.5609	-1.0973	0.0	-5.0984
10	40	VALLEY	0.0324	-0.0584	2.3422	17.5253
		$\frac{1}{4}$	-1.2098	-0.5698	2.1783	4.7116
		$\frac{1}{2}$	-2.3239	-0.9296	1.6901	-3.9661
		$\frac{3}{4}$	-3.1702	-1.1377	0.9280	-8.2289
		CROWN	-3.4957	-1.2053	0.0	-9.4040
20	30	VALLEY	0.0324	-0.0078	1.1500	2.3178
		$\frac{1}{4}$	-0.2424	-0.6500	1.2684	-0.7174
		$\frac{1}{2}$	-0.1363	-1.2704	1.3535	-0.7950
		$\frac{3}{4}$	-0.9967	-1.8371	0.9439	0.2132
		CROWN	-1.4482	-2.0794	0.0	0.6353
20	35	VALLEY	0.0324	-0.0113	1.4196	3.4760
		$\frac{1}{4}$	0.1996	-0.6909	1.5087	-0.9477
		$\frac{1}{2}$	-0.2778	-1.3032	1.5284	-1.3367
		$\frac{3}{4}$	-1.3034	-1.8293	1.0378	0.2344
		CROWN	-1.8447	-2.0492	0.0	1.0387
20	40	VALLEY	0.0324	-0.0150	1.7107	4.7903
		$\frac{1}{4}$	0.0947	-0.7326	1.7596	-1.1335
		$\frac{1}{2}$	-0.4929	-1.3381	1.6899	-1.9211
		$\frac{3}{4}$	-1.6351	-1.8227	1.1099	0.1799
		CROWN	-2.2324	-2.0189	0.0	1.3658

BOUNDARY CONDITIONS: CASE (V).

HALF CENTRAL ANGLE $\phi_e = 80^\circ$, GA 22.

RADIUS	SPAN	ϕ/ϕ_e	\bar{N}_x	\bar{N}_ϕ	$\bar{N}_{x\phi}$	\bar{M}_ϕ
10	30	VALLEY	0.0324	-0.0158	1.2444	4.9898
		$\frac{1}{4}$	0.0414	-0.3572	1.2584	1.4952
		$\frac{1}{2}$	0.0191	-0.6421	1.2706	-0.8545
		$\frac{3}{4}$	-0.0186	-0.9509	1.2705	-2.7776
		CROWN	-0.0324	-1.3519	1.2601	-4.0583
10	35	VALLEY	0.0324	-0.0273	1.5103	9.1070
		$\frac{1}{4}$	0.0602	-0.3867	1.5255	2.8898
		$\frac{1}{2}$	0.0416	-0.6900	1.5430	-1.7510
		$\frac{3}{4}$	-0.0093	-1.0186	1.5481	-5.2632
		CROWN	-0.0324	-1.4409	1.5402	-7.1416
10	40	VALLEY	0.0324	-0.0450	1.8303	15.4335
		$\frac{1}{4}$	0.0812	-0.4327	1.8467	5.0242
		$\frac{1}{2}$	0.0660	-0.7646	1.8687	-3.1354
		$\frac{3}{4}$	0.0004	-1.1226	1.8781	-9.0747
		CROWN	-0.0324	-1.5751	1.8722	-11.8594
20	30	VALLEY	0.0324	-0.0060	1.1889	1.4276
		$\frac{1}{4}$	0.0548	-0.6566	1.2285	-0.6109
		$\frac{1}{2}$	-0.0880	-1.2042	1.2225	0.2748
		$\frac{3}{4}$	-0.1237	-1.7532	1.1289	0.4044
		CROWN	-0.0324	-2.4320	1.0776	-1.3814
20	35	VALLEY	0.0324	-0.0066	1.4031	1.6754
		$\frac{1}{4}$	0.0300	-0.6616	1.4276	-0.5370
		$\frac{1}{2}$	-0.0889	-1.2004	1.4123	0.2830
		$\frac{3}{4}$	-0.1098	-1.7510	1.3388	0.2642
		CROWN	-0.0324	-2.4511	1.2985	-1.6834
20	40	VALLEY	0.0324	-0.0071	1.6106	2.0126
		$\frac{1}{4}$	0.0149	-0.6631	1.6267	-0.3942
		$\frac{1}{2}$	-0.0862	-1.1978	1.6089	0.2644
		$\frac{3}{4}$	-0.0926	-1.7520	1.5500	0.0261
		CROWN	-0.0324	-2.4677	1.5173	-2.0802

MAXIMUM INTENSITY OF SNOW LOAD FOR
DIFFERENT CASES OF BOUNDARY CONDITIONS

GA 22, $\phi_e = 80^\circ$

SPAN (feet)	15	20	25	30	35	40
RADIUS (feet)	10	10	10	10	10	15
LOAD (psf): For CASE (I)	45	20	11	7	4	12
LOAD (psf): For CASE (II)	50	42	23	10	5	18

TABLE (A)

SPAN (feet)	30	40	20	30	40	50
RADIUS (feet)	10	10	15	15	15	15
LOAD (psf): For CASE (III) $\phi_e = 90^\circ$	13	6	44	22	12	6

TABLE (B)

SPAN (feet)	30	35	40	30	35	40
RADIUS (feet)	10	10	10	20	20	20
LOAD (psf): For CASE (IV)	22.5	16	11	20	14	10
LOAD (psf): For CASE (V)	50	50	48	50	50	45

TABLE (C)

Example:

The analysis of a simply supported cylindrical shell by the use of tables will be illustrated in this example.

Design a shell roof made of corrugated sheets with longitudinal stiffeners at the valleys. The shell has the following parameters:

Span = 20 Feet

Radius = 10 Feet

$$\phi_e = 80^\circ$$

Maximum intensity of snow load is 15 psf.

Solution:

From table A, the roof with the given dimensions can be built with Gage 22 and can carry a maximum intensity of 20 psf snow load. From table (I), the stress-resultants can be calculated from the following formulae:

$$N_x = \bar{N}_x \cdot p \cdot \cos \frac{\pi x}{L} \quad (\text{lb/in})$$

$$N_\phi = \bar{N}_\phi \cdot p \cdot \cos \frac{\pi x}{L} \quad (\text{lb/in})$$

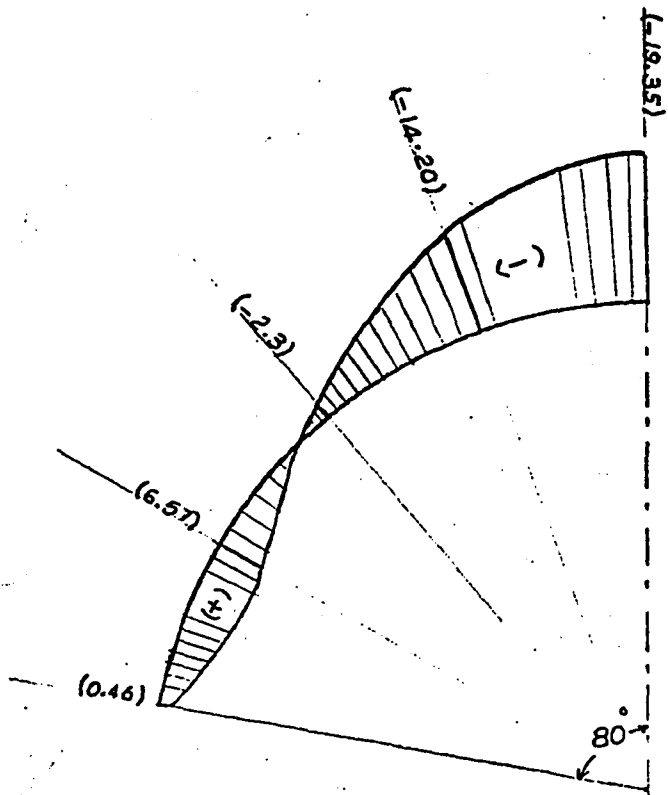
$$N_{x\phi} = \bar{N}_{x\phi} \cdot p \cdot \sin \frac{\pi x}{L} \quad (\text{lb/in})$$

$$M_\phi = \bar{M}_\phi \cdot p \cdot \cos \frac{\pi x}{L} \quad (\text{lb/in})$$

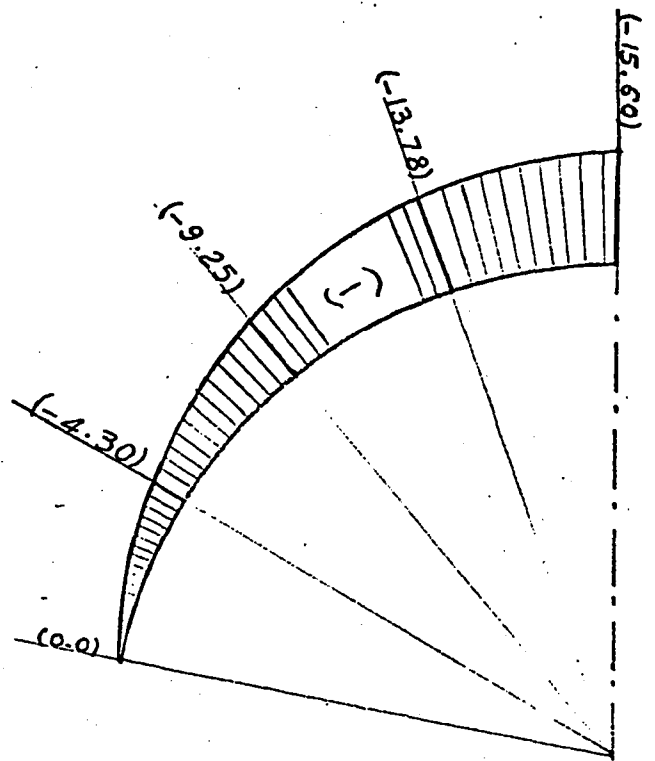
$$\text{where } p = 15 \text{ psf}$$

Figures (a, b, c & d) show the distribution of the stress-resultants.

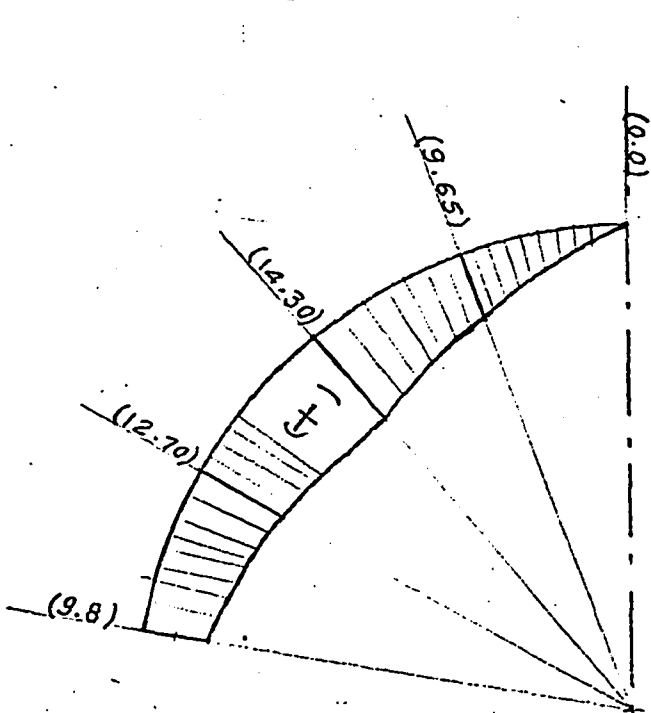
$$\text{Area of stiffener} = \frac{15 \times L}{\pi \times \sigma_x} \cdot 0.6565 = 0.118 \text{ in}^2$$



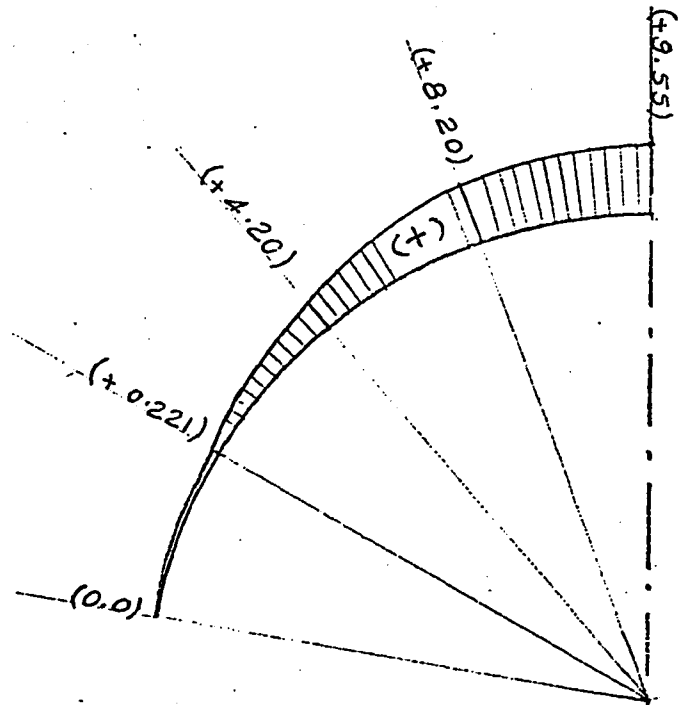
N_x - Distribution (lb/in)
at mid-span.
Fig. (a)



N_ϕ - Distribution (lb/in)
at mid-span.
Fig. (b)



$N_{x\phi}$ - Distribution (lb/in)
at support.
Fig. (c)

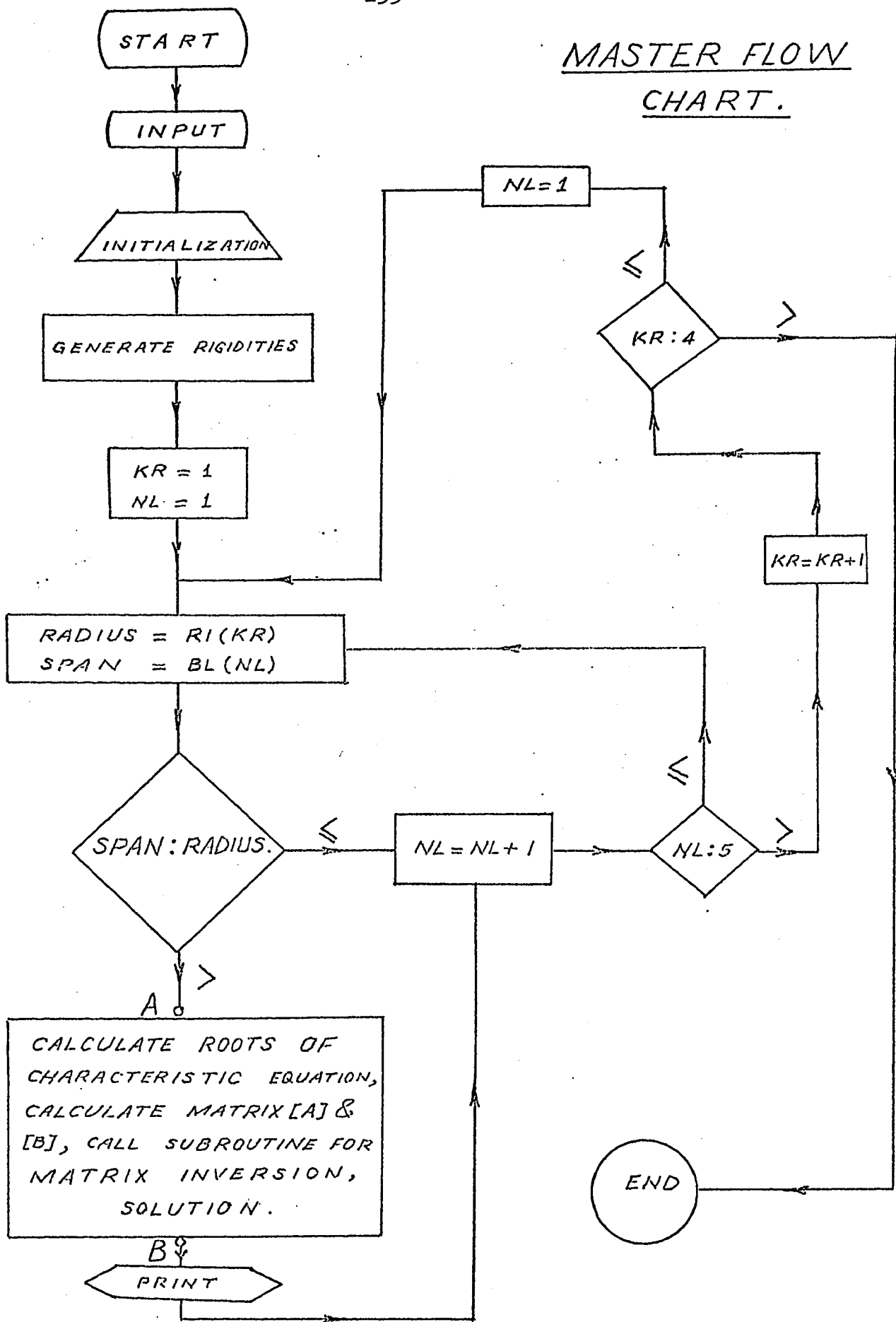


M_ϕ - Distribution (lb/in)
at mid-span
Fig. (d)

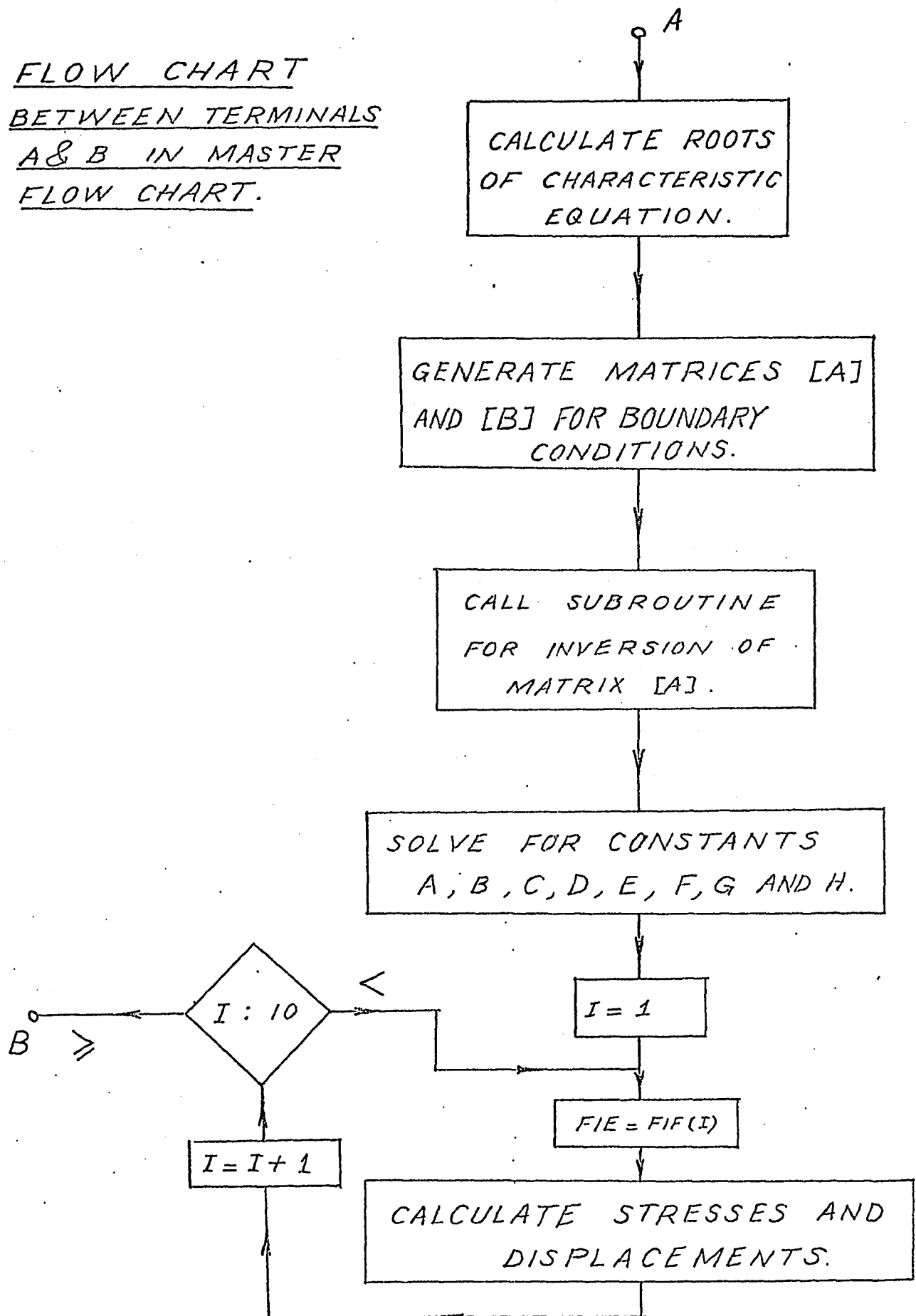
APPENDIX (IV)

FLOW CHARTS

MASTER FLOW CHART.



FLOW CHART
BETWEEN TERMINALS
A & B IN MASTER
FLOW CHART.



REFERENCES

1. Abdel-Sayed, G., "Critical Shear Loading of Curved Panels of Corrugated Sheets", Journal of E.M. Division, ASCE, Dec. 1970, pp. 895-912.
2. Abdel-Sayed, G., "Critical Shear Loading of Curved Panels of Corrugated Sheets with Restrained Edges" Proc. of 1st specialty Conference on Cold-Formed Steel Structures, Rolla, Missouri, Aug. 1971, pp. 167-172.
3. Abdel-Sayed, G., "Effective Width of Steel Deck-Plate in Bridges", Journal of the Structural Division, ASCE, No. ST7, July, 1969, pp. 1459.
4. "Bin Wall Design and Construction", ACI Journal, July, 1968, Reported by ACI Committee 313.
5. Cornelius, W., Die Berechnung der ebenen Flachentragwerke mit Hilfe der Theorie der orthogonalen anisotropen Platte Stahlbau, 1952, p. 21.
6. Donnell, L.H., Stability of Thin-Walled Tubes Under Torsion, NACA Report No. 479, 1933, p. 12.
7. Donnell, L.H., "A Discussion of Thin-Shell Theory", Journal of Applied Mechanics, Proc. 5th Internat. Cong. Appl. Mech., Cambridge, 1927.
8. El-Atrouzy, M.N., Structural Properties of Corrugated Sheets used in Cylindrical Shells, M.Sc. Thesis University of Windsor, Windsor, Ontario, Canada, 1969.
9. El-Atrouzy, M.N., Abdel-Sayed, G., "Cylindrical Shells Made of Corrugated Sheets", International Association of Bridge and Structural Engineering, 1972.
10. Flugge, W., Stresses in Shells, Springer-Verlag, Berline/Cöttingen/Heidelberg, 1962.
11. Hoff, N.J., "The Accuracy of Donnell's Equations" Journal of Applied Mechanics, September, 1955.
12. Huber, M.T., Die Theorie Der Kreuzweise Bewehrten Eisenbetonplatten Nebst Anwendungen Auf Mehrere Bautechnisch Wichtige Ausgaben Uber Rechteckige Platten, December, 1923, p. 354 and 392.

13. Johannes Moe, C.E., Trondheim, "On the Theory of Cylindrical Shells, Explicit Solution of the Characteristic Equations and Discussion of the Accuracy of Various Shell Theories", International Association of Bridge and Structural Engineering, Publication 13, 1953.
14. Joseph Kempner, "Remarks on Donnell's Equations," Journal of Applied Mechanics, Vol. 22, March, 1955.
15. Kraus, H., Thin Elastic Shells, John Wiley & Sons, Inc. N.Y., 1967.
16. Love, A.E.H., The Mathematical Theory of Elasticity, Cambridge University Press, Cambridge, 1927.
17. Luttrell, L.D., Structural Performance of Light Gage Steel Diaphragms, Report 319, Department of Structural Engineering, Cornell University, August, 1965.
18. Nilson, A.H., "Shear Diaphragms of Light Gage Steel" Journal of the Structural Division, ASCE, Vol. 86, ST11, Nov., 1960.
19. Nilson, A.H., "Folded Plate Structures of Light Gage Steel", ASCE, Transactions Paper No. 3514, (Vol. 128, 1963, Part II), pp. 848-880.
20. El-Dakhakhini, W. M. and Bryan, E.R., "Shear of Thin Plates with Flexible Edge Members", Proceedings of ASCE, Vol. 90, No. St4, August, 1964.
21. Ramaswamy, G.S., Design and Construction of Concrete Shell Roofs, McGraw-Hill, N.Y. (1968)
22. The James F. Lincoln, Orthotropic Bridges - Theory and Design, AISC, 101 Park Av., N.Y. (1962).
23. Timoshenko, S., Theory of Elasticity, McGraw-Hill Book Co., N.Y. Second edition, (1952).
24. Timoshenko, S., Theory of Plates and Shells, McGraw-Hill Book Co., N.Y. Second edition (1959).

VITA AUCTORIS

- 1943 Born August 21 in Cairo, Egypt.
- 1960 Entered the University of Ain Shams in Cairo.
- 1965 Graduated with Bachelor of Science of Engineering. Appointed as an instructor in the Faculty of Engineering, Ain Shams University in Cairo.
- 1968 Awarded a Teaching and Research Assistantship for graduate study at the University of Windsor.
- 1969 Graduated with a Master of Applied Science in Civil Engineering from the University of Windsor.
- 1969 In November, he continued studies at the University of Windsor in order to obtain the Degree of Doctor of Philosophy in Civil Engineering.
- 1972 Accepted as a member of the Association of Professional Engineers of Ontario.